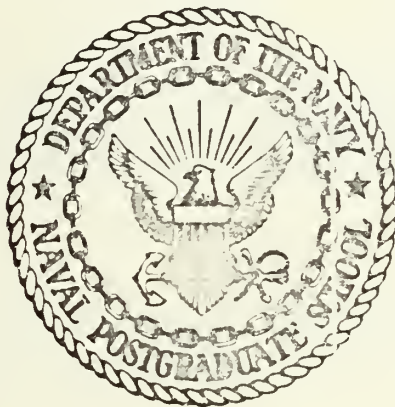


AN EVALUATION OF A NUMERICAL WATER ELEVATION
AND TIDAL CURRENT PREDICTION MODEL
APPLIED TO MONTEREY BAY

by

Sheldon Mark Lazanoff

United States Naval Postgraduate School



THE SIS

AN EVALUATION OF A NUMERICAL WATER ELEVATION
AND TIDAL CURRENT PREDICTION MODEL
APPLIED TO MONTEREY BAY

by

Sheldon Mark Lazanoff

Thesis Advisor:

E. B. Thornton

March 1971

Approved for public release; distribution unlimited.

U138003



— — —

An Evaluation of a Numerical Water Elevation
and Tidal Current Prediction Model
Applied to Monterey Bay

by

Sheldon Mark Lazanoff
Civilian, United States Naval Oceanographic Office
B. S., Pennsylvania State University, 1963

Submitted in partial fulfillment of the
requirements for the degree of

MASTER OF SCIENCE IN OCEANOGRAPHY

from the

NAVAL POSTGRADUATE SCHOOL
March 1971

ABSTRACT

The Hansen Hydrodynamical - Numerical model was evaluated for Monterey Bay with actual field data. Tides and winds are the principal driving forces of the Hansen model. Analysis of the field data indicated that the principal driving force of the circulation in the bay was the oceanic currents and not the tides and winds. The tidal heights and phases and current directions were calculated correctly by the model, but the calculated current speeds were an order of magnitude too large. The inaccuracy of the current speeds was attributed to the inaccurate calculations of the currents along the open boundary and the large bathymetric gradients of the Monterey Submarine Canyon.

TABLE OF CONTENTS

I. INTRODUCTION -----	12
A. REVIEW -----	12
B. OBJECTIVES -----	14
II. THE HANSEN HYDRODYNAMICAL MODEL -----	17
A. MATHEMATICAL MODEL -----	17
B. COMPUTER MODEL -----	22
C. MONTEREY BAY -----	27
1. Grid -----	31
2. Time Step -----	33
3. Tides -----	33
4. Horizontal Eddy Diffusivity -----	37
5. Bottom Stress -----	38
6. Wind Stress -----	39
III.COMPUTER MODEL RESULTS AND DATA ANALYSIS -----	40
A. DATA ANALYSIS -----	40
B. COMPUTER MODEL RESULTS -----	48
IV. CONCLUSION -----	56
APPENDIX A -----	59
BIBLIOGRAPHY -----	142
INITIAL DISTRIBUTION LIST -----	144
FORM DD 1473 -----	147

LIST OF FIGURES

1	Hansen Coordinate System -----	18
2	Model Grid System -----	23
3	Tide, Wind and Current Meter Stations -----	28
4	Depth of Canyon Thalweg -----	29
5	Transverse Profiles of Monterey Canyon -----	30
6	Hansen Grid System for Monterey Bay -----	32
7	Computed vs. Actual Tide at Santa Cruz -----	36
8	Semi-diurnal Rotary Tidal Current -----	42
A-1	Actual Tides at Monterey and Santa Cruz for 12-13 August 1970 -----	60
A-2	Actual Tides at Monterey and Santa Cruz for 18-19 August 1970 -----	61
A-3	Actual Tides at Monterey and Santa Cruz for 6-7 November 1970 -----	62
A-4	Actual Tides at Monterey and Santa Cruz for 8-9 November 1970 -----	63
A-5	Actual Tides at Monterey and Santa Cruz for 10-11 November 1970 -----	64
A-6	Actual Tides at Monterey and Santa Cruz for 12-13 November 1970 -----	65
A-7	Actual Tides at Moss Landing for 6-7 November 1970 -----	66
A-8	Actual Tides at Moss Landing for 8-9 November 1970 -----	67
A-9	Actual Tides at Moss Landing for 10-11 November 1970 -----	68
A-10	Actual Tides at Moss Landing for 12-13 November 1970 -----	69
A-11	Tracks of Drogues 1-5 -----	70
A-12	Tracks of Drogues 6-13 -----	71

A-13	Tracks of Drogues 28-32 -----	72
A-14	Tracks of Drogues 34-Z -----	73
A-15	Tracks of Drogues 35-38 -----	74
A-16	Tracks of Drogues 35-36 continued and closed. current system between Pt. Ano Nuevo and Santa Cruz -----	75
A-17	Currents vs. Tides and Winds for Droque 1 -----	76
A-18	Currents vs. Tides and Winds for Droque 2 -----	77
A-19	Currents vs. Tides and Winds for Droque 4 -----	78
A-20	Currents vs. Tides and Winds for Droque 5 -----	79
A-21	Currents vs. Tides and Winds for Droque 6 -----	80
A-22	Currents vs. Tides and Winds for Droque 7 -----	81
A-23	Currents vs. Tides and Winds for Droque 8 -----	82
A-24	Currents vs. Tides and Winds for Droque 10 -----	83
A-25	Currents vs. Tides and Winds for Droque 12 -----	84
A-26	Currents vs. Tides and Winds for Droque 13 -----	85
A-27	Currents vs. Tides and Winds for Droque 28 -----	86
A-28	Currents vs. Tides and Winds for Droque 29 -----	87
A-29	Currents vs. Tides and Winds for Droque 30 -----	88
A-30	Currents vs. Tides and Winds for Droque 31 -----	89
A-31	Currents vs. Tides and Winds for Droque 33 -----	90
A-32	Currents vs. Tides and Winds for Droque 34 -----	91
A-33	Currents vs. Tides and Winds for Droque x -----	92
A-34	Currents vs. Tides and Winds for Droque y -----	93
A-35	Currents vs. Tides and Winds for Droque z -----	94
A-36	Currents vs. Tides and Winds for Droque 35 -----	95
A-37	Currents vs. Tides and Winds for Droque 36 -----	96
A-38	Currents vs. Tides and Winds for Droque 37 -----	97
A-39	Currents vs. Tides and Winds for Droque 38 -----	98

A-40	Currents vs. Tides and Winds for Current Meter Station 1 -----	99
A-41	Currents vs. Tides and Winds for Current Meter Station 1 -----	100
A-42	Currents vs. Tides and Winds for Current Meter Station 2 -----	101
A-43	Currents vs. Tides and Winds for Current Meter Station 3 -----	102
A-44	Current in Lagrangian Format for Current Meter Station 1 -----	103
A-45	Currents in Ocean adjacent to Monterey Bay -----	104
A-46	Currents in Ocean adjacent to Monterey Bay -----	105
A-47	Calculated Tides and Currents in Monterey Harbor for 7 November 1970 -----	106
A-48	Calculated Tides and Currents in Monterey Harbor for 8 November 1970 -----	107
A-49	Calculated Tides and Currents at Santa Cruz for 7 November 1970 -----	108
A-50	Calculated Tides and Currents at Santa Cruz for 8 November 1970 -----	109
A-51	Calculated Tides and Currents at Moss Landing for 7 November 1970 -----	110
A-52	Calculated Tides and Currents at Moss Landing for 8 November 1970 -----	111
A-53	Calculated Tides and Currents in Deep Part of Monterey Canyon 8 November 1970 -----	112
A-54	Calculated Tides and Currents in Shallow Part of Monterey Canyon for 8 November 1970 -----	113
A-55	Calculated currents in Monterey Bay at Higher Low Water plus 0.5 hours -----	114
A-56	Calculated currents in Monterey Bay at Lower High Water minus 2 hours -----	115
A-57	Calculated currents in Monterey Bay at Lower High Water plus 1 hour -----	116
A-58	Calculated currents in Monterey Bay at Lower Low Water minus 2.5 hours -----	117

A-59	Calculated currents in Monterey Bay at Lower Low Water -----	118
A-60	Calculated currents in Monterey Bay at Lower Low Water plus 3.5 hours -----	119
A-61	Calculated currents in Monterey Bay at Higher High Water minus 2.5 hours -----	120
A-62	Calculated currents in Monterey Bay at Higher High Water plus 0.5 hours -----	121
A-63	Calculated currents in Monterey Bay at Lower Low Water minus 2.5 hours -----	122

LIST OF TABLES

A-I	Comparison of Tides at Monterey Bay Reference Stations -----	123
A-II	Wind Measurements in Monterey Bay -----	126
A-III	Drogues Course/Speed Data -----	135

LIST OF SYMBOLS

A_b	area of Monterey Bay
A_j	Fourier constituent
A_n	tidal amplitude of n^{th} constituent
B_j	Fourier constituent
C	De Chezy coefficient
D	thickness of fluid
DL	1/2 mesh length
DT	1/2 time step
H	total water depth
K_h	horizontal eddy diffusivity
M	Hansen grid coordinate
M_2	semi diurnal tidal constituent
N	Hansen grid coordinate
P	fluid pressure
P_o	atmospheric pressure
U_i	horizontal velocity over depth
$(V_o + U_n)$	value of equilibrium of the n^{th} tidal constituent
W	wind velocity
Z	Hansen symbolic grid point
a'	wind, bottom and lateral shear stresses combined
f	Coriolis parameter (planetary vorticity)
f_n	factor for reducing tidal amplitude A_n to year of prediction
g	gravitational attraction of the earth
h	distance from ocean bottom to mean sea level

\bar{h}_e	average depth across the entrance of the bay
h_{\max}	maximum depth of the bay
l	grid mesh length
l_e	length of the entrance of the bay
n	bathymetry line perpendicular to flow
r	bottom stress coefficient
t	time
u	current velocity
\bar{u}_e	average velocity at the bay entrance
X	grid coordinate
α	horizontal viscosity parameter
κ_n	tidal epoch of the n^{th} constituent
λ	wind drag coefficient
η	deviation of water surface from mean sea level
$\bar{\eta}_b/T$	average increase in water elevation in the bay during a given time period
ζ	relative vorticity
ρ	fluid density
σ	Fourier frequency
τ	time step between two grid points
τ^b	bottom shear stress
τ^w	wind stress
ν	horizontal eddy viscosity

ACKNOWLEDGEMENT

The author wishes to express his sincere appreciation to Professor Edward B. Thornton, under whose direction this paper was written. His encouragement and criticism were invaluable in the completion of this research.

In addition, the author is indebted to Captain Willard S. Houston, Commanding Officer, Fleet Numerical Weather Central (FNWC) for permission to run the Monterey Bay numerical model on FNWC computers. The author also wishes to thank Dr. Taivo Laevastu and Mr. Chuck Hines, FNWC, for technical and programming assistance respectively; Leo J. Fisher and Donald B. Burns, U. S. Naval Oceanographic Office for providing oceanographic instrumentation; the staff of Monterey office of the National Marine Fisheries Service for technical advice and typing services; and Professor Jerry Galt, whose discussions of numerical modeling were stimulating and educational.

Finally, the author is deeply grateful to his wife, Linda, without whose ability the graphics for this report could not have been completed.

I. INTRODUCTION

A. REVIEW

During the normal course of events, tidal circulation in coastal areas, estuaries and rivers affects a diverse number of parameters including: marine life in the inter-tidal and near shore zones; the flow of man-made sewage and other pollutants dumped into the water; off-shore structures, channel dredging and other engineering projects; and, of course, ship traffic. Furthermore, in areas where intense storms occur, the wind can create storm surges which combined with the tides can kill and injure people and destroy property on the surrounding low lands. Before the advent of high speed digital computers, the prediction of tidal heights and currents was difficult and cumbersome. The tidal circulation in deep water is primarily due to the attraction by the moon and sun; however, the tides in shallow water are also strongly affected by the geography and bathymetry of the area.

The techniques for tide prediction developed by the US Coast and Geodetic Survey (USCGS) and the British Admiralty, among other international agencies, in the late nineteenth century have become standard throughout the world. The procedure requires tidal height and current data measured for at least 29 days which covers the principal lunar constituents, preferably for a year which covers the principal solar constituents and ideally for 18.6 years which covers all possible

tidal constituents. The tidal constituents, or harmonic coefficients, are then used to predict the tidal elevation. The accuracy of the predictions increase with the length of the record. The data are analyzed by harmonic techniques and tidal constituents are produced. In the past the tidal constituents were used as input to large tide prediction machines which produced hourly heights and tidal currents (Schureman, 1958). The machine needed at least twelve hours to produce yearly predictions for one station. One serious problem with this technique is that if tide data are not available for a location of interest, then the predictions have to be interpolated between known stations as shown in the USCGS Tide Tables. The interpolated tide values can be inaccurate and more detrimental than helpful for real time operational planning. The U.S. Navy became acutely aware of this problem when using French tide tables for riverine and coastal operations in Vietnam.

The necessary equations of motion needed to describe the tides were developed by Bernoulli and Laplace in the 18th century. However, because the equations are non-linear, simplfying assumptions had to be made and tedious analytical methods were used to obtain solutions. Analytical methods are not practical for real time predictions. By using computers these equations can be solved in less time by more sophisticated methods. For example, yearly tide predictions for one station can now be calculated on a computer in 1.7 minutes (Pore and Cummings, 1967) compared to twelve hours for the mechanical tide prediction machine. Several

computerized mathematical models using different numerical schemes and boundary conditions have been developed to predict assorted circulation parameters in a two dimensional field rather than for one point. An operational hydrodynamical model to compute water elevations and currents has been developed by Professor Walter Hansen, Universität Hamburg. The two driving forces in the model are the tides at the open boundary and the wind stress acting at the surface over the entire grid. The Hansen Model was initially begun in 1938 (Laevastu and Stevens, 1969), culminating in a two dimensional model of the North Sea in 1952 (Mungall and Matthews, 1970). In 1966 the North Sea model was programmed for the computer by Jensen, Weywadt, and Jensen (1966). The predictions compared favorably with field observations. Some of the general characteristics of Hansen's two dimensional model are that density is uniform over depth; the water transport is averaged over depth; bottom and wind stresses are represented by quadratic formulas; Coriolis force is assumed to be constant over small geographical areas; the effect of atmospheric pressure is neglected; and there are no more than two open boundaries on the rectangular grid.

B. OBJECTIVES

Since June 1968 Fleet Numerical Weather Central (FNWC) and U.S. Naval Oceanographic Office (NAVOCEANO) personnel have modified and adapted the Jensen, et.al. program to other geographic areas such as the South China Sea, DaNang Bay, Gulf of Tonkin, Straits of Gibraltar, Gulf of Mexico and the

Chesapeake Bay. Even though Hansen himself has indicated (Hansen, 1966) that synoptic field data are extremely important in verifying the results of the computer calculations, the results for the above mentioned projects have only been compared to atlas data and sparse field data, leaving some doubt as to the accuracy of the predictions. The U.S. Naval Oceanographic Office does oceanographic surveys in shallow water, semi-enclosed embayments throughout the world to fulfill specific requirements in supporting naval operations such as mine sweeping and diffusion studies. Because of ever changing world politics, oceanographic surveys cannot always be made in vital areas before they are needed and then, circumstances can prevent a proper survey from being made in these areas. Such situations have occurred in Vung Tau and DaNang Bay in the Republic of Vietnam. Thus, the object of this report is to evaluate the accuracy of Hansen's mathematical model for a shallow water, semi-enclosed embayment; varying parameters such as boundary conditions and the horizontal eddy viscosity parameter to determine their effects on the predicted elevations and currents and to determine the minimum field data requirements needed to satisfactorily verify the computer results.

For several reasons Monterey Bay appeared to be an excellent site to evaluate the model. Monterey Bay has similar geometrical features to many of the NAVOCEANO areas of interest. Unlike Southeast Asia areas there is no significant river run-off to influence the results (Lazanoff and Clarke, 1970). Winds are fairly steady and predictable over a long

period of time allowing the model to be evaluated for two steady-state conditions-summer calm conditions and fall and winter storm conditions. Finally, Monterey Bay, which is bisected by one of the deepest submarine canyons in the world allows the model to be tested over a large change of depth in a short horizontal distance.

II. THE HANSEN HYDRODYNAMICAL MODEL

A. MATHEMATICAL MODEL

Although the Hansen two-dimensional model is detailed by Jensen, et. al., the following is a review of the more important characteristics of the model. The coordinate system and surface and boundary conditions are shown in Figure 1. Some of the basic assumptions made in the analysis scheme are:

- 1) the fluid is homogeneous and incompressible,
- 2) the fluid is in hydrostatic equilibrium in the vertical direction,
- 3) the geographical and the vertical variations of the Coriolis force is neglected.

The equations used in the Hansen model are derived from the conservation of momentum and the conservation of mass which are respectively: the conservation of momentum

$$\frac{\partial u_i}{\partial t} + u_j \frac{\partial u_i}{\partial X_j} + (-1)^{(j+1)} f u_j + \frac{1}{\rho} \frac{\partial P}{\partial X_i} + a_i' + g_i = 0 \quad (1)$$

where, $i, j = 1, 2, 3$

u_i is the velocity component in the i^{th} direction,

t is time,

f is the Coriolis parameter,

ρ is the fluid density and, based on assumption (1),
is constant over depth,

P is the pressure of the fluid,

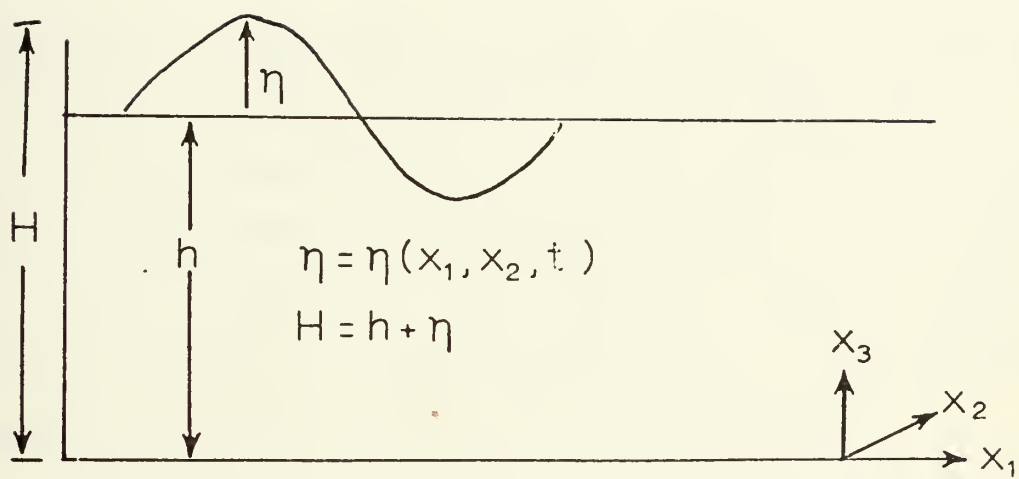


Figure 1. Hansen Coordinate System.

a_i' represents the wind, bottom and lateral shear stresses combined,

g_i represents external body force which is here limited to the gravitational attraction of the earth.

and the conservation of mass.

$$\frac{\partial \rho}{\partial t} + \frac{\partial \rho u_i}{\partial X_j} = 0 \quad j=1,2,3 \quad (2)$$

The density of sea water is assumed constant by assumption (1). This assumption is a limitation of the model and was made because of computer memory and time limitations at the time of the development of the original model. A multi-layer model is being developed at Fleet Numerical Weather Central under the guidance of Professor Hansen and Dr. Taivo Laevastu. The model was not available for use in Monterey Bay.

From assumption (2), equation (2) in the vertical direction reduces to

$$\begin{aligned} P &= \int_{-h}^{\eta} \rho(X_3) g dX_3 + P_0 \\ &= \rho g (\eta+h) + P_0 \end{aligned} \quad (3)$$

where P_0 is the atmospheric pressure.

The boundary condition at the bottom, $X_3 = 0$, is

$$\vec{u}_i \cdot \vec{n} = 0 \quad (4)$$

where n is the unit normal to the bottom.

The boundary condition at the surface, $x_3 = \eta + h$ is

$$\frac{\partial \eta}{\partial t} + u_{\eta_i} \frac{\partial \eta}{\partial x_i} = u_{\eta_3} \quad i = 1, 2 \quad (5)$$

where η is the water surface elevation and u_3 is the velocity in the vertical direction.

The barotropic atmospheric pressure term has been eliminated from the Monterey Bay model. Admittedly, the water height will increase by one centimeter as the atmospheric pressure decreases or increases one millibar (Lazanoff, 1969); however, this fluctuation is relatively insignificant compared to the fluctuations caused by the wind stress (Jensen, et. al.) and over the distance of Monterey Bay the atmospheric pressure varies only slightly except during very stormy periods.

The convective terms, $u_j \frac{\partial u_i}{\partial x_j}$, has also been neglected from the Hansen model. If a rather large value of 100 cm/sec (about 2 knots) is assigned to both u_j and the change of u_i with respect to x_j and the distance between grid points is 900 meters (actual mesh length for Monterey Bay), then the convective term has a value in the order of 10^{-5} cm/sec². Under the same conditions, the local acceleration term will be of order one; the Coriolis term will be on the order of 10^{-3} cm/sec and the gravitational term will be at least on the order of 10^{-2} cm/sec². Thus, the convective term will at least two order of magnitude less than any of the other terms in the equation.

By integrating the remainder of terms in equations (1) and (2) over depth, combining terms and defining the mean

velocity as

$$U_i = \frac{1}{H} \int_{-h}^{\eta} u_i dx_3 \quad i = 1, 2 \quad (6)$$

where $H = \eta + h$ and is the total water depth, the following equations arise:

$$\frac{\partial U_i}{\partial t} + (-1)^{(j+1)} f U_j - v \frac{\partial^2 U_i}{\partial x_j^2} = \frac{\tau_{\eta i}^w - \tau_{\eta i}^h}{\rho H} - g_i \frac{\partial \eta}{\partial x_i} \quad (7)$$

$i, j = 1, 2$

and

$$\frac{\partial \eta}{\partial t} + \frac{\partial (H U_i)}{\partial x_i} = 0 \quad (8)$$

where v is horizontal eddy diffusivity coefficient (lateral shear stress coefficient),

τ_i^w is the wind stress in the x_i direction in dynes/cm²

τ_i^b is the bottom shear stress in the x_i direction in dynes/cm².

Equations (7) and (8) are the equations used in the Hansen model.

The wind stress term ($\tau_{x_i}^w$), as used in Hansen's model, is assumed to be a quadratic expression in windspeed. This expression is

$$\tau_{\eta i}^w = \rho \lambda W_i (W_i^2 + W_j^2)^{1/2} \quad (9)$$

where λ is the wind drag coefficient (dimensionless) and W_i and W_j are the wind components.

The bottom stress term ($\tau_{X_i}^b$) is represented similarly to the wind stress term and is

$$\tau_{X_i}^b = \rho r U_i (U_i^2 + U_j^2)^{1/2} \quad (10)$$

where r is the bottom friction coefficient (dimensionless) and is assumed constant.

Both the bottom stress and wind stress terms are nonlinear and have been derived by empirical means. This formulation is an approximation and its applicability to deep water is questionable as it was originally formulated for shallow water application.

B. COMPUTER MODEL

A central differencing scheme is used to program equations (7) and (8). The grid system is shown in Figure 2 (Laevastu and Stevens, 1970). A "leap frog" method is used whereby the grid is staggered in time and space (Mungall and Matthews, 1970). N and M correspond respectively to the X_1 and X_2 coordinates. The Z points are the symbolic depths indicating land, sea and boundary points.

The finite approximations (Ortiz, 1964) are:

$$\eta_{(N,M)}^{(t,\tau)} = \tilde{\eta}_{(N,M)}^{(t)} - \tau/\ell \left(H_{U_1(N+1,M)}^{(t-\tau)} U_1^{(t)}(N+1,M) - H_{U_1(N-1,M)}^{(t-\tau)} U_1^{(t)}(N-1,M) \right. \\ \left. + H_{U_2(N,M-1)}^{(t-\tau)} U_2^{(t)}(N,M-1) - H_{U_2(N,M+1)}^{(t-\tau)} U_2^{(t)}(N,M+1) \right) \quad (11)$$

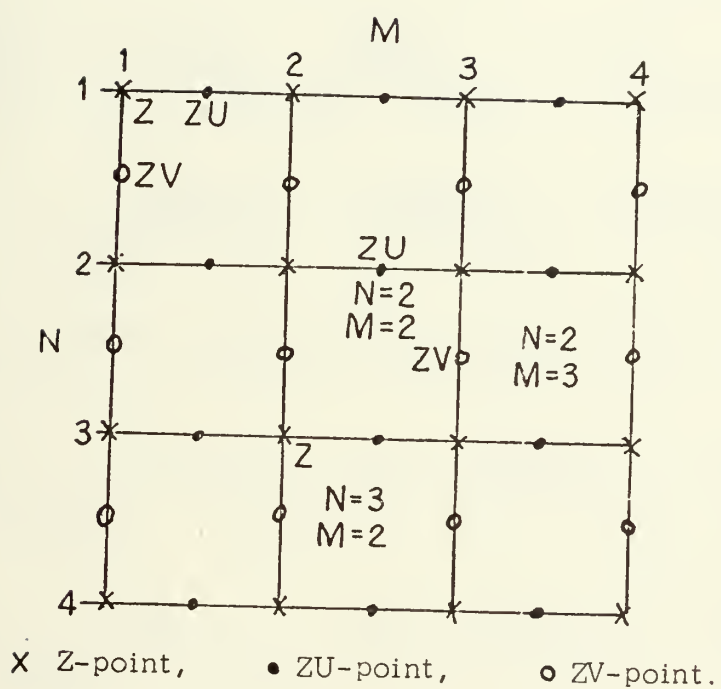


Figure 2. Model Grid System.

where τ is the time step between two Z points and ℓ is the mesh length between two Z points

$$U_{(N,M)}^{(t+2\tau)} = (1 - Q_{(N,M)}^{X_1(t)}) \tilde{U}_{1(N,M)}^{(t)} + 2\tau f U_{2(N,M)}^*(t) - \frac{\tau}{\ell} g. \quad (12)$$

$$\left(\eta_{(N+1,M)}^{(t+\tau)} - \eta_{(N-1,M)}^{(t+\tau)} \right) - 2\tau \tau_{X_i}^W(t)_{(N,M)}$$

Similarly,

$$U_{2(N,M)}^{(t+\tau)} = \left(1 - Q_{X_2(N,M)}^{(t)} \right) \tilde{U}_{2(N,M)}^{(t)} - 2\tau f U_{1(N,M)}^* - \frac{\tau}{\ell} g \quad (13)$$

$$\left(\eta_{(N,M+1)}^{(t+\tau)} - \eta_{(N,M-1)}^{(t+\tau)} \right) + 2\tau \tau_{X_2}^W(t)_{(N,M)}$$

The terms used in the previous equation can be defined as:

$$H_{U_1(N,M)}^{(t)} = h U_{1(N,M)} + 1/2 \left(\eta_{(N+1,M)}^{(t-\tau)} + \eta_{(N-1,M)}^{(t-\tau)} \right) \quad (14)$$

$$H_{U_2(N,M)}^{(t)} = h U_{2(N,M)} + 1/2 \left(\eta_{(N,M-1)}^{(t-\tau)} + \eta_{(N,M+1)}^{(t-\tau)} \right) \quad (15)$$

$$Q_{X_1(N,M)}^{(t)} = 2r\tau \left[\left(\tilde{U}_{1(N,M)}^{(t)} \right)^2 + \left(U_{2(N,M)}^*(t) \right)^2 \right]^{1/2} / H_{U_1(N,M)}^{(t+\tau)} \quad (16)$$

$$Q_{X_2(N,M)}^{(t)} = 2r\tau \left[\left(U_{1(N,M)}^*(t) \right)^2 + \left(U_{2(N,M)}^*(t) \right)^2 \right]^{1/2} / H_{U_2(N,M)}^{(t+\tau)} \quad (17)$$

U_1^* and U_2^* are the averaged velocities for the four Zu and Zv points about a Z point.

$$\begin{aligned} \tilde{U}_1^{(t)}(N,M) = & \alpha U_1^{(t)}(N,M) + \frac{1-\alpha}{4} \left(U_1^{(t)}(N+1,M) + U_2^{(t)}(N-1,M) \right. \\ & \left. + U_1^{(t)}(N,M-1) + U_1^{(t)}(N,M+1) \right) \end{aligned} \quad (18)$$

$$\begin{aligned} \tilde{U}_2^{(t)}(N,M) = & \alpha U_2^{(t)}(N,M) + \frac{1-\alpha}{4} \left(U_2^{(t)}(N+1,M) + U_2^{(t)}(N-1,M) \right. \\ & \left. + U_2^{(t)}(N,M-1) + U_2^{(t)}(N,M+1) \right) \end{aligned} \quad (19)$$

$$\begin{aligned} \eta^{(t)}(N,M) = & \alpha \eta^{(t)}(N,M) + \frac{1-\alpha}{4} \left(\eta^{(t)}(N+1,M) + \eta^{(t)}(N-1,M) \right. \\ & \left. + \eta^{(t)}(N,M-1) + \eta^{(t)}(N,M+1) \right) \end{aligned} \quad (20)$$

Alpha (α) is a function of the horizontal eddy diffusivity term, mesh length and time ($0 \leq \alpha \leq 1$). This term will be discussed in more detail in a later section.

If any of the above calculations occur at a boundary, then the values of η , U_1 and U_2 are taken at the actual point rather than from the surrounding points.

The primary forcing function for this model is the tide at the open boundary points. When the model was applied to other areas, predicted tides were generated for each time step using the following equation (Schureman):

$$\eta = A_0 + \sum_{n=1}^N f_n A_n \cos [a_n t + (V_0 + U_n) - \kappa_n] \quad (21)$$

where, η = height of the tide at any time
 A_o = mean height of water level above datum line,
 A_n = amplitude of the n^{th} amplitude
 f_n = factor for reducing amplitude A to year of predictions,
 A_n = speed of the n^{th} constituent,
 t = time calculated from some initial epoch such as beginning of year of predictions,
 $(V_o + U_n)$ = value of equilibrium of the n^{th} constituent when $t = 0$,
 κ_n = epoch of the n^{th} constituent.

Equation (21) is applied only at the open boundary. Since the objective of this particular project is to evaluate Hansen's hydrodynamical model and not the prediction of astronomical tides, a different method was used to calculate the input at the open boundary points. A Fourier analysis was made of the actual tide records which are used in this study. The Fourier constituents were used in the following equation:

$$\eta = 1/2 A_o + \sum_{j=1}^N (A_j \cos_j \sigma t + B_j \sin_j \sigma t) \quad (22)$$

where, A_o , A_j and B_j are the Fourier constituents, determined from the actual records

N is the total number of constituents used,

j is any given constituent,

$\sigma = \frac{2\pi}{T}$ and T is the length of time that spans the entire record.

The principal parts of the Hansen hydrodynamical model have now been detailed and the following section describes the application of the model to Monterey Bay.

C. MONTEREY BAY

Monterey Bay (Figure 3) is a semi-enclosed (one open boundary), approximately symmetrical embayment. Because Monterey Canyon very nearly bisects the bay, there is an unusually large variation of depth (400 fathoms) in a relatively small area (approximately 175.5 square miles). The depth of the canyon thalweg from the mouth of the bay to the shoreline is shown in Figure 4. The thalweg from the shoreline to six miles off the coast has an extremely steep slope of 1:18. Two transverse profiles of the bay are shown in Figure 5. The gradients of the canyon wall is steeper on the south side than on the north side but both canyon walls are extremely steep. Lynch (1970) found that the canyon tends to divide the bay into two distinct basins in which long period oscillations such as seiche occur independent of each other. The results of the Hansen model appear to indicate that this also occurs for tides which have longer periods than seiches.

The total circulation of Monterey Bay is affected by density gradients as well as tides, wind stress and air pressure gradients. All these mechanisms can be important and it is not really correct to separate the density gradients from the other parameters. Unfortunately, the complex computer models needed to combine these parameters would consume too much computer storage and running time to be practical and economically feasible on the present day computers.

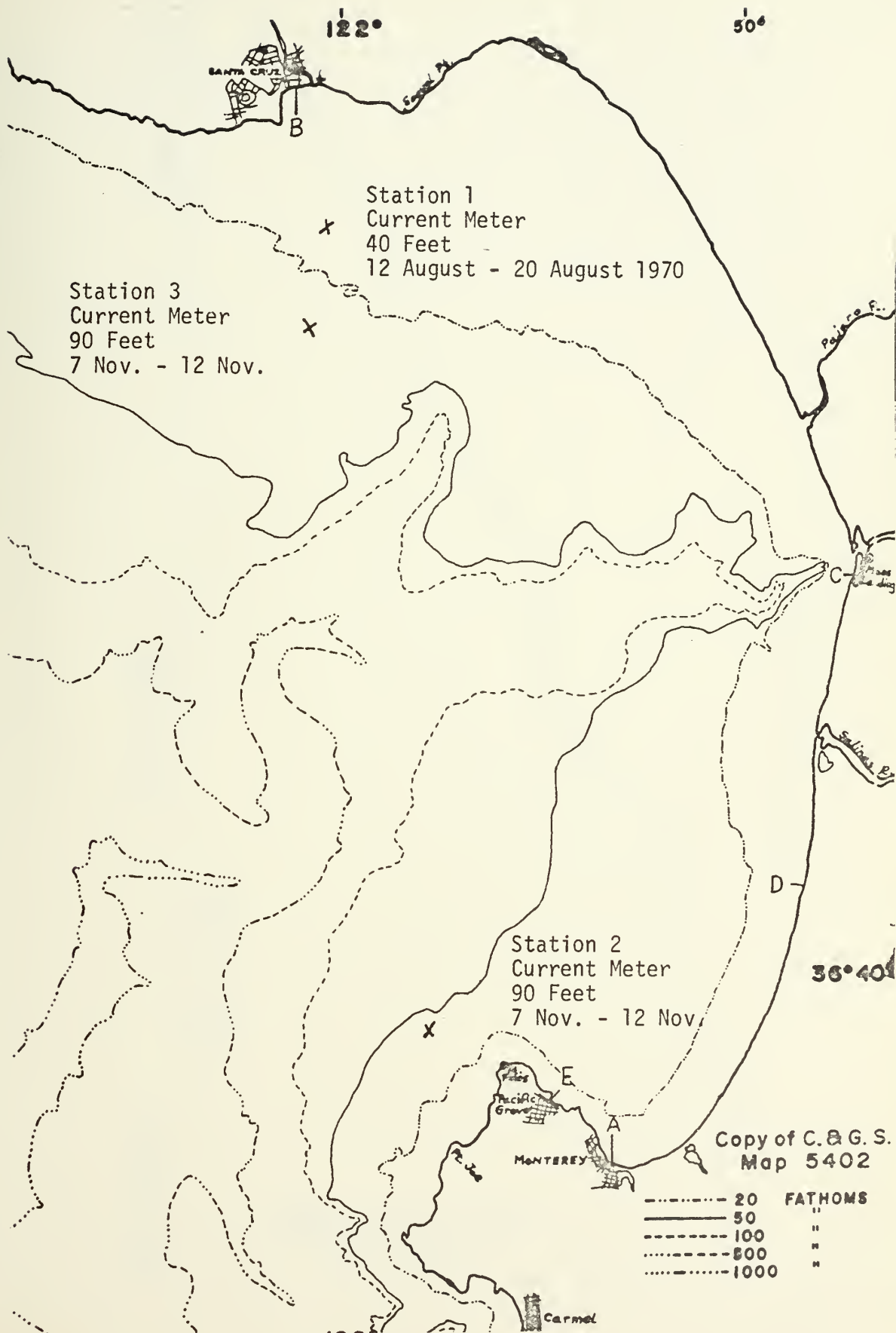


Figure 3. Tide, Wind and Current Meter Stations.

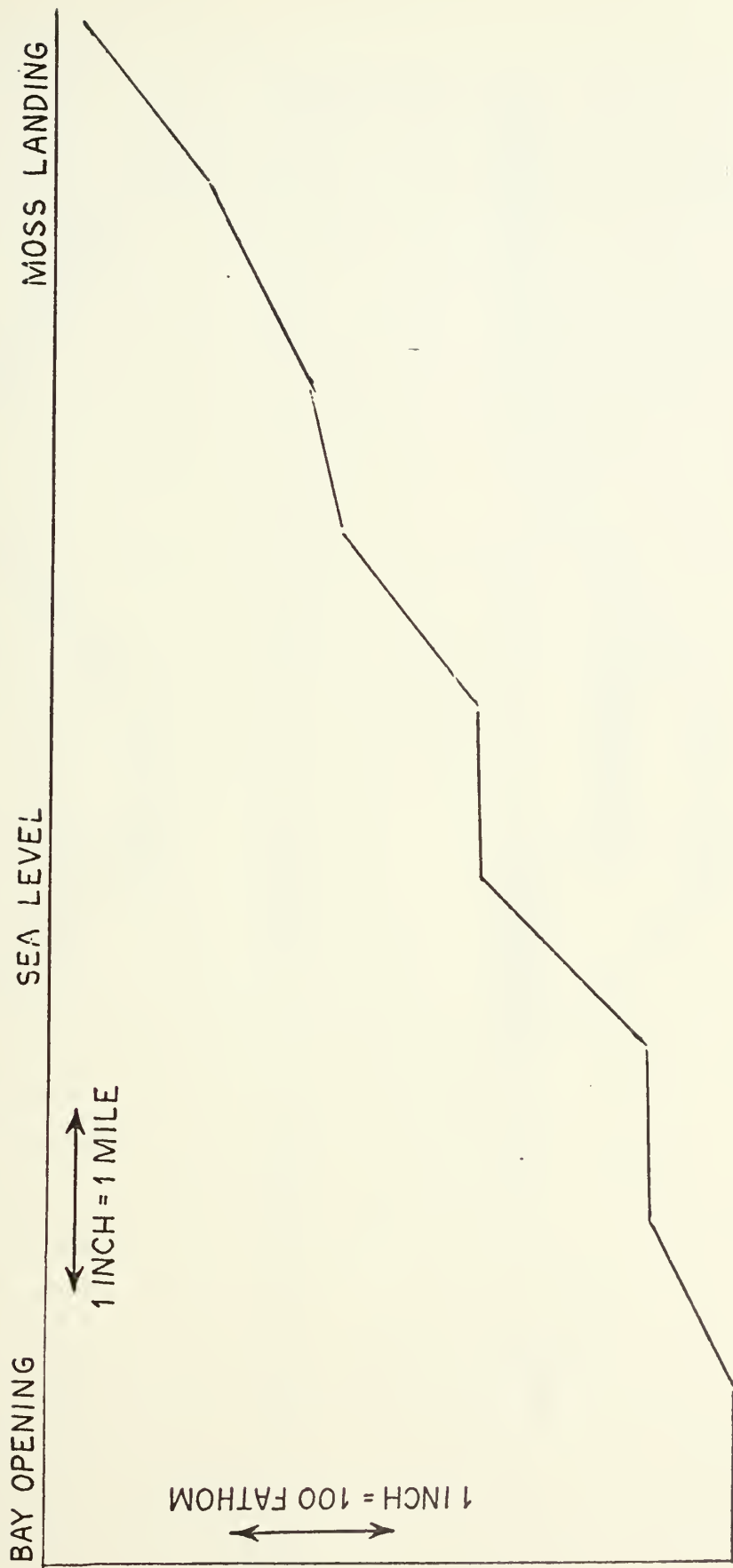


Figure 4. Depth of Canyon Thalweg.

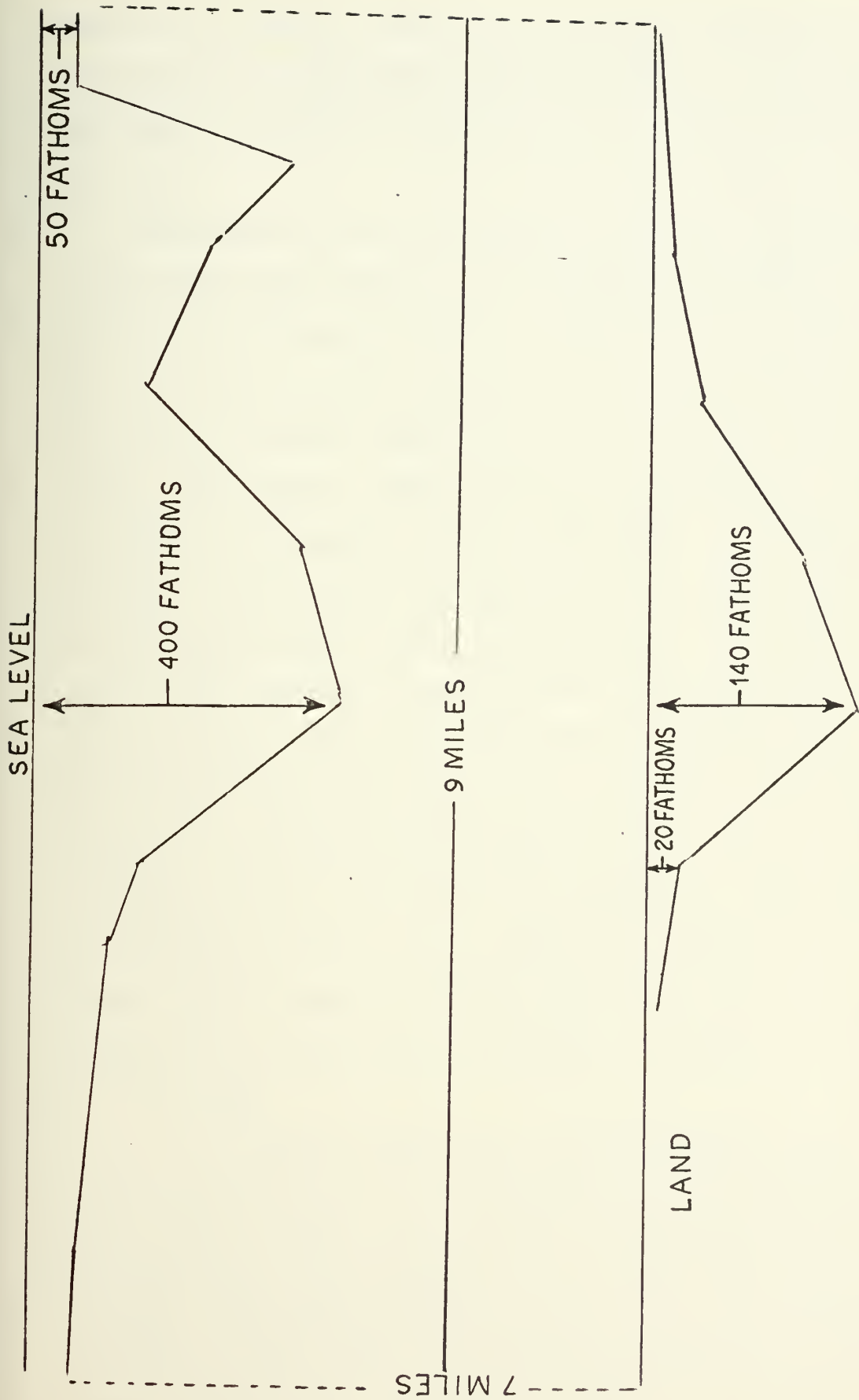


Figure 5. Transverse Profiles of Monterey Canyon.

However, to complete the picture of the circulation of Monterey Bay, some mention should be made of the semi-permanent density currents that occur in the ocean adjacent to the bay.

Depending on the climatological season, the circulation in Monterey Bay appears to be strongly influenced by the California or Oceanic current, Davidson current and upwelling. The California current can be as much as 420 miles in breadth and have an average speed of 0.5 knots (Carter and Kazmierczak, 1968). The current flows south during September, October and a portion of November. During the months of November through February, the Davidson current, which is approximately 40 miles wide and has a maximum velocity of 0.44 knots, flows north. The upwelling period extends from March through July. Carter, et.al. claim that the upwelling current flows south in the open ocean and north along the coast. The upwelling current velocities average about 0.5 knots over depth with a maximum speed of 0.6 knots at the surface. The influence of the Monterey Canyon on the oceanic currents is not really known and the currents created inside the bay do not necessarily flow in the same direction as the oceanic current.

1. Grid

The chosen grid size is 19 (ordinate) by 46 (abscissae) with a mesh length of 0.5 nautical miles (Figure 6). The bottom depths were obtained from C & GS Chart No. 5403 (Scale 1:50000) which was updated in June 1970. The grid was selected so that the open boundary coincides with the natural opening of the bay and Monterey Canyon is adequately defined.

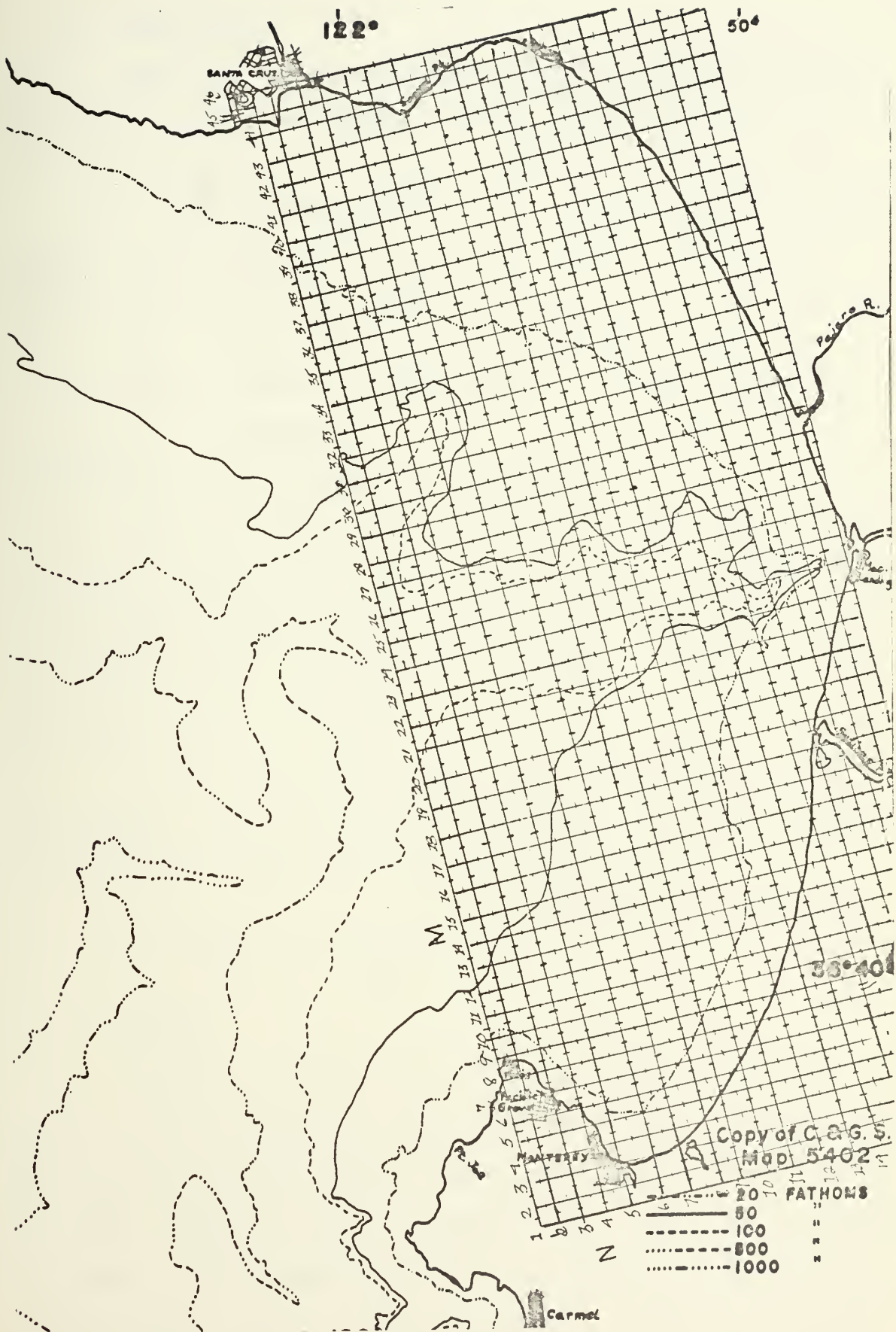


Figure 6. Hansen Grid for Monterey Bay.

2. Time Step

The time step between grid points was determined by using the Courant-Friedrich-Lewy criterion which is

$$\frac{DT}{DL} \leq 1/(2gh_{\max})^{1/2} \quad (23)$$

where, DT = 1/2 time step,

DL = 1/2 mesh length (1500) ft.

h_{\max} = Maximum bottom depth of the grid area (400 fathoms)

In this case the maximum DT is 3 seconds.

If a time step greater than the maximum allowed by the Courant-Friedrich-Lewy criteria is selected, then the results of the model rapidly diverge. The author has experimentally verified this when applying Hansen's model to the South China Sea and the Gulf of Mexico.

It is interesting to note that when equation (23) is rearranged, then the formula is different only by a factor of $\sqrt{2}$ from the deep water wave celerity formula:

$$\frac{DL}{DT} \leq \sqrt{2} \sqrt{gh_{\max}} \quad (24)$$

3. Tides

Since the tides are the primary forcing function across the open boundary, they need to be accurately defined. Ideally the tides should be known at every point on the open boundary; however, this is impractical. The optimum situation for Monterey Bay would have been to measure the tides at three points along the open boundary - at both ends of the

boundary and in the canyon which bisects the open boundary. Unfortunately, the tides were only measured near the open boundary at Monterey Wharf No. 2 (Point A on Figure 3) which is 3.3 miles from the closest open boundary point at the southern end of the grid and the Santa Cruz Municipal Pier (Point B on Figure 3) which 0.3 miles from the closest northern open boundary point. It had been planned to place a submerged tide guage in the Canyon but the necessary equipment could not be assembled before the field survey commenced.

Hourly tidal height records from Monterey and Santa Cruz are shown in figures (A-1) through (A-6) and for Moss Landing in figures (A-7) through (A-10). The Monterey records have been corrected to a datum level. The tide records for the other stations contain the correct phases and relative amplitudes. The relative amplitudes for the three stations are compared to each other in Table A-1. The maximum difference between amplitudes of any two stations is less than 0.75 feet and for most cases there was no difference at all. The Santa Cruz and Moss Landing records compared more favorably with each other than they did with the Monterey Wharf records. The fact that the tides at Santa Cruz and Moss Landing were measured by the same type of instrument while the tides at Monterey were measured by a different type of recorder may explain part of the difference. Since the tidal phases and amplitudes at Santa Cruz and Monterey were very nearly equal and there was no knowledge of the tidal behavior in deep water, only the Santa Cruz data were Fourier analyzed.

The Santa Cruz constituents were used at every open boundary point. An example of the computed tide compared to the actual tide is shown in Figure (7).

Before actual tide data were used as input to the model, a test run was made to determine the length of running time needed for the model to propagate the tidal wave throughout the entire bay. The M_2 (lunar-semi diurnal tide) sine wave recycles every 12 hours, 25 minutes. The Monterey M_2 constituent was used for the test runs. The tide travelled from the mouth of the bay to Moss Landing in less than a half hour. This does not mean that all the perturbations caused by the initial wave placed on the grid have been dampened. In the original Hansen model the wave heights at all the grid points were set equal to zero and then the initial wave was inserted at the open boundary points. It seemed that if the initial tide was at either high or low water, then large transients would be induced as the tide travelled across the grid. Several test runs were made to test if the entire grid should be initialized at the same tidal elevation rather than just at the mouth of the bay. It had been hoped that this would keep the initial shock of the induced wave to a minimum. Unfortunately, this technique caused a separate wave to be generated along the closed boundary. It was decided that for Monterey Bay all computer runs would be made so that the initial tide would be at mean sea level. Then, since the tide moves quite rapidly across the bay, the transients would be kept to a minimum.

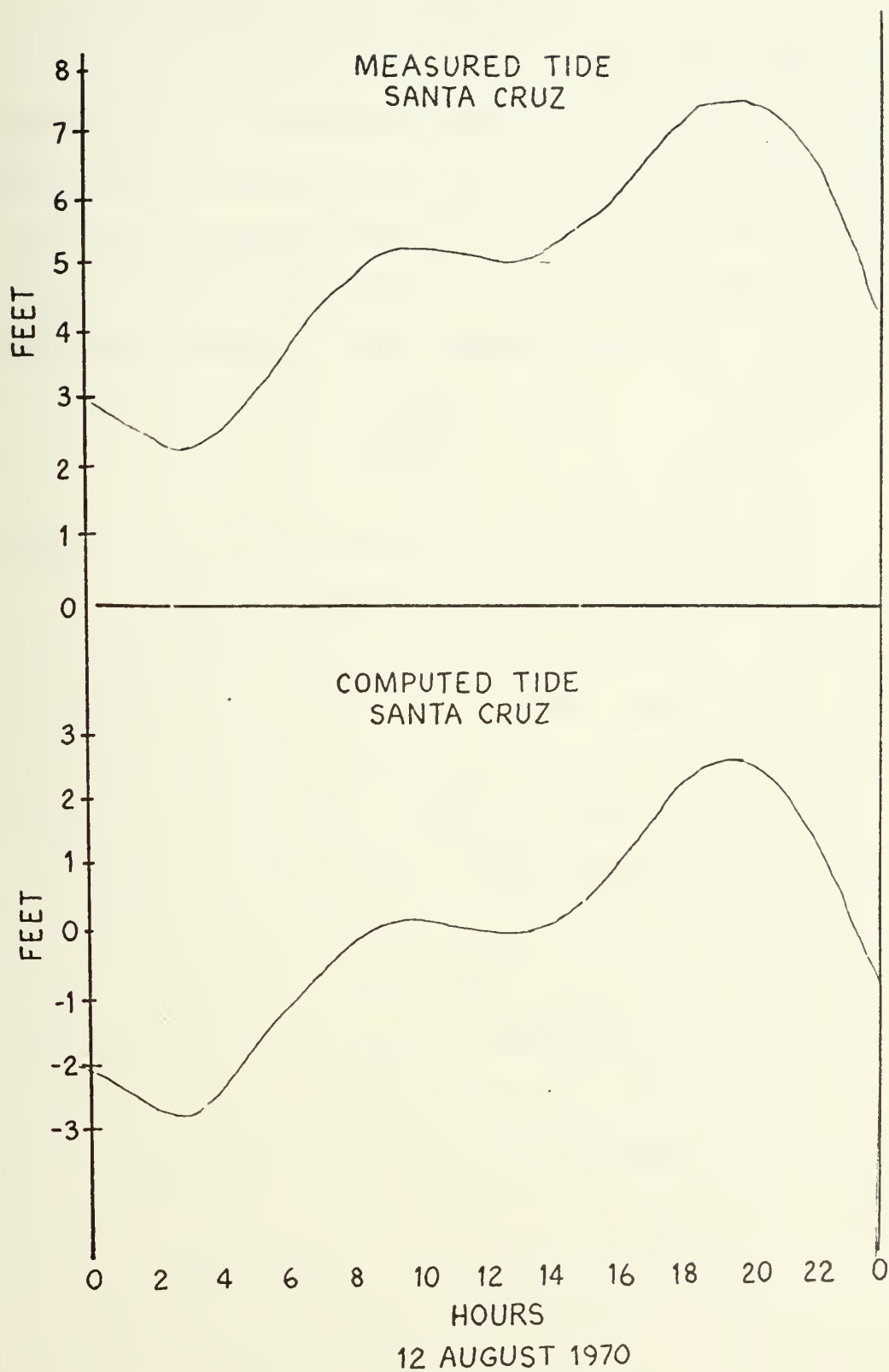


Figure 7. Computed vs. Actual Tide at Santa Cruz.

4. Horizontal Eddy Diffusivity

The parameter alpha (Equations 20-22) which is a function of the horizontal eddy diffusivity coefficient, mesh length and time step has been described as a horizontal viscosity parameter (Laevastu and Stevens) and as a stability factor (Mungalls and Matthews and Hansen, 1966). Ortiz (after Lax and Richtmeyer, 1956) defines alpha as

$$\alpha = 1 - 4 \frac{K_h DT}{DL^2} \quad (25)$$

where, K_h is the horizontal eddy diffusivity term.

Ortiz and Hansen claim that the numerical calculations converge analytically as alpha approaches 1, but are unstable when alpha is equal to one. Alpha equal to one implies the eddy diffusivity coefficient K_h is equal to zero, i.e. no diffusion of momentum. Since the time step and mesh length are arbitrarily selected for each problem, alpha depends primarily on the variability of the horizontal eddy diffusivity term. A general solution does not exist for eddy diffusivity. Empirical solutions must be developed for specific areas of interest. Garcia (1971) claims that the value of horizontal eddy diffusivity for Monterey Bay ranges from 10^7 to 10^8 dynes/cm². The latter produces an alpha of less than 0.5 which is unrealistic. The former value produces an alpha of approximately 0.94 which is far more satisfactory. Test runs were made with alpha equal to 0.95, 0.990 and 0.998 for the M₂ constituent and 0.900, 0.940 and 0.950 for the actual tide. The best results for the tidal heights appeared to be

obtained with alpha equal to 0.950. This corresponds to a value of K_h equal to slightly less than 10^7 dynes/cm². Current speeds were not satisfactory but if alpha was decreased, then the tidal heights were over-dampened.

5. Bottom Stress

As previously mentioned the quadratic expression (Equation 12) used to represent bottom stress has been in existence for sometime; however, there seems to be some discussion as to what value should be assigned to the bottom stress coefficient (r). The bottom stress coefficient is defined as

$$r = g \cdot C^{-2} \quad (26)$$

where C (cm^{1/2}/sec) is the DeChezy coefficient and is a function of bottom roughness and bottom material.

Experience in the coastal waters around the Netherlands (Dronkers, 1964) has shown that a reasonable range for r varied from 2.4×10^{-3} to 2.8×10^{-3} with 2.7×10^{-3} the most common value used. Although Hansen (1966) used the values of 2.8×10^{-3} , 3×10^{-3} and 8.6×10^{-3} for r without comment, it appeared that 2.8×10^{-3} was used when the model depth was equal to or less than 50 meters (25 fathoms). Mungalls, et.al., used 4×10^{-3} for Cook Inlet, Alaska which has numerous mud flats and shoals. Pekeris and Accad (1969) suggested that 2×10^{-3} should be used in shallow water. Test runs were made with r equal to 3.0×10^{-3} , 8.6×10^{-3} and 3.2×10^{-3} for Monterey Bay. It will be shown in the

following section that the errors in the current speeds calculated by the mathematical model appeared to be quite large and the adjusting of the bottom friction coefficient does not seem to change the results significantly. The value of 8.6×10^{-3} seems to be the most satisfactory value to use.

6. Wind Stress

If little is known about bottom stress, less is known about the interaction of the atmosphere and sea water. It is exceedingly difficult to make the micro-measurements needed to accurately determine the wind stress coefficient. The wind stress or drag coefficient (λ) is defined similarly to the bottom stress coefficient. Munk and others used the value of 2.6×10^{-3} (dimensionless) for wind velocities from 12 to 40 knots (Dronkers). The drag coefficient is a function of the elevations at which the velocities were measured. Based on Cardone's investigation (1970), a drag coefficient of 1×10^{-3} was selected for Monterey Bay. The bottom stress term originally included the density of sea water and the wind stress term included the density of air. Thus, when equation (1) was divided by the density of sea water, density was eliminated from the bottom stress term but not from the wind stress term.

III. COMPUTER MODEL RESULTS AND DATA ANALYSIS

A. DATA ANALYSIS

Tides, currents and winds were measured on 12, 13, 18 and 19 August and 6-13 November 1970 for the purpose of evaluating the mathematical model. The tides were measured at the three stations mentioned in the previous section by mechanical gauges. Non-linear time errors can occur on the tide records if the mechanical gauges are not maintained properly. The Monterey and Santa Cruz tide records were timed by chronometers. The August tide records for Moss Landing were not accurately timed and contain errors. Thus, only the tidal amplitudes from the August records of Moss Landing were used for comparison. The tides were mixed (almost diurnal) during the 12-13 August time period, semi-diurnal during the 18-19 August time period and shifted from semi-diurnal to mixed during the 6-13 November 1970 time period.

Wind data obtained from land stations and the USNS De Steiguer are listed in Table A-2. The land stations were located at the shore line. The exact location of the USN De Steiguer at any given time can be determined by noting when the current meters were emplaced and the current drogues were launched. Since Monterey Bay is a small geographical area for large-scale climatological parameters and the wind records from the various stations around the bay appear to be in fairly good agreement, the complete wind records from Moss Landing

(Figure 3) were considered to be representative of the entire grid for each analysis period.

Currents were measured in a Lagrangian sense by current drogues and, during portions of the survey, in an Eulerian sense by current meters. The structure and application of the current drogues are described by Stoddard (1971). Drogues were not placed north of the Monterey Canyon as there were no facilities to track them. The tracks of the current drogues are shown in Figures (A-11) - (A-16) and the hourly speeds and directions are shown in Table 3. The location and depth of the current meters are shown in Figure 3. The relationship between the currents derived from the drogues and some of the current meters, winds and tides are shown in Figures (A-17) - (A-43). Data from other current meters did not appear to be realistic and were not used. The currents are plotted on the tidal curves. The heads of the current and wind vectors are set in the direction in which the parameters are moving.

Tidal currents can either be the reversing type where the currents are zero at the anti-nodes and a maximum at the nodal points or the elliptical type where the current direction passes through all points of the compass and the speed is seldom zero. Reversing currents can be found along the coast or in rivers. Elliptical or rotary currents, as shown in Figure (8), occur in the open ocean or large embayments. The elliptical currents move in a clock-wise direction in the Northern Hemisphere. Maximum speeds usually occur mid-way between turning points and minimum speeds at high and low waters. If surface currents are primarily induced by wind

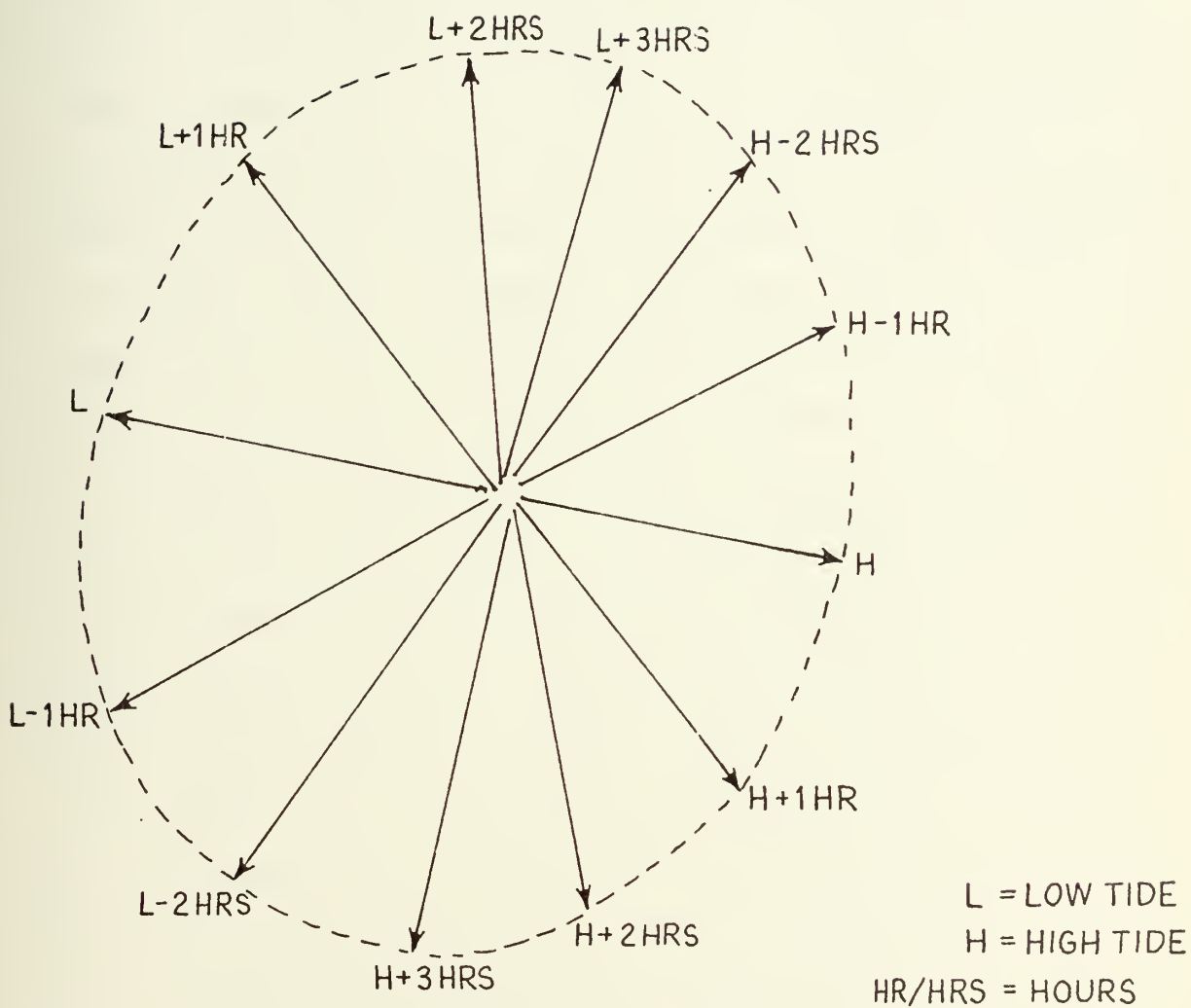


Figure 8. Semidiurnal Rotary Tidal Current

Current meter data (Station 1 in Figure 3), plotted in a Lagrangian format (Format A-44) indicated that the currents at this location, with only slight deviations, flowed in a steady northwesterly direction. Thus, the NPGS data seems to indicate that the oceanic currents had more influence during these surveys on the circulation in Monterey than the tides and winds.

Professor William Broenkow, Moss Landing Laboratories, has measured surface currents in the vicinity of Moss Landing with drift poles (personal communication). The measurements were made during April, May, November and December, 1970. The poles were never tracked for longer than 3 hours and 15 minutes. The maximum current speed occurred during flood tide and was perpendicular to the coast. Currents with speed up to 1.5 knots and moving parallel to the coast were measured north of the canyon. South of the canyon, the speeds never exceeded 0.7 knots. The maximum current speeds occurred either during flood or ebb tide in some cases. In other cases, the maximum speed occurred at high water. There were not enough observations at this point to accurately correlate the currents near Moss Landing with the tides; however, it did appear that the current flowed southwest during ebb tide and northwest during flood tide. In most cases, the poles travelled along equal depth lines

McKay (1970), towed a Geomagnetic Electrokinetograph (GEK) from a moving ship in Monterey Canyon during July and August 1970 to measure the currents. The GEK only performed satisfactorily in areas where the water depth was greater than 75

fathoms. McKay believed that the measured currents which ranged in speeds from 0.05 to 1.35 knots, were dependent on tides. Closer observation of the data indicated that the GEK was probably measuring extremities or eddies of the California or up-welling current. In one case, which McKay stated that the currents were a result of flood tides, the currents flowed in a direction that would not be usually associated with flood tides. The average speed of the current was 0.5 knots. As with the other current measurements, most of the GEK measurements tended to follow the contour lines of the canyon.

Defant (1961) indicates that if a strong current or up-welling exists in the adjacent ocean, standing vortices can occur in coastal bays such as Monterey Bay. The flow of the standing vortex is such that the currents on the seaward side of the bay follows the main current while on the landward side the current is opposite the main current. Theoretically, standing vortices would have the same water mass circulating within it and there would be no water transfer from the main current. In actuality, this is not the case. Variations in the oceanic current or upwelling will perturb the stationary vortex and renew the water circulating in the bay.

Carter and Kazmierczak claims that a permanent closed circulation system which moves in a counter-clockwise direction extends from Ano Nuevo, north of Monterey Bay, to Moss Landing (Figure A-16). The average speed of the system is 0.1 knots. Coastal engineers at Pacific Gas and Electric Company (P.G. & E.) believe that they have accumulated enough field data to confirm this phenomena (personal communication).

Over a three year period P.G. & E. has launched a number of drogues at the 6 fathom line north of Monterey Canyon. The drogues were launched during all three climatic seasons and at different phases of the tidal cycle. The drogues consistently follow the contour line towards the northwest. The maximum speed of the drogues never exceeded 0.5 knots and usually was quite less.

The field data collected by NPGS in the bay during August and November 1970 only implied, but did not absolutely prove, that the oceanic currents and upwelling were the primary forces of the circulation of Monterey Bay. It should be noted that the oceanic currents and upwelling were the primary driving forces of the circulation of Monterey Bay. The NPGS data were collected during the transitory times between the upwelling and California currents and the California and Davidson currents respectively. To properly correlate the currents in the bay with the oceanic circulation, measurements were needed in the adjacent ocean. Twelve hydrocasts were made in the open ocean during 8-9 November and again during 13-14 November 1970. Five current drogues were also launched on 8 November 1970. The results from this data are shown in Figures (A-45) and (A-46). The dynamic height calculations for the first time period indicate that the oceanic current diverged, with speeds ranging from 0.1 to 0.6 knots, as it approached the coast. The drogues which were launched north of the canyon continued to move north fairly rapidly. The second set of dynamic height calculations showed a more complicated current pattern in the ocean. A large eddy was

present southwest of Monterey Bay. The current speeds for this set of data were similar to that of the first set. The oceanic flow may be affected by Monterey Canyon. The current north of the canyon moves north and vice-versa. The observations in the bay seems to substantiate the oceanic data. However, there was very little current data available for the north basin of Monterey Bay and more surveys need to be made in this area. Ideally, simultaneous current measurements should be made in the ocean and the bay on a seasonal basis to really understand the circulation patterns in the bay and the adjacent ocean. It is obvious that measurements in the bay without corresponding measurements in the ocean are really not significant. It should also be noted that the Hansen hydrodynamical model is not designed to handle density currents and their presence will not appear in the computer calculations for the bay.

One point should be made about the tendency of the current measurements to follow lines of constant bathymetry. This implies that potential vorticity is being conserved. Potential vorticity is comprised of several components. The planetary vorticity, or Coriolis parameter (f), is related to the rotation of the earth and varies as the flow of water moves from the poles to the equator and vice-versa. In a small area such as Monterey Bay, planetary vorticity can be considered constant. Relative vorticity (ζ) is a function of the motion of a fluid relative to the earth and can be defined as

$$\zeta = \frac{\partial u_2}{\partial x_1} - \frac{\partial u_1}{\partial x_2} \quad (27)$$

The sum of the relative and planetary vortices is the absolute vorticity. The conservation of vorticity equation (Stommel, 1966) is

$$\frac{d}{dt} \left(\frac{f + \zeta}{D} \right) = 0 \quad (28)$$

where D is the thickness of the fluid.

When equation (28) is integrated, it can be shown that potential vorticity is

$$\frac{f + \zeta}{D} = \text{constant} \quad (29)$$

If flow is along lines of constant bathymetry ($D = \text{constant}$), and f is assumed constant, then absolute vorticity, ζ , is constant.

B. COMPUTER MODEL RESULTS

The computer results were compared with the field data. The parameters compared were water elevation heights and phases and current speeds and directions. The results were plotted in two different formats by an automated plotter. One format shows the current circulation in the entire bay at any given time. Only every third row is plotted in this format and some of the calculated details, especially along the coast, are now shown. The other format shows the currents plotted on the tidal curve for individual grid points. The calculated water heights and phases compared quite favorably with the real tides at Monterey Harbor, Santa Cruz and Moss Landing as can be seen when Figures (A-47) through (A-52) are compared to Figures (A-3), (A-4), (A-7) and (A-8) and Table

A-1. The model indicated that the tidal range was less in the canyon than it was in shallow water as seen in Figures (A-53) and (A-54). Although this could be expected, it would have been more satisfying if there had been actual tide data available in the canyon to indicate if this was correct.

The calculated directions also seemed to be accurate. Some of the calculated circulation patterns in Monterey Bay are shown in Figures (A-55) through (A-63). As anticipated, the model produced two gyres - one in the northern basin and the other in the southern basin - separated by the canyon. The gyres were more predominant during the ebb and flood periods. The northern gyre rotated in a counter-clockwise direction (Figure A-61) and the southern gyre rotated in a clockwise direction (Figure A-60) on the flood tide and vice versa on the ebb tide. The maximum currents occurred at high water (Figure A-62) and low water (Figure A-59). At high water the currents diverged from the canyon into the basins and at low water the currents converged towards the canyon. The currents in the canyon are shown to be reversing currents. Although not shown in the figures, the model also depicted the currents along the coast-line as reversing currents.

With few exceptions, the calculated circulation pattern is dissimilar to the circulation pattern depicted by the field measurements. This is another indication that the tidal current is dominated by the oceanic currents.

The calculated current speeds appear to be an order of magnitude too large. Except for near Moss Landing, the maximum current speeds measured in the bay was 0.7 knots and the

average speed was 0.3 knots. Since it has been concluded that the oceanic currents have more influence in Monterey Bay than the tides and winds, then it would be expected that the tidal currents would be in the order of 0.1 knots or less. There are two other reasons to expect that tidal currents would be low. First, the fact that the tidal phases are nearly equal throughout the bay implies that the horizontal current speeds would be low. Second, the magnitude of the current is a function of the water mass displaced horizontally during the rise and fall of the tides and the cross-sectional area through which it moves, (Simmons, 1966). Mathematically, this can be represented by

$$(\bar{u}_e) (\bar{h}_e) (\ell_e) = A_b (\bar{\eta}_b/T) \quad (30)$$

where, \bar{u}_e is the average velocity at the entrance of the bay,
 \bar{h}_e is the average depth across the entrance of
 Monterey Bay (approximately 612 feet),
 ℓ_e is the length of the entrance of Monterey Bay
 (19.5 miles),
 A_b is the area of Monterey Bay (approximately 175.5
 square miles)
 $(\bar{\eta}_b/T)$ is the average increase in water elevation in the
 bay during the time period T

As an example, on 7 November 1970 there was an increase of two feet in water elevation from low to high water in 5 hours and 30 minutes. Then \bar{u}_e is approximately 0.05 knots. For the same time period, the model calculated an average

speed 0.1 knots for the south end of the opening; 0.2 knots for the canyon; and close to 1.0 knots at the north end of the opening. Thus, it appears that the model does not correctly calculate the current speeds in Monterey Bay.

The model computer program was checked thoroughly for errors. The continuity equation (Equation 11) and the conservation of momentum equations (Equations 12 and 13) were checked by hand calculations. Decreasing the viscosity parameter (α) and increases the stress coefficient (r) dampens the current velocities; however, if either term is varied too greatly, then the water elevations are over-dampened. This occurred in the test cases when α and r were set equal to 0.90 and 3.2×10^{-2} respectively. These two parameters are useful only when the computer results need a fine adjustment.

During most of the test runs, the computer program was only run out to 24 hours. It was thought possibly that even though all the tidal heights on the grid reached their correct height in a short time, the transients created by the initial waves moving across the grid would need more time to be completely damped. One case, commencing 1900 PST, 6 November 1970, was run out to 64 hours. The length of the computer run did not improve the calculations, which implies equilibrium conditions are obtained after about one hour.

Several test runs were made so that the computer calculations at every time step between 0 and 120 seconds and 7200 to 7320 seconds could be observed. It became apparent that the velocities increased greatly as the waves moved from the

deep canyon areas to the much more shallow basins. Some irregularities in the currents occurred along the very shallow (less than 5 fathoms) coastal boundaries. It was decided to smooth the bottom by the following technique:

$$h_{(N,M)} = 0.5 h_{(N,M)} + 0.125 (h_{(N+1,M)} + h_{(N-1,M)} + h_{(N,M+1)} + h_{(N,M-1)}) \quad (31)$$

There was approximately a ten percent improvement in the current speeds, particularly about the canyon, when the bathymetry was smoothed once and approximately 15 percent improvement when the bathymetry was smoothed twice using equation (31). It would appear that the model, employing the grid spacing used here, has difficulty coping with the great variance in depth over as small an area as Monterey Bay. The large lateral and transverse slopes of the canyon (Figure 4 and Figure 5) are significant bathymetric problems. It is believed that if a finer grid was used, the accuracy of the calculated current velocities would be improved. This point was proved in reverse when the grid was changed to 12 x 25 with a mesh length of one nautical mile, the currents became larger.

Assuming that the present grid is inadequate for Monterey Bay, some mention about the computer requirements for this model need to be made. Remembering that the grid size is 19 x 46 and the time step is 6 seconds, the Control Data Computer (CDC) 6500 computer at FNWC utilizes 53000 computer words, requiring 3.25 hours to compute a real time interval

of 24 hours. If a finer grid and, thus, a smaller time step was used, the computer core storage and running time would be greatly increased and the model would be impractical to use.

At the suggestion of Dr. Tiavo Laevastu, FNWC research oceanographer, the bathymetry of all grid points which were less than 10 fathoms, were increased to 10 fathoms. This suggestion seemed to be appropriate since the current speeds would then become less along the coast and possibly the lower speeds would be diffused into the rest of the bay. A test run was made for 24 hours. The calculated current speeds did improve at the head of the canyon and other areas where there was a large slope in the bathymetry, but in the flat basins the currents speeds became larger.

A more serious problem than the large variation in the Monterey Bay bathymetry is the inability of the model to correctly calculate the currents along the open boundary of the grid. Equation (30) and analysed field data indicate that for Monterey Bay the average tidal currents across the open boundary should be less than 0.1 knots. The current speeds calculated by the model were an order of magnitude larger. The difference between the calculated and actual current speeds seem to remain fairly constant throughout the bay. The inability to calculate the proper currents along the open boundary may be an inherent trait of the Hansen model. This author has found that the model produced unusually large currents at the entrances of the Gulf of Mexico and the South China Sea. Maury Pelto, National Marine

of 24 hours. If a finer grid and, thus, a smaller time step was used, the computer core storage and running time would be greatly increased and the model would be impractical to use.

At the suggestion of Dr. Tiavo Laevastu, FNWC research oceanographer, the bathymetry of all grid points which were less than 10 fathoms, were increased to 10 fathoms. This suggestion seemed to be appropriate since the current speeds would then become less along the coast and possibly the lower speeds would be diffused into the rest of the bay. A test run was made for 24 hours. The calculated current speeds did improve at the head of the canyon and other areas where there was a large slope in the bathymetry, but in the flat basins the currents speeds became larger.

A more serious problem than the large variation in the Monterey Bay bathymetry is the inability of the model to correctly calculate the currents along the open boundary of the grid. Equation (30) and analysed field data indicate that for Monterey Bay the average tidal currents across the open boundary should be less than 0.1 knots. The current speeds calculated by the model were an order of magnitude larger. The difference between the calculated and actual current speeds seem to remain fairly constant throughout the bay. The inability to calculate the proper currents along the open boundary may be an inherent trait of the Hansen model. This author has found that the model produced unusually large currents at the entrances of the Gulf of Mexico and the South China Sea. Maury Pelto, National Marine

Fisheries Service, has observed the same phenomena when using the model for Bristol Bay, Alaska. The large currents at the open boundaries of these three models did not seem to be transmitted across the grid. However these areas were much larger than Monterey Bay and the mesh lengths were of the same order of magnitude as the entire Monterey grid. It may be that for larger geographical areas, the frictional terms in Equation (7) may dampen out the higher speeds as the tides move across the grid.

There may be an additional problem with the Monterey Bay open boundary. The assumption that the tidal ranges and phases were equal for all the grid points along the open boundary may be part of the reason that the current speeds were too large. As mentioned previously, since the Monterey and Santa Cruz tide records were in good agreement, the Santa Cruz tides were used along the open boundary. In most embayments, this would have posed no problems; however, since the canyon crosses the entrance of Monterey Bay, the tidal range in the canyon could be different than the range at the more shallow end points. If the tidal range was less in the canyon area, then the current speeds would have been smaller as the wave moved into the basins. It then becomes quite apparent that the tides and currents along the open boundary have to be more accurately defined.

Since the calculated current velocities did not appear to be correct, it did not seem apropos to run the model with wind fields. Only one twenty-four hour run was made with a

wind field included. The run began 1200 PST, 12 August 1970. The wind field had a velocity of 10 knots and a direction of 225°. Although it is difficult to make a general statement about the influence of a wind field on Monterey Bay based on one computer run, in this case the tidal range seemed to be increased by approximately one foot and the current speeds by 0.1 to 0.2 knots. It should be remembered that the actual tides and not the predicted tides are inserted at the open boundary and the wind effects are already included. By adding a wind field, the additional increases in water elevation and current speed result in slight over predictions.

IV. CONCLUSION

As the field data analysis and the computer test runs progressed, it became quite obvious that the assumption that Monterey Bay would be an excellent site to evaluate the Hansen numerical model was invalid. First, field data collected by NPGS and other groups indicated that the principal driving force of the circulation in Monterey Bay was the adjacent oceanic current rather than the tides. At least one standing vortex appears to exist in Monterey Bay. Except for the Moss Landing area, maximum current speeds in the southern basin was 0.70 knots. Currents at the head of Monterey Canyon are undoubtedly influenced by the tides where the currents reached measured speeds of 1.5 to 2.2 knots. The canyon may also influence the oceanic flow but there was not enough data to really confirm this hypothesis. Comprehensive field surveys need to be made on a seasonal basis in the bay and adjacent ocean to fully understand the circulation patterns of the area.

If the density currents are the predominant currents in Monterey Bay, then the tidal-induced currents would be less than the density currents and, except for the shallow coastline, should be on the order of 0.1 knots. The computed velocities were as much as an order of magnitude too high. It is speculated that the steep slopes of the canyon and conditions imposed at the open boundary are the principle

cause of the large errors in the current speeds. A finer grid system may solve the problem but would not be practical on present-day computers. Smoothing the bathymetry and adjusting the horizontal eddy viscosity parameter and the bottom stress coefficient did not improve the current prediction results appreciably. Increasing the shallow water depths to a minimum of ten fathoms did improve the results. The calculations of water elevation and phase and current direction which indicates that separate gyres exist in the northern and southern basins appears to be correct.

This thesis points out the important fact that when the Hansen model or any other numerical model is applied to specific areas of interest, the calculations should be correlated with actual field data. Parameters such as the horizontal eddy diffusivity term and bottom stress coefficient can be considered empirical in nature and vary from location to location. It is very important to properly define the tide and current input along the open boundary. If, as in Monterey Bay, there is a large variance in the depths across the open boundary, then the tides should be accurately measured at all locations. Depending on the size and complexity of the area of interest, at least one and preferably several tide gauges should be used along the closed boundary. In the case of Monterey Bay, there was a noticeable lack of field data for the north basin. Thus, it was difficult to make definite conclusions about the circulation in this area.

Finally, this report demonstrated the need to understand all the forces that govern the circulation in embayments. In

cases similar to Monterey Bay, where either permanent or seasonal oceanic currents exists, one must look at the embayment as part of a larger system. Ideally, computer models should include all the factors governing the circulation in an embayment but the amount of computer time required for these more sophisticated models makes this suggestion impractical on present-day computers. Thus, in applying any model to an area, there should be some prior knowledge as to which model would be more significant for the area.

APPENDIX A

Monterey Bay Tide, Current and Wind Data
for 12-13, 18-19 August and 6-13 November 1970

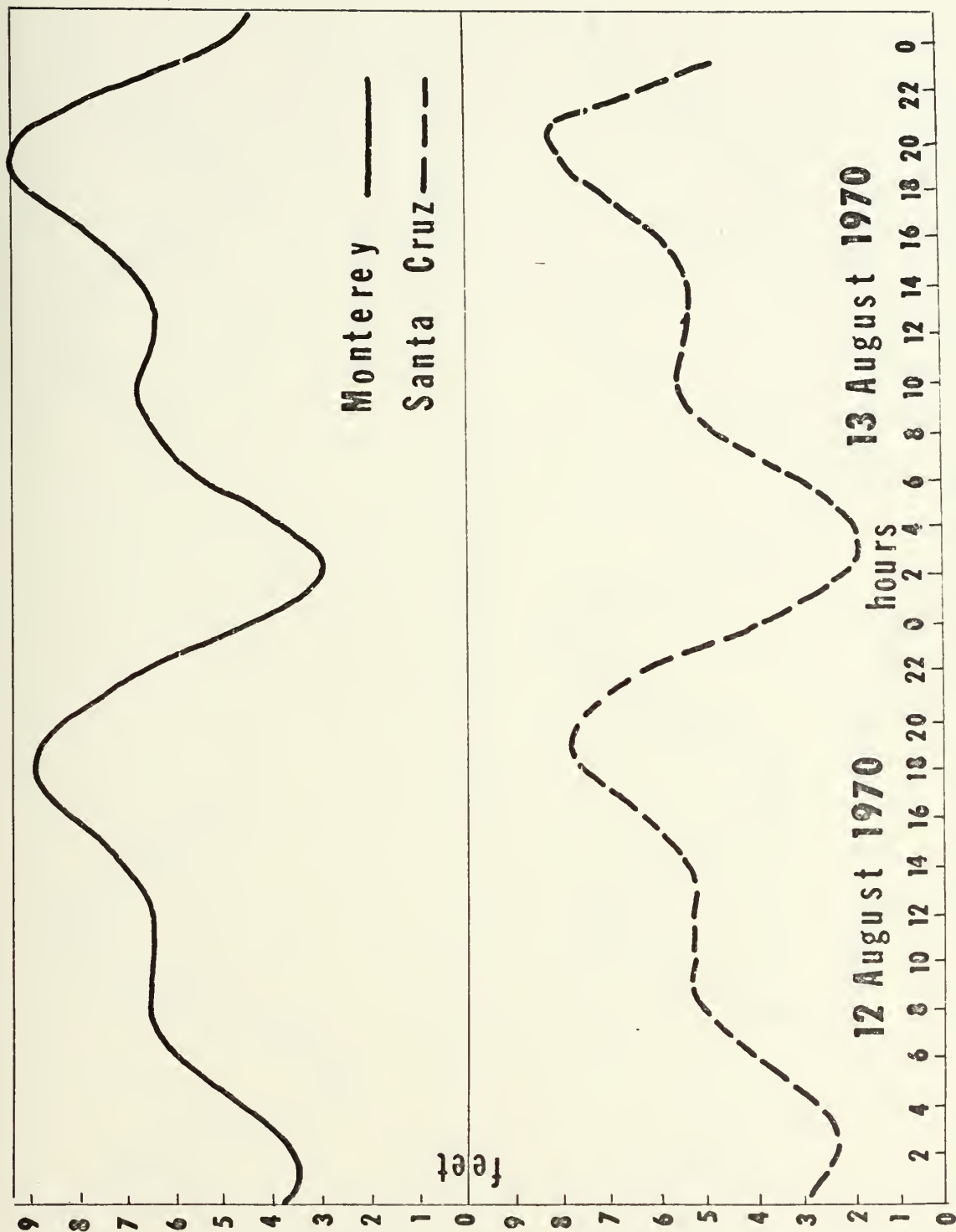


Figure A-1. ACTUAL TIDES FOR MONTEREY AND SANTA CRUZ.

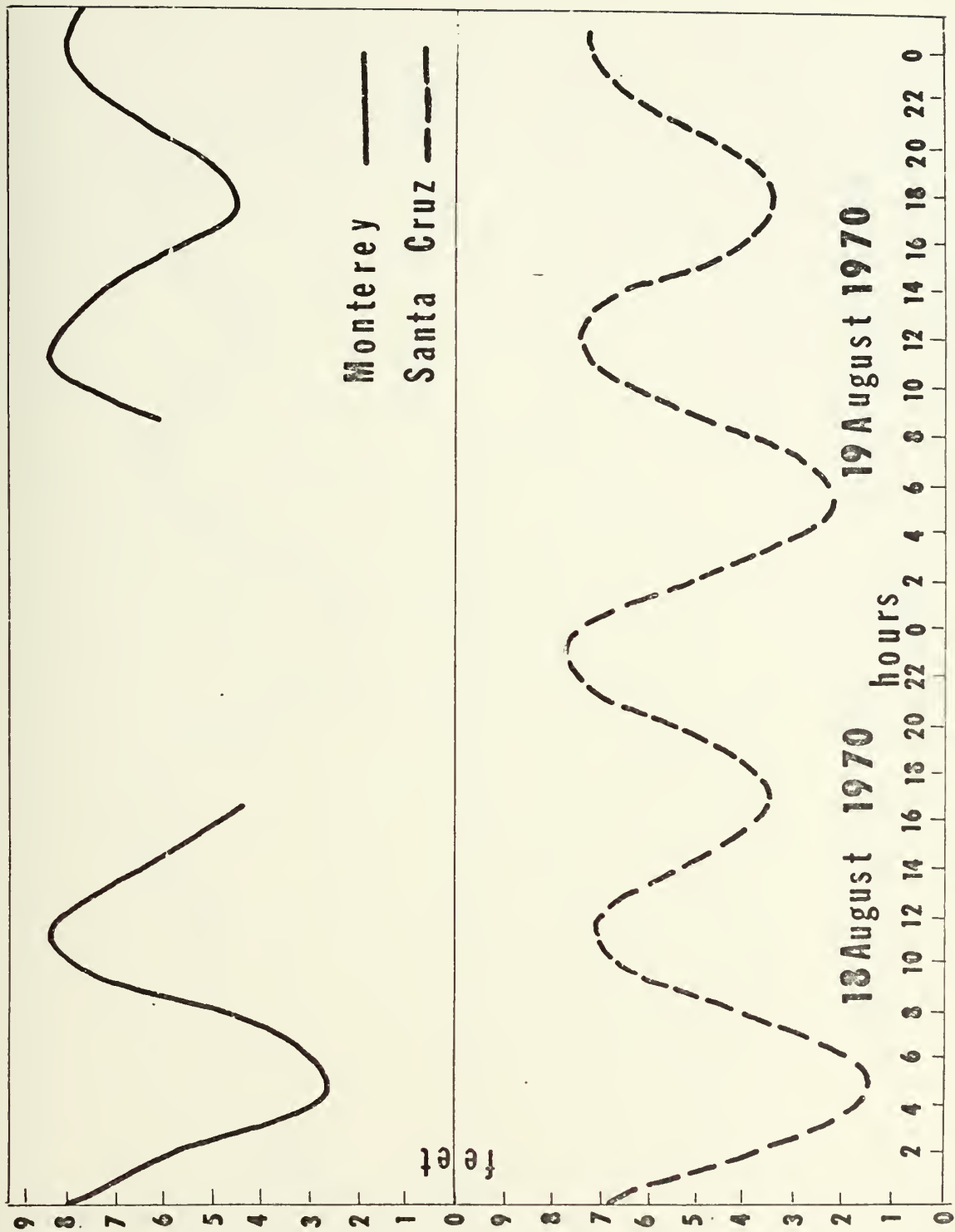


Figure A-2. ACTUAL TIDE AT MONTEREY AND SANTA CRUZ.

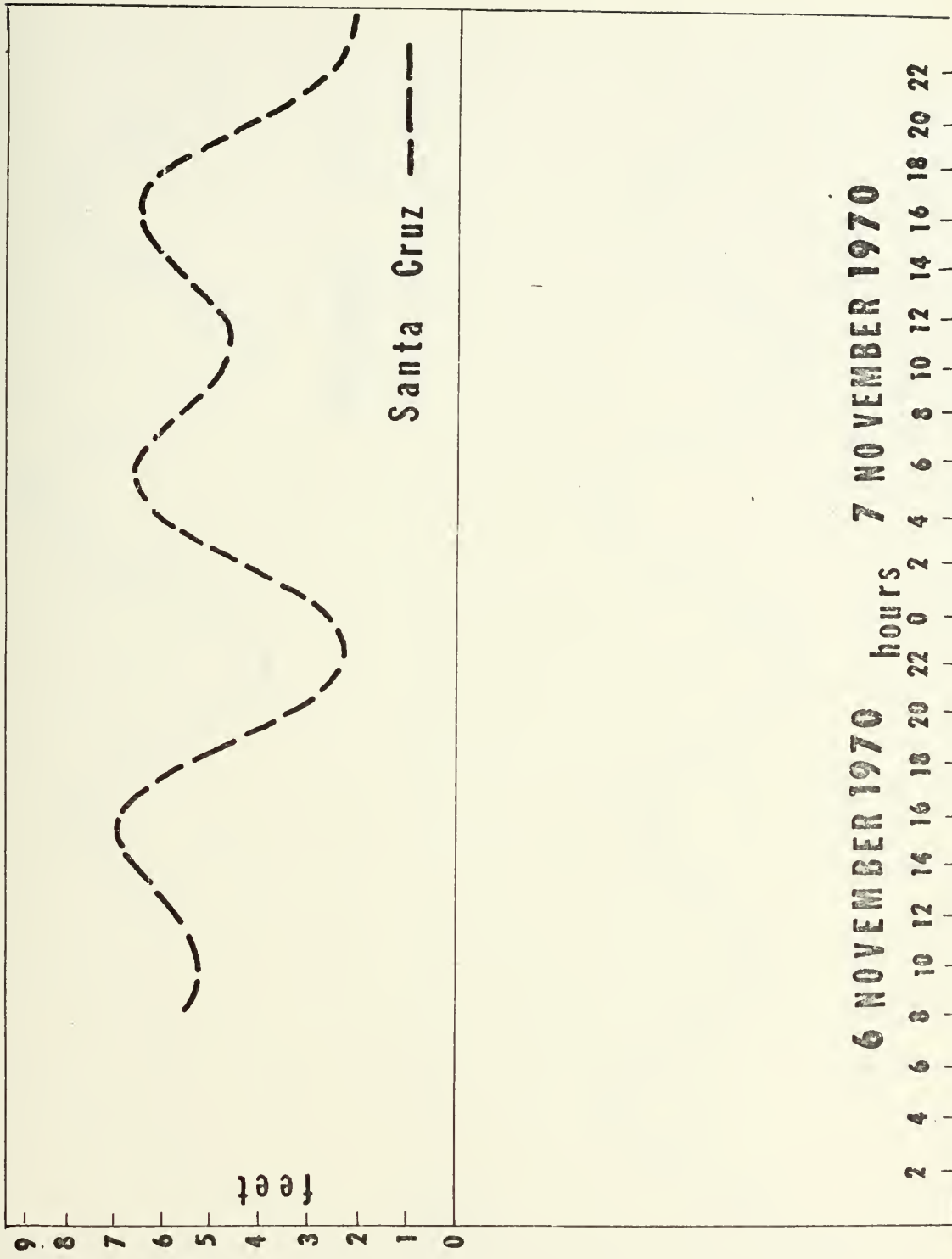


Figure A-3. ACTUAL TIDES AT MONTEREY AND SANTA CRUZ.

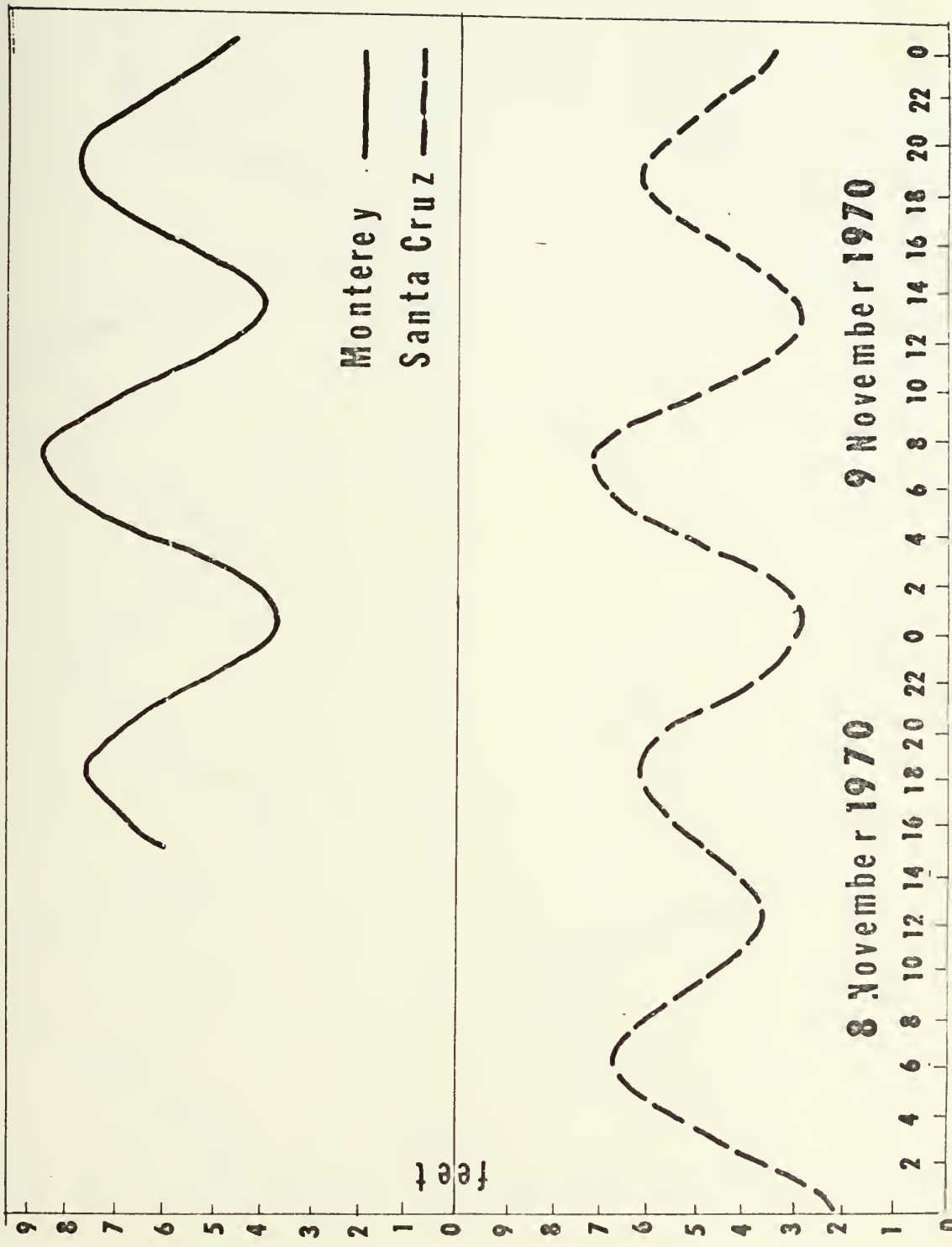


Figure A-4 ACTUAL TIDES AT MONTEREY AND SANTA CRUZ.

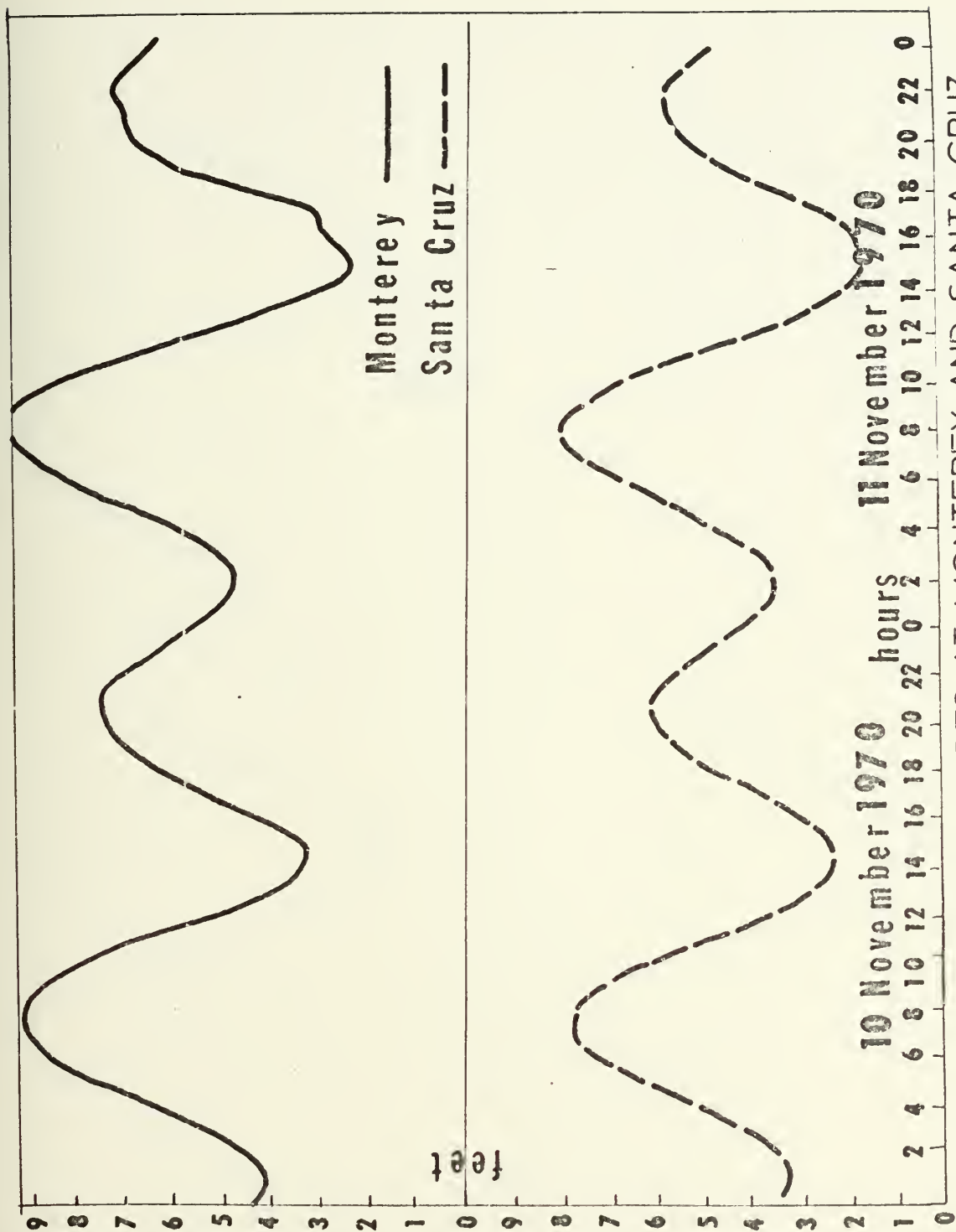


Figure A-5 ACTUAL TIDES AT MONTEREY AND SANTA CRUZ.

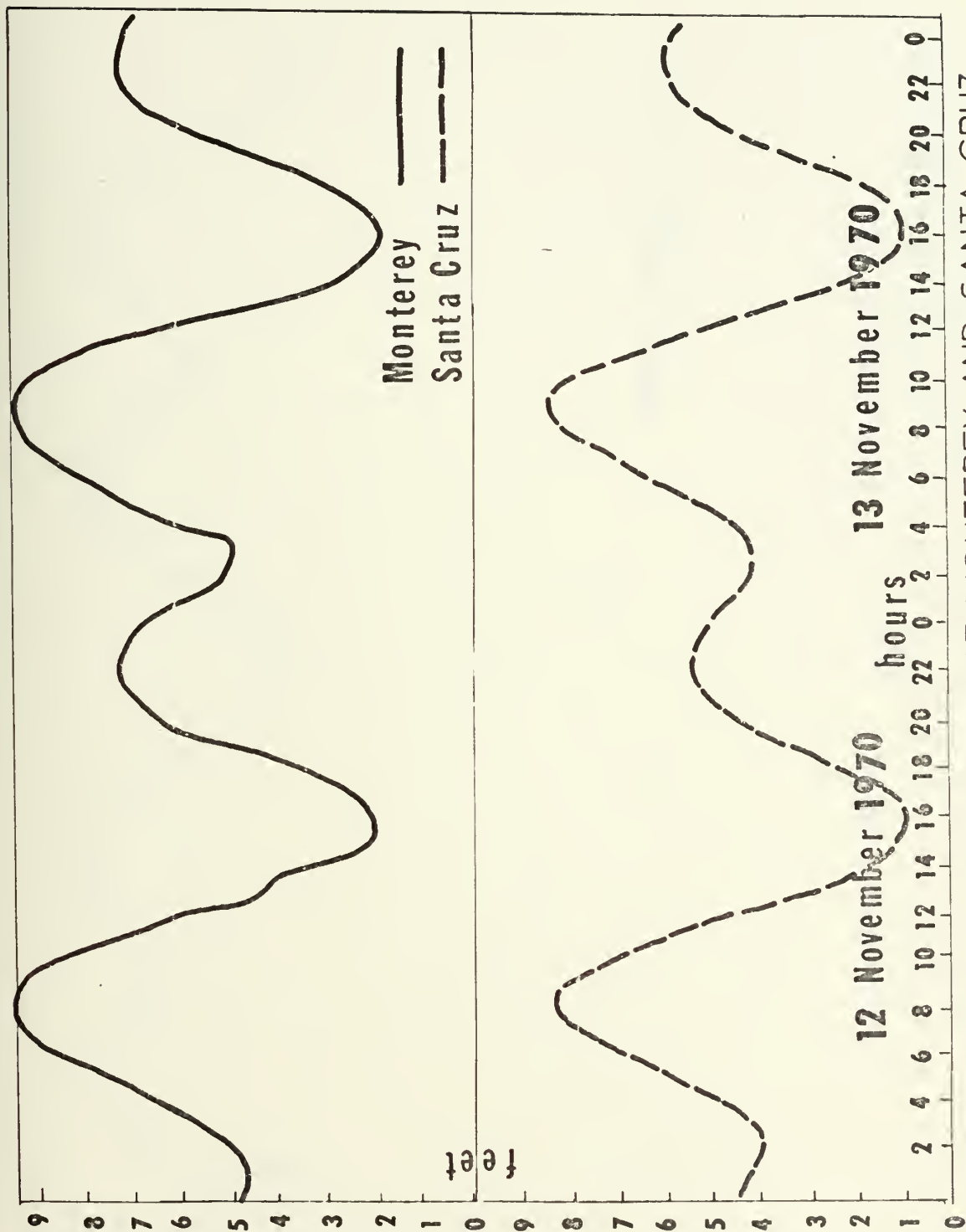
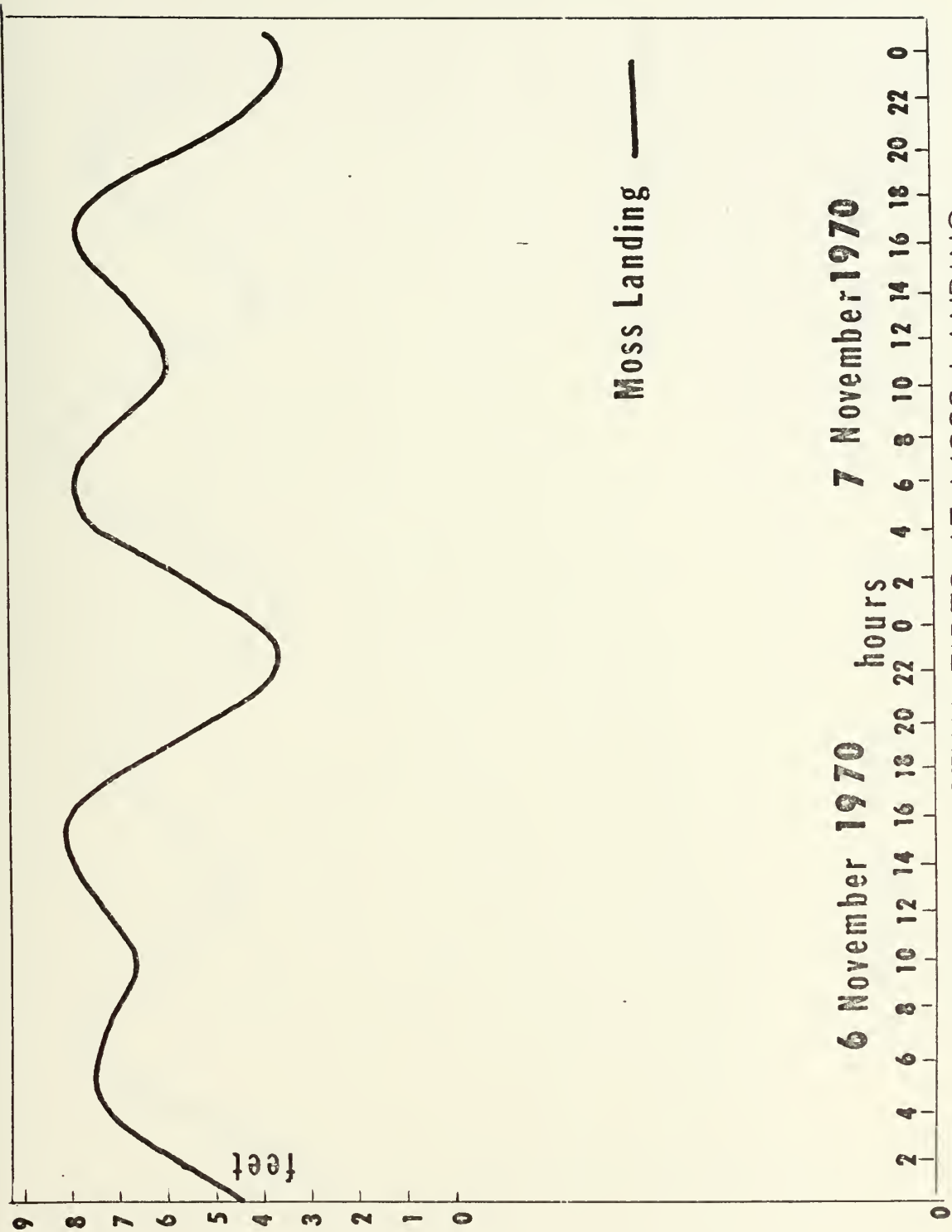


Figure A-6 ACTUAL TIDES AT MONTEREY AND SANTA CRUZ.



Moss Landing —

Figure A-7. ACTUAL TIDES AT MOSS LANDING.

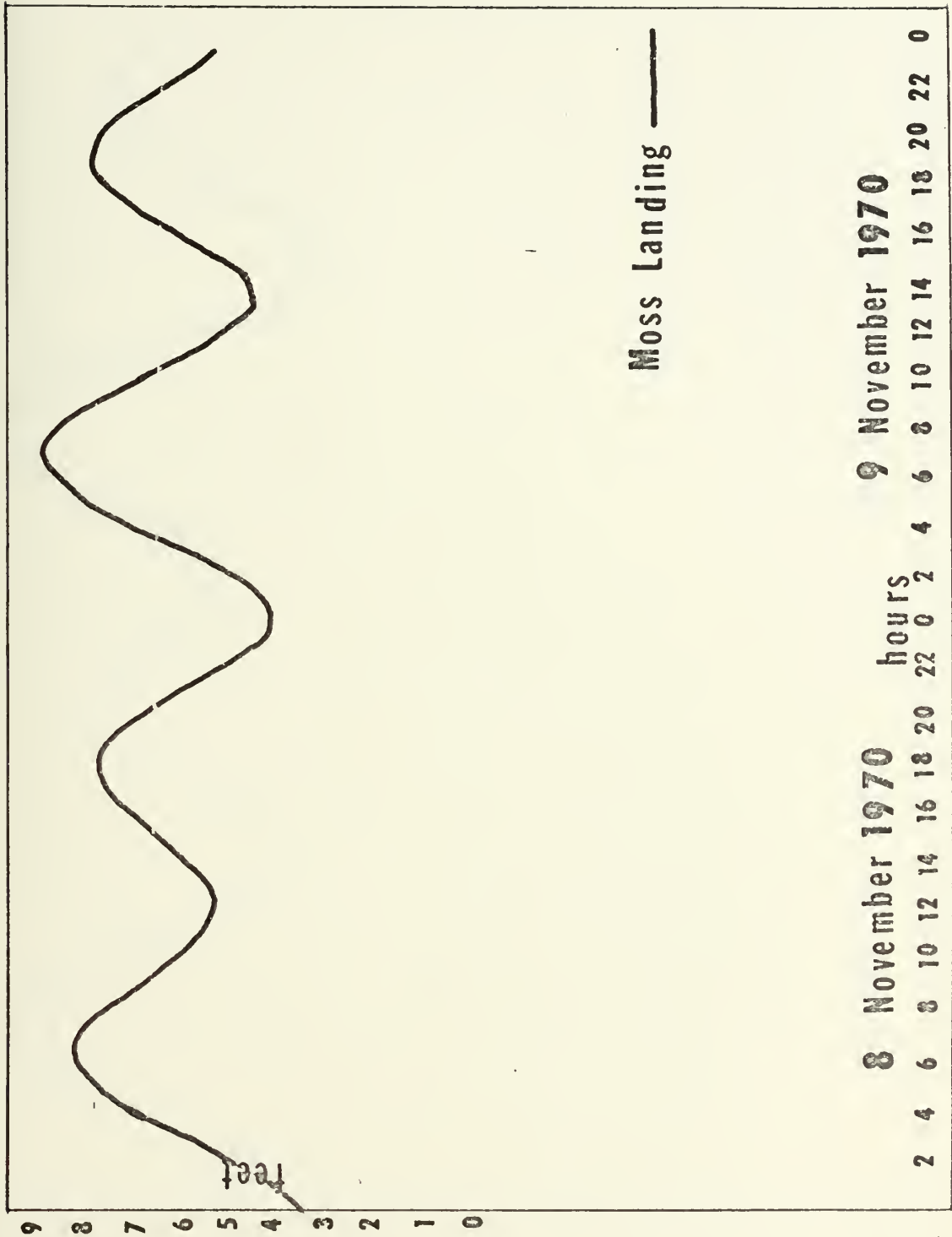
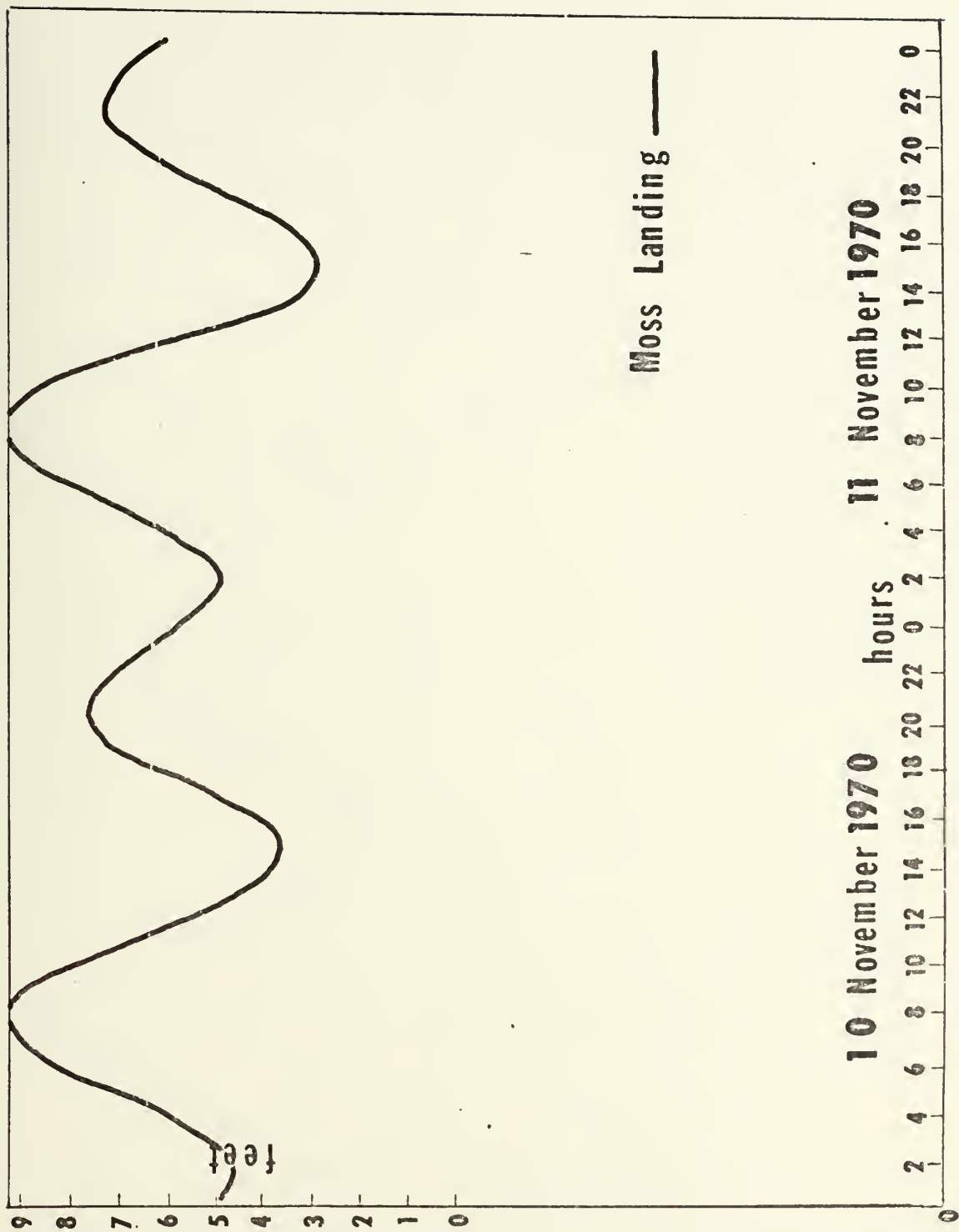


Figure A-8. ACTUAL TIDES AT MOSS LANDING.



Moss Landing —

10 November 1970 hours 11 November 1970

Figure A-9. ACTUAL TIDES AT MOSS LANDING.

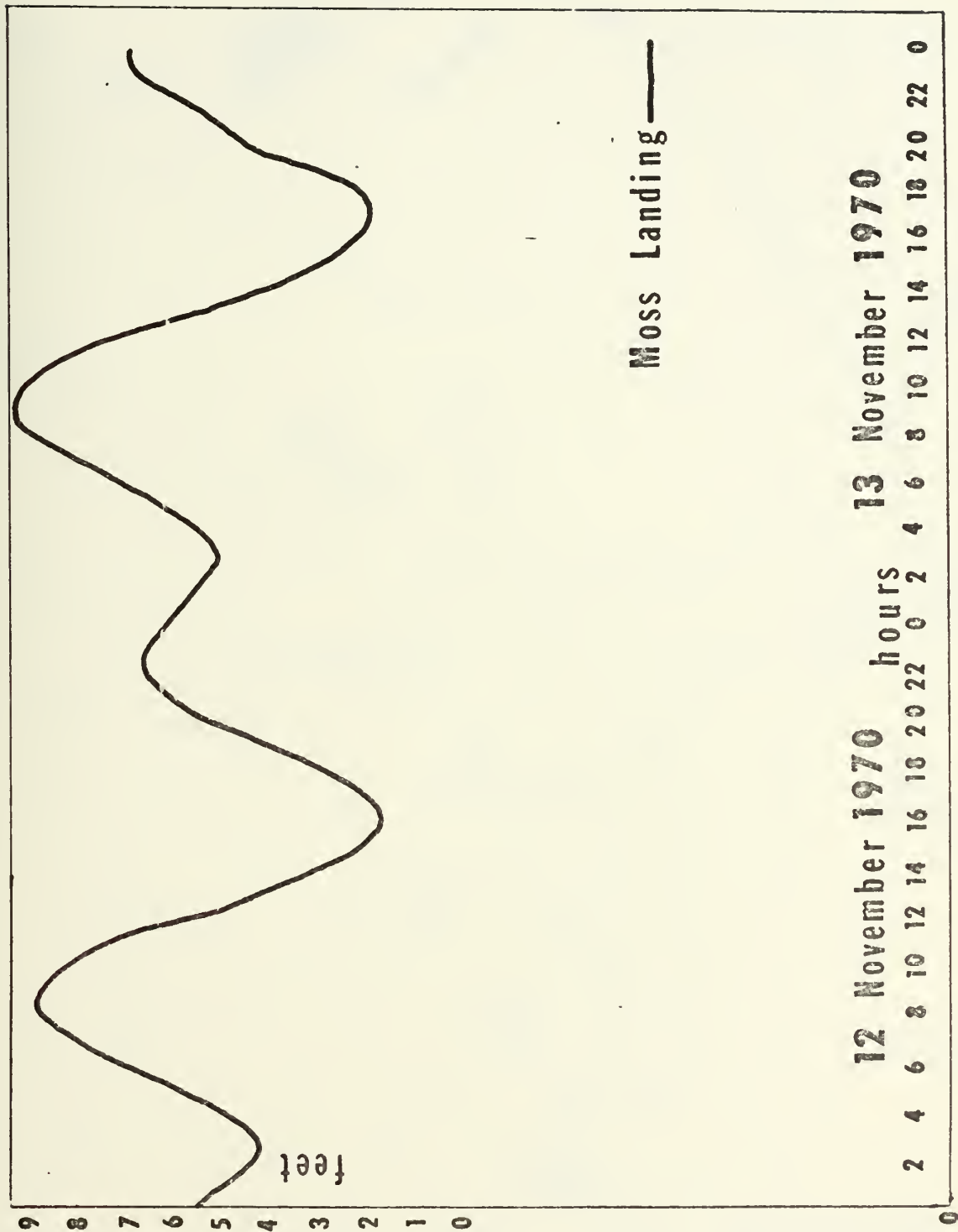


Figure A-10. ACTUAL TIDES AT MOSS LANDING.

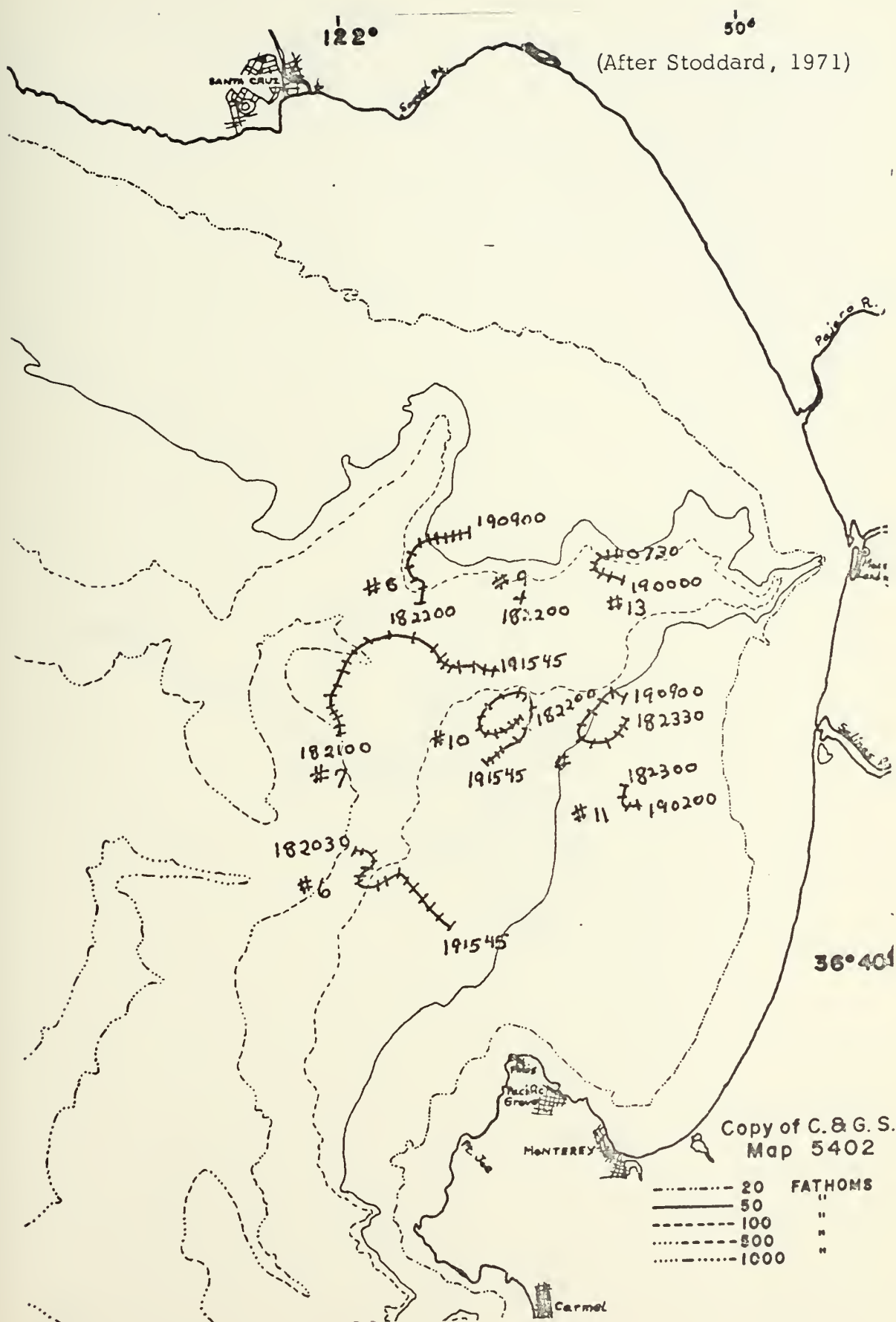


Figure A-12. Tracks of Drogues 6-13.

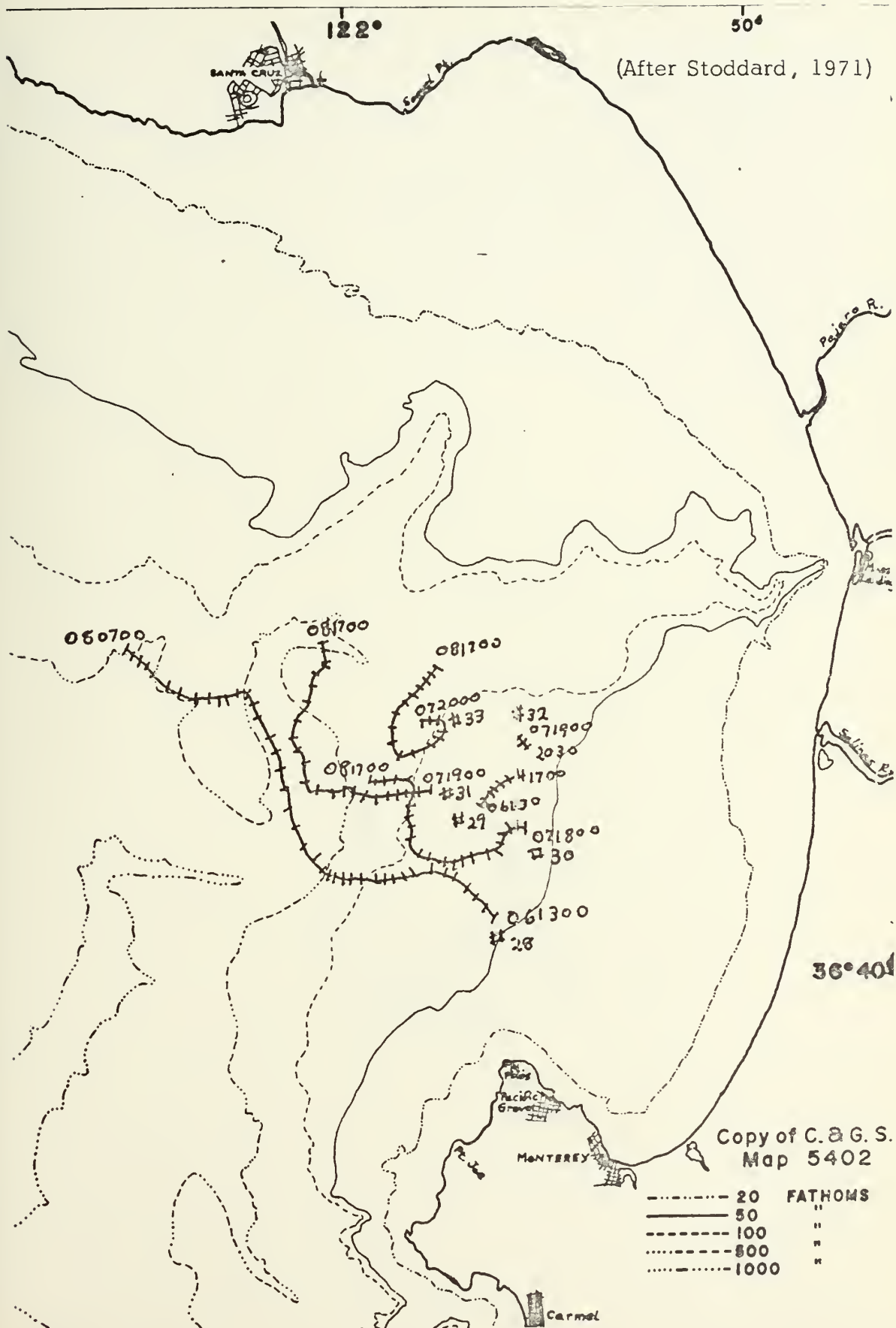
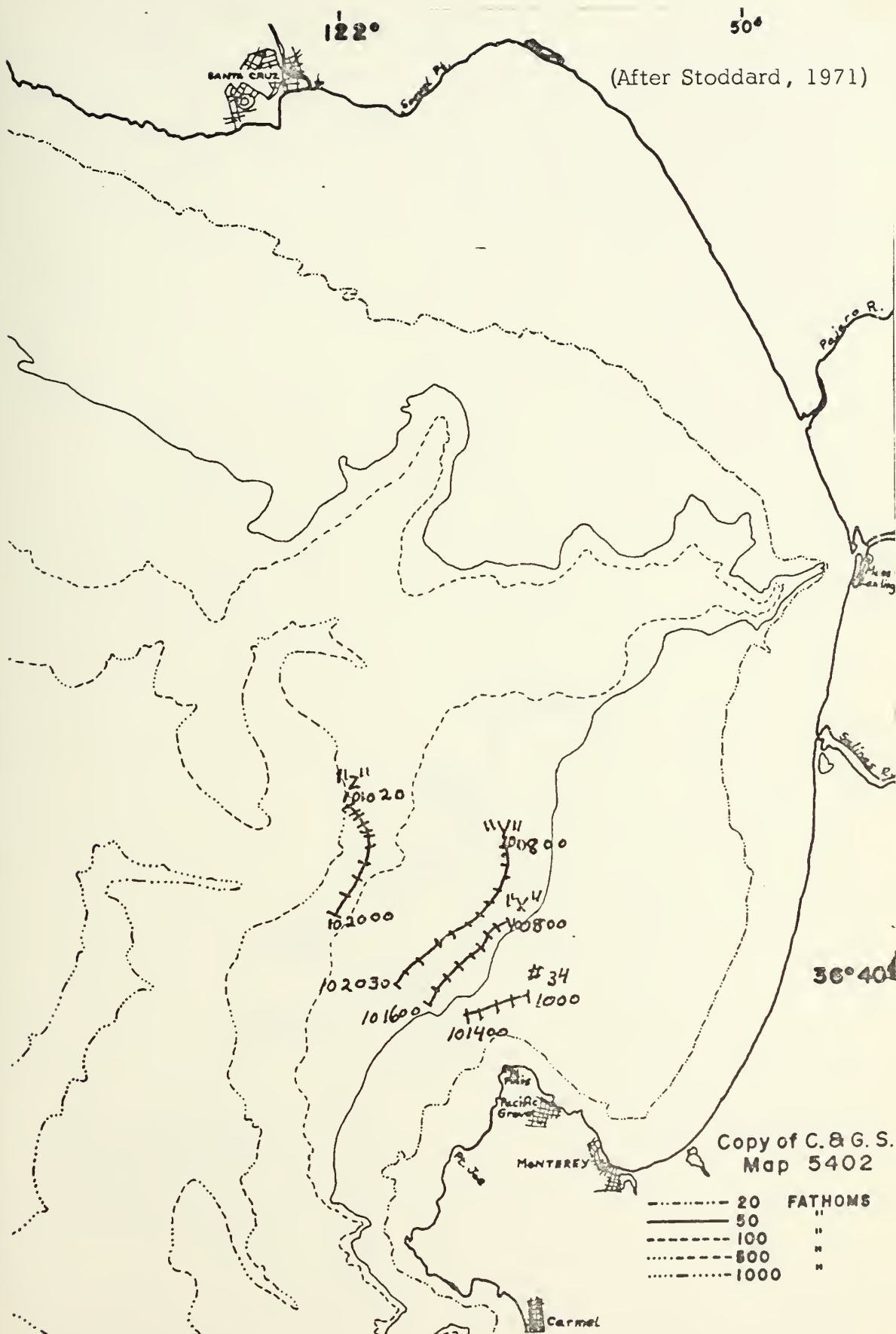


Figure A-13. Tracks of Drogues 28-32.



(After Stoddard, 1971)

Figure A-14. Tracks of Drogues 34- Z.

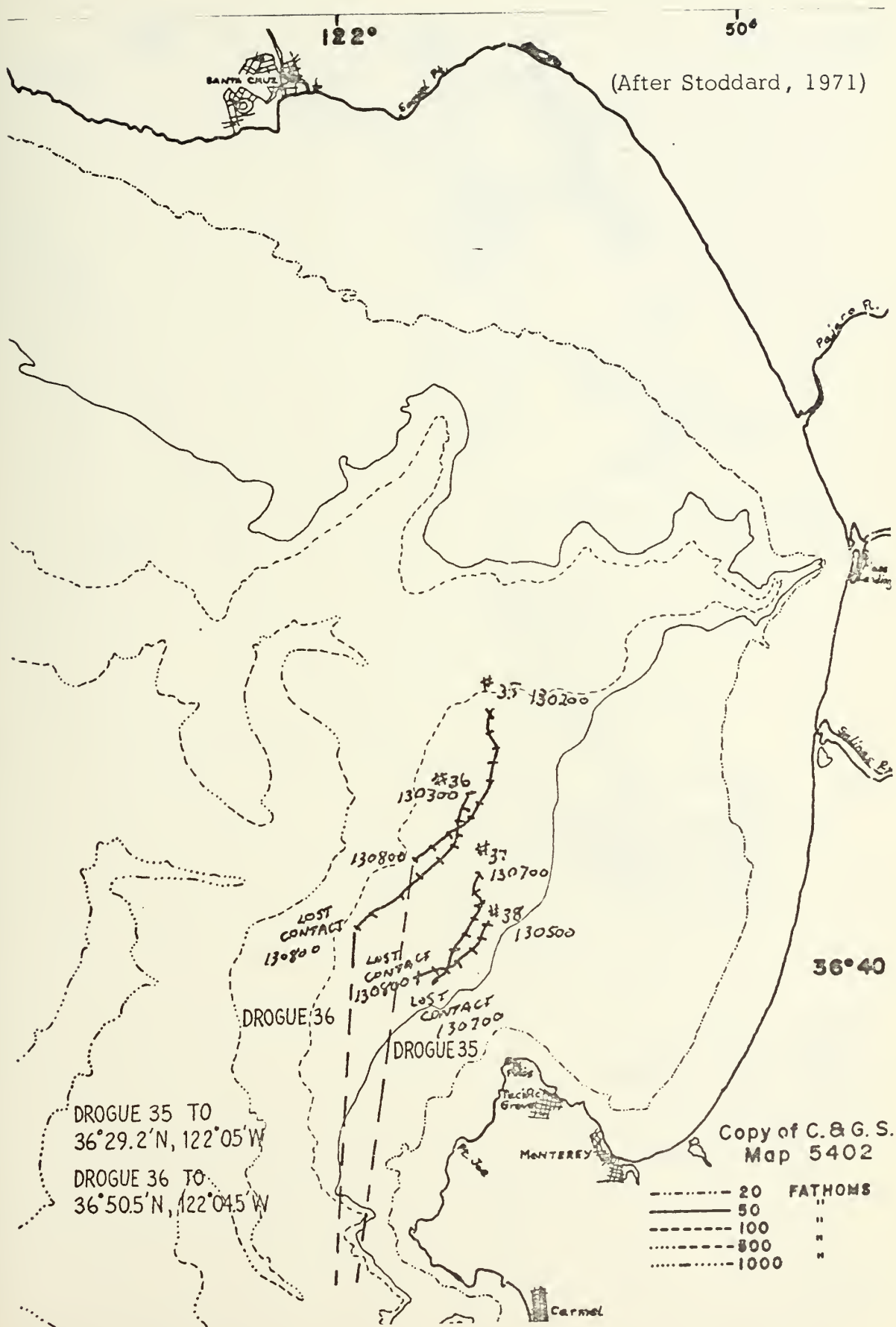


Figure A-15. Tracks of Drogues 35-38.

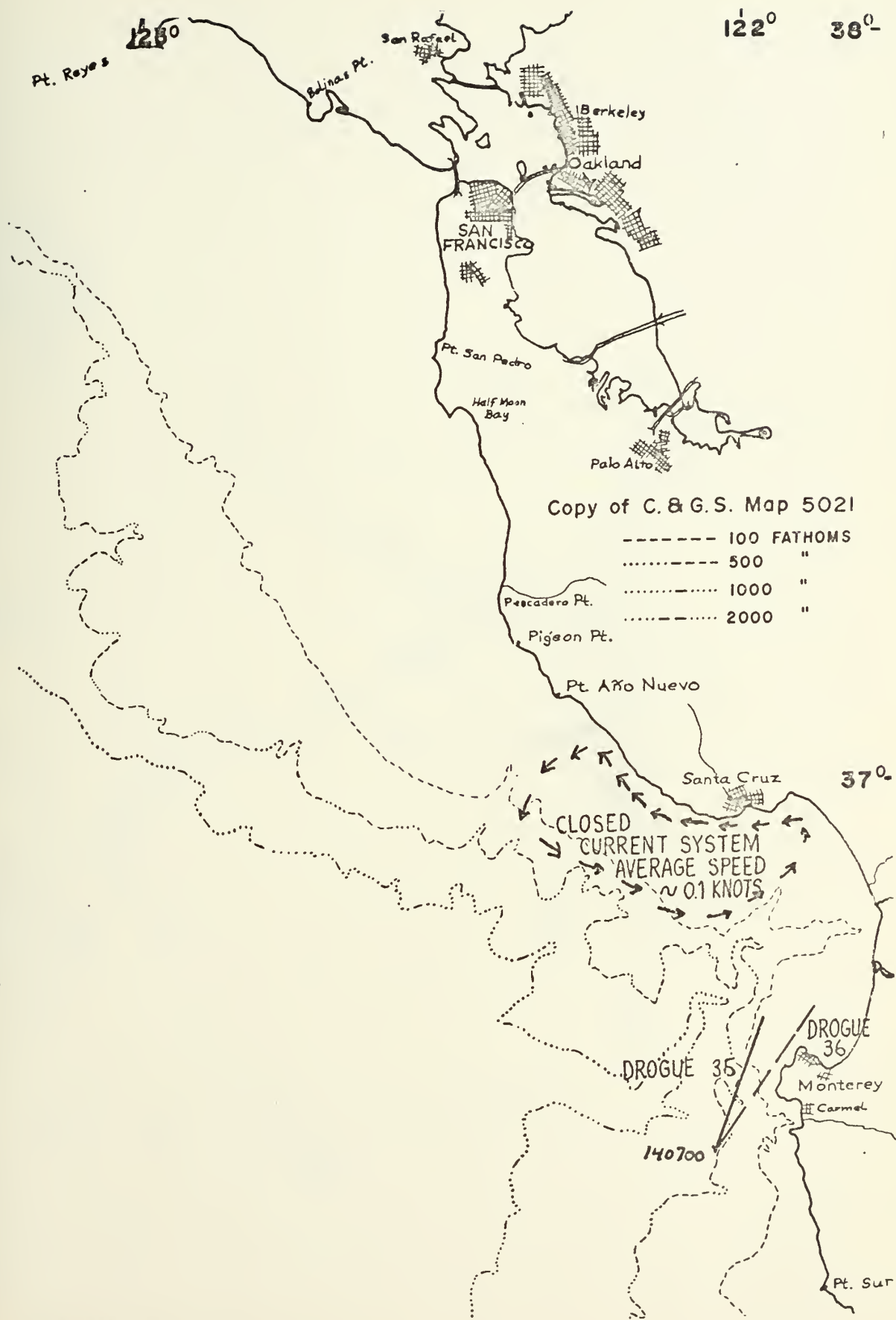


Figure A-16. Tracks of Drogues 35-36 continued and closed current system between Pt. Año Nuevo and Santa Cruz.

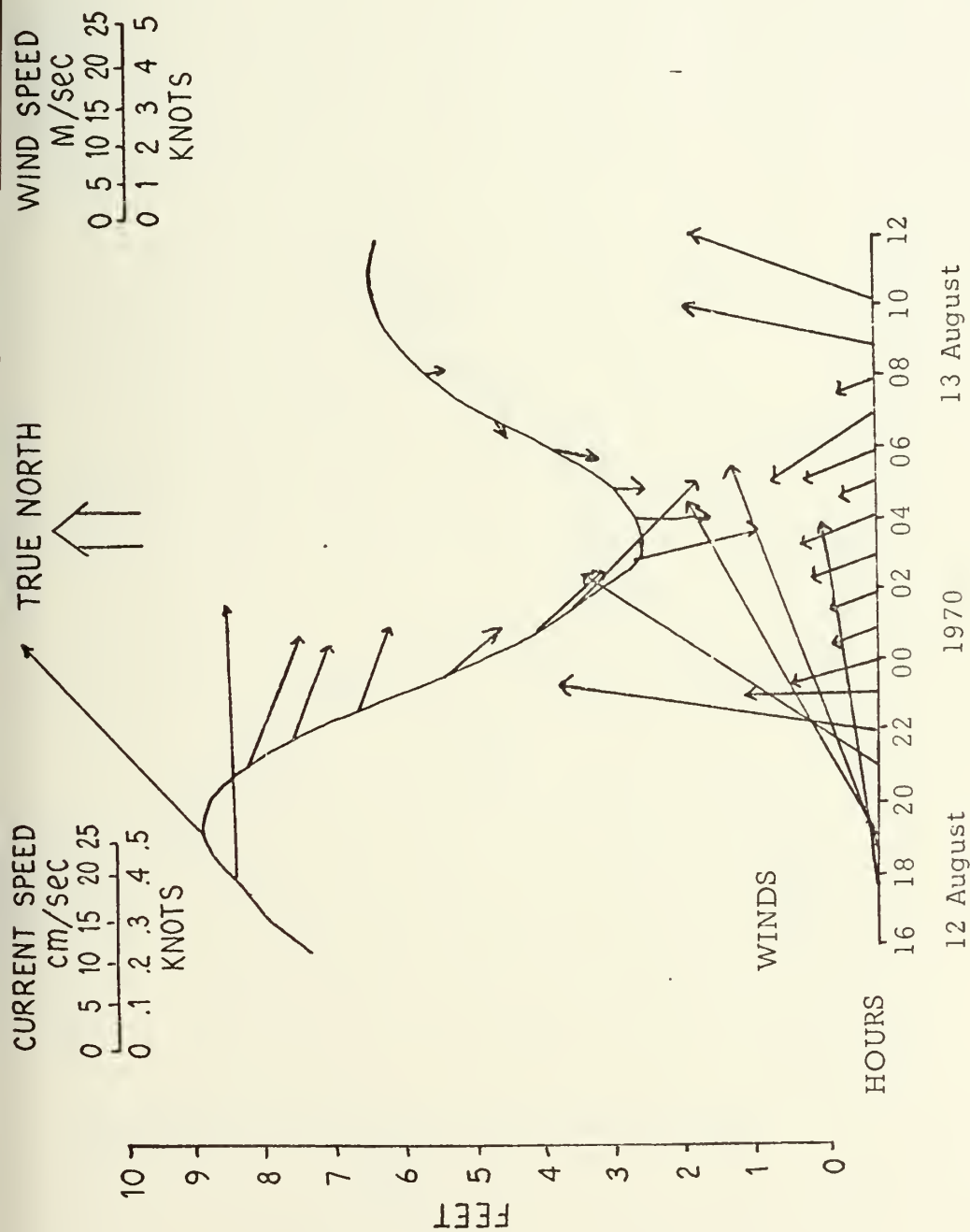


Figure A-17. Currents vs. Tides and Winds for Droque 1.



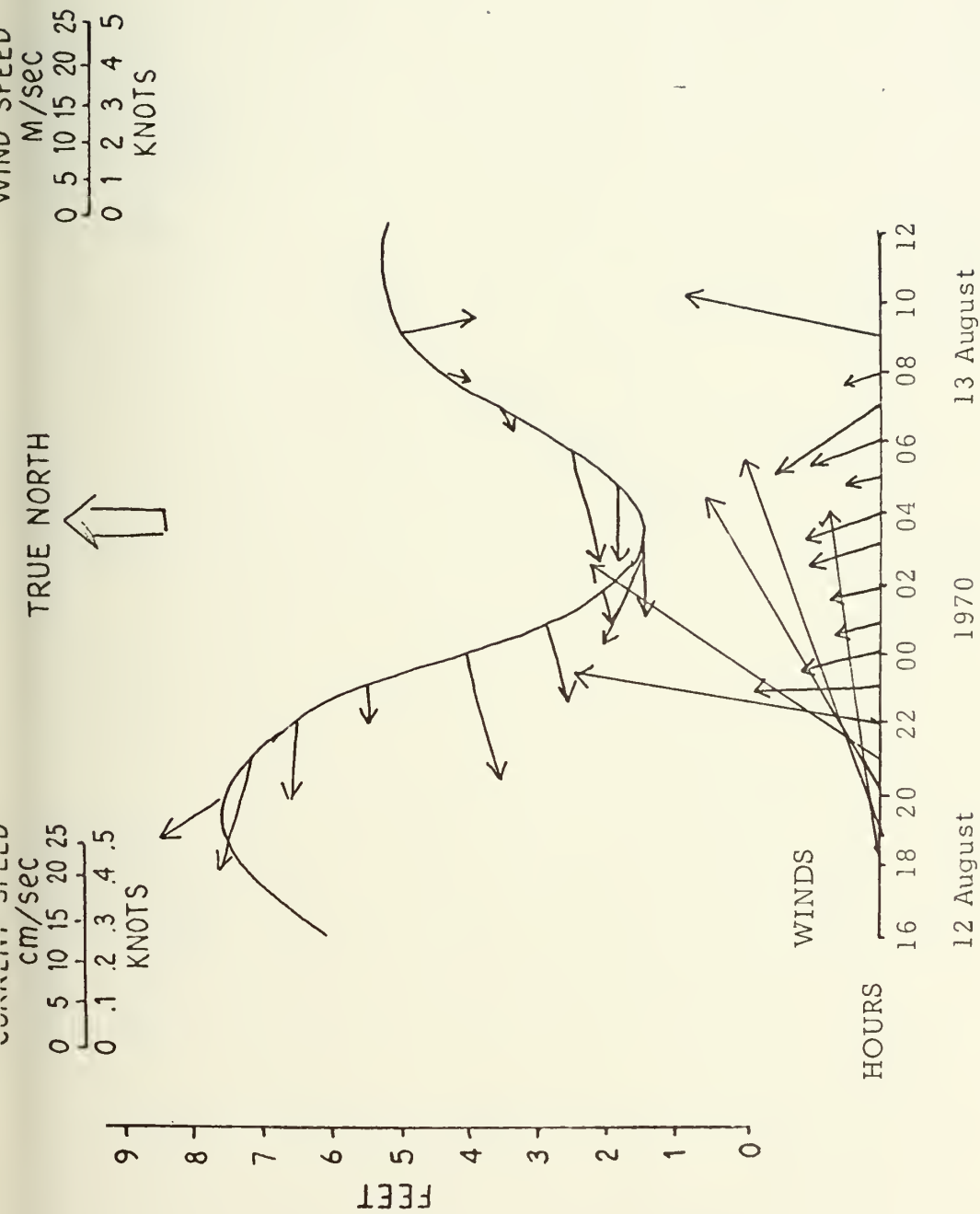


Figure A-18. Currents vs. Tides and Winds for Drogue 2.

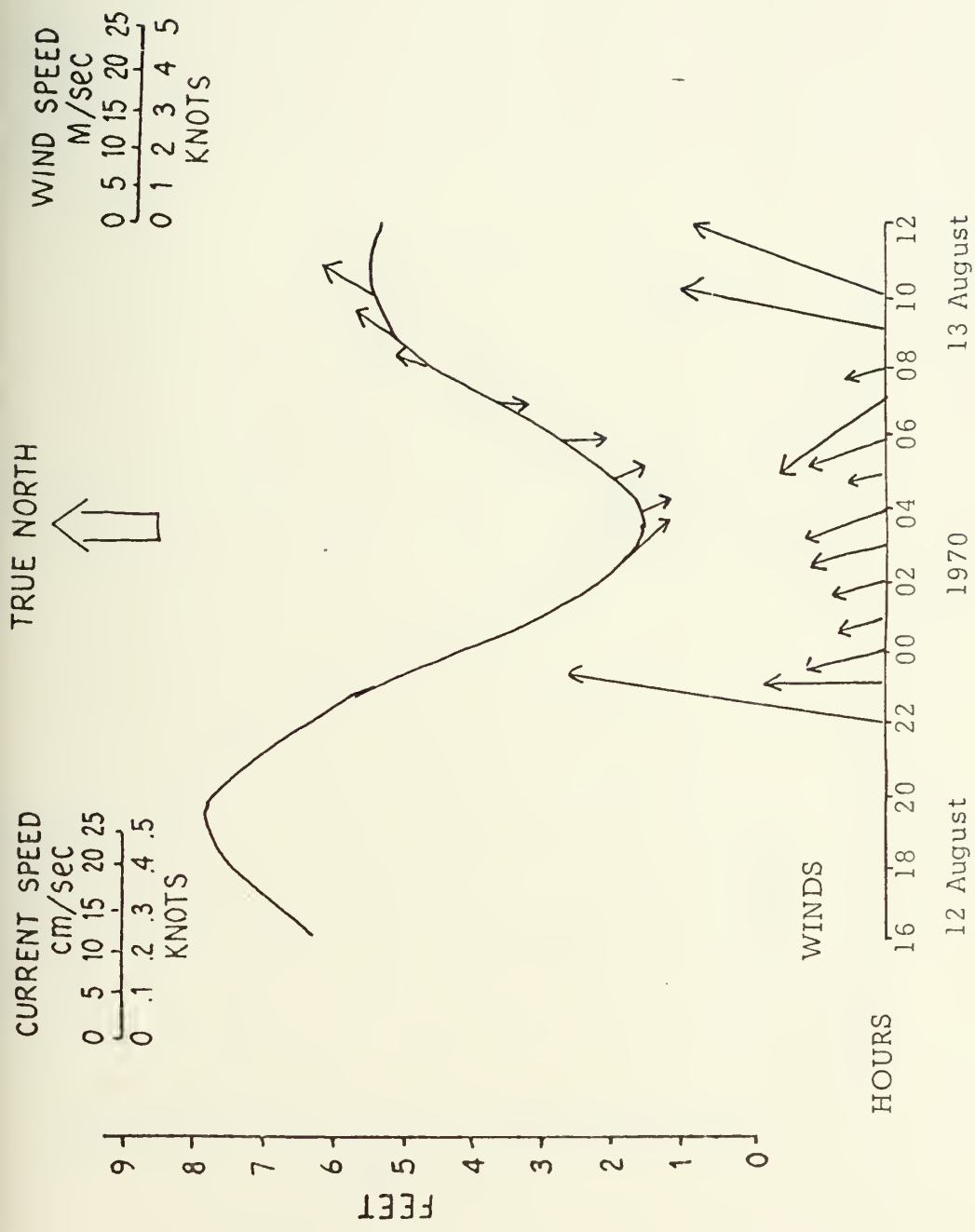


Figure A-19. Currents vs. Tides and Winds for Droque 4.

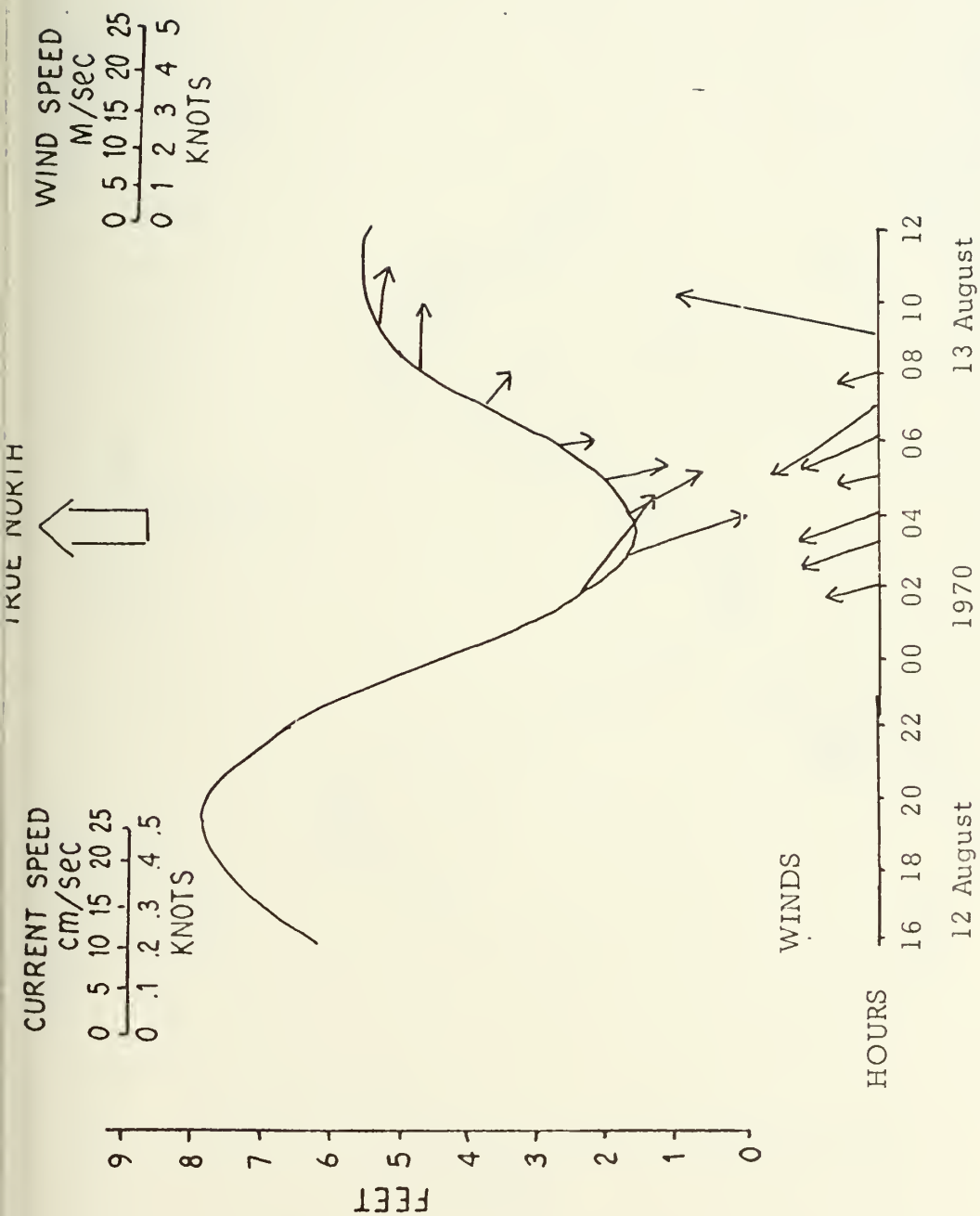


Figure A-20. Currents vs. Tides and Winds for Droque 5.

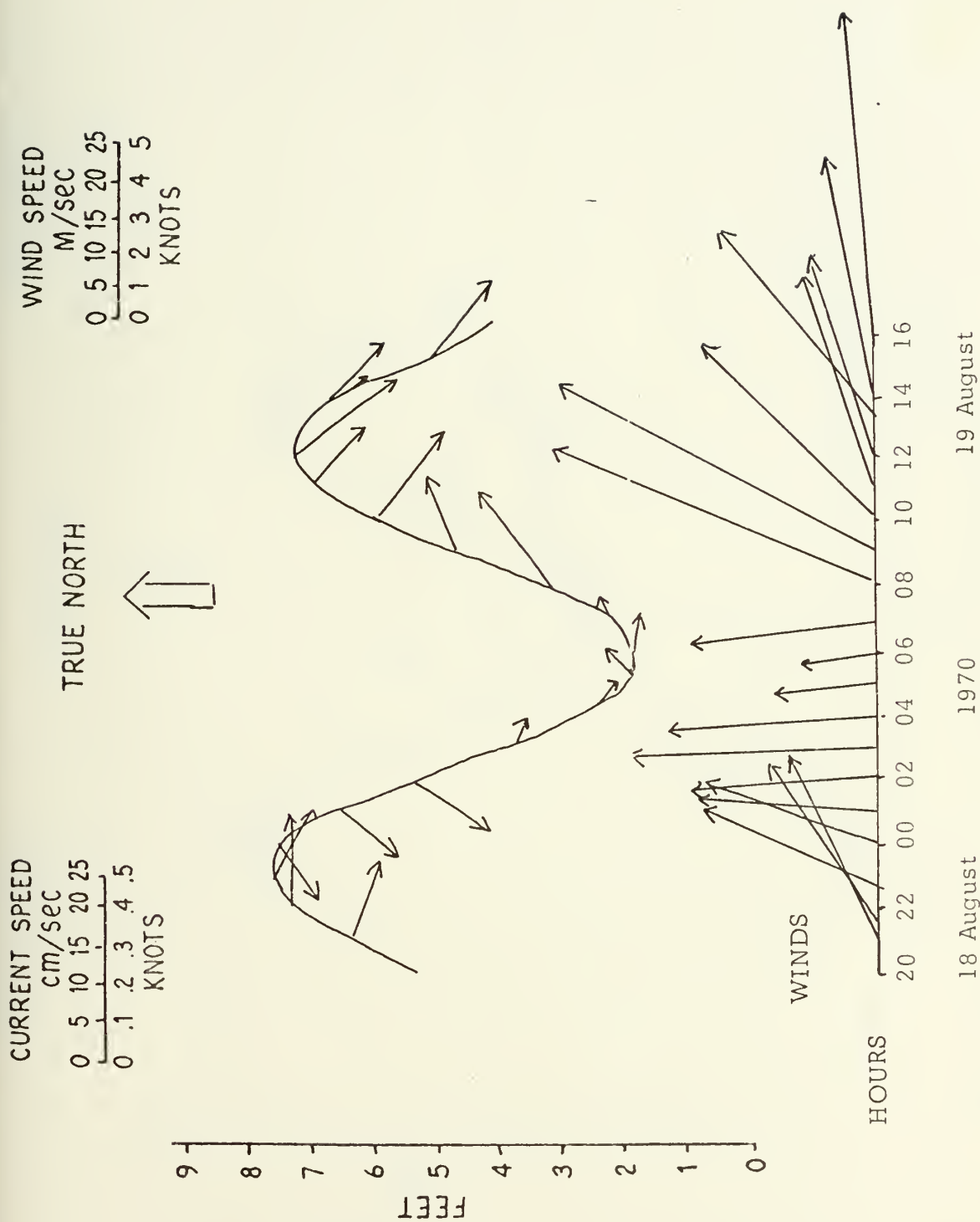


Figure A-21. Currents vs. Tides and Winds for Droque 6.

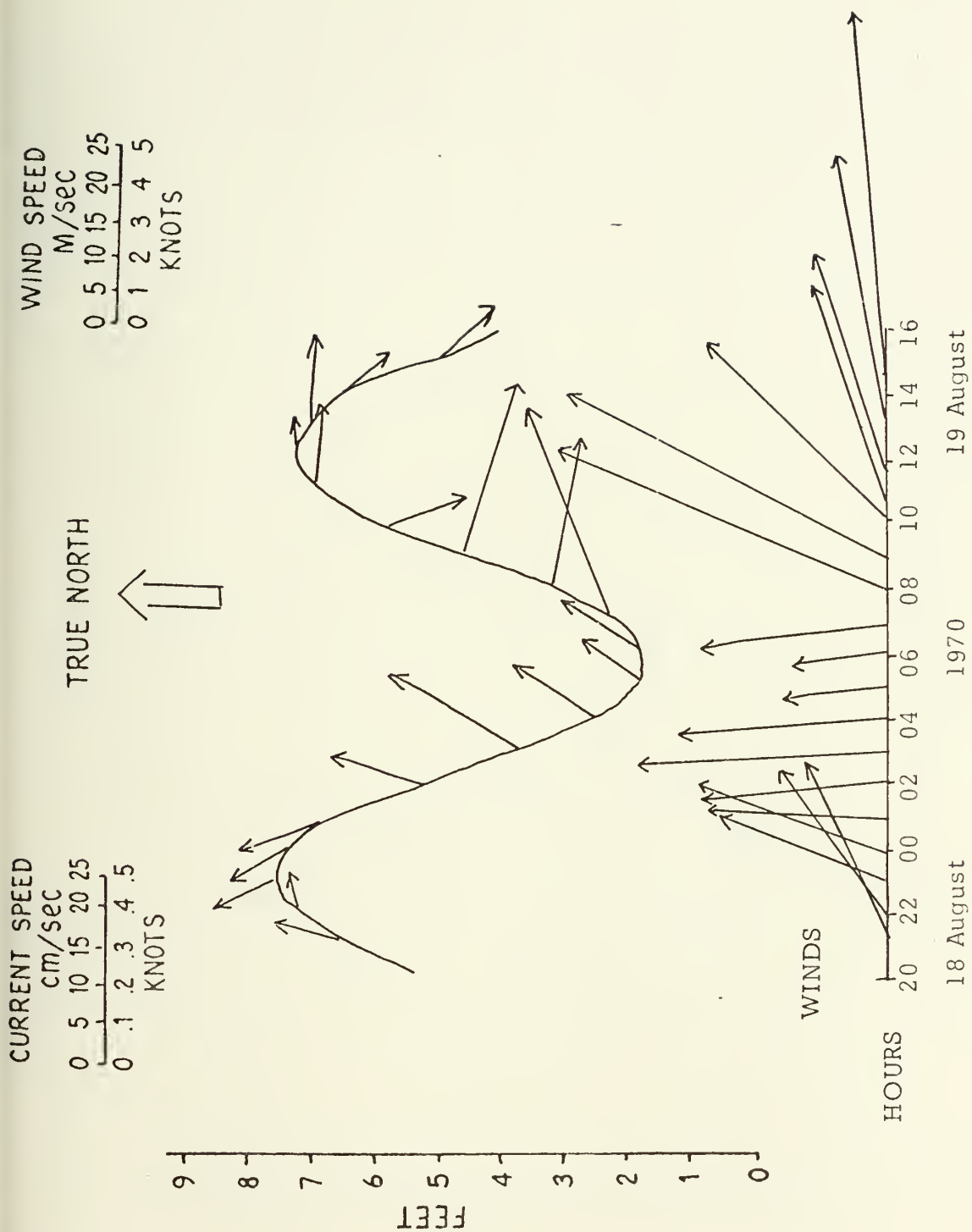


Figure A-22. Currents vs. Tides and Winds for Drogue 7.

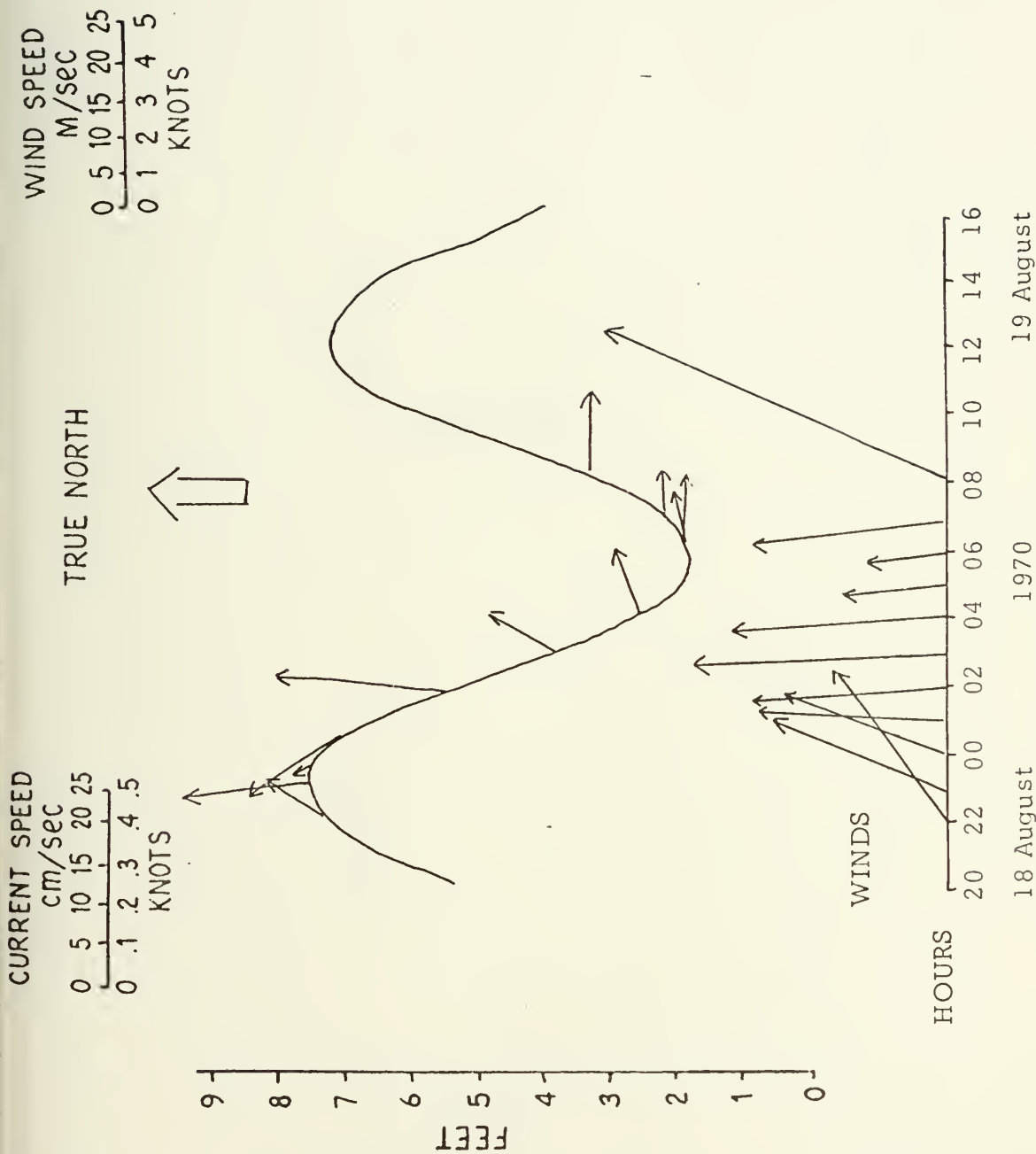


Figure A-23. Currents vs. Tides and Winds for Droque 8.

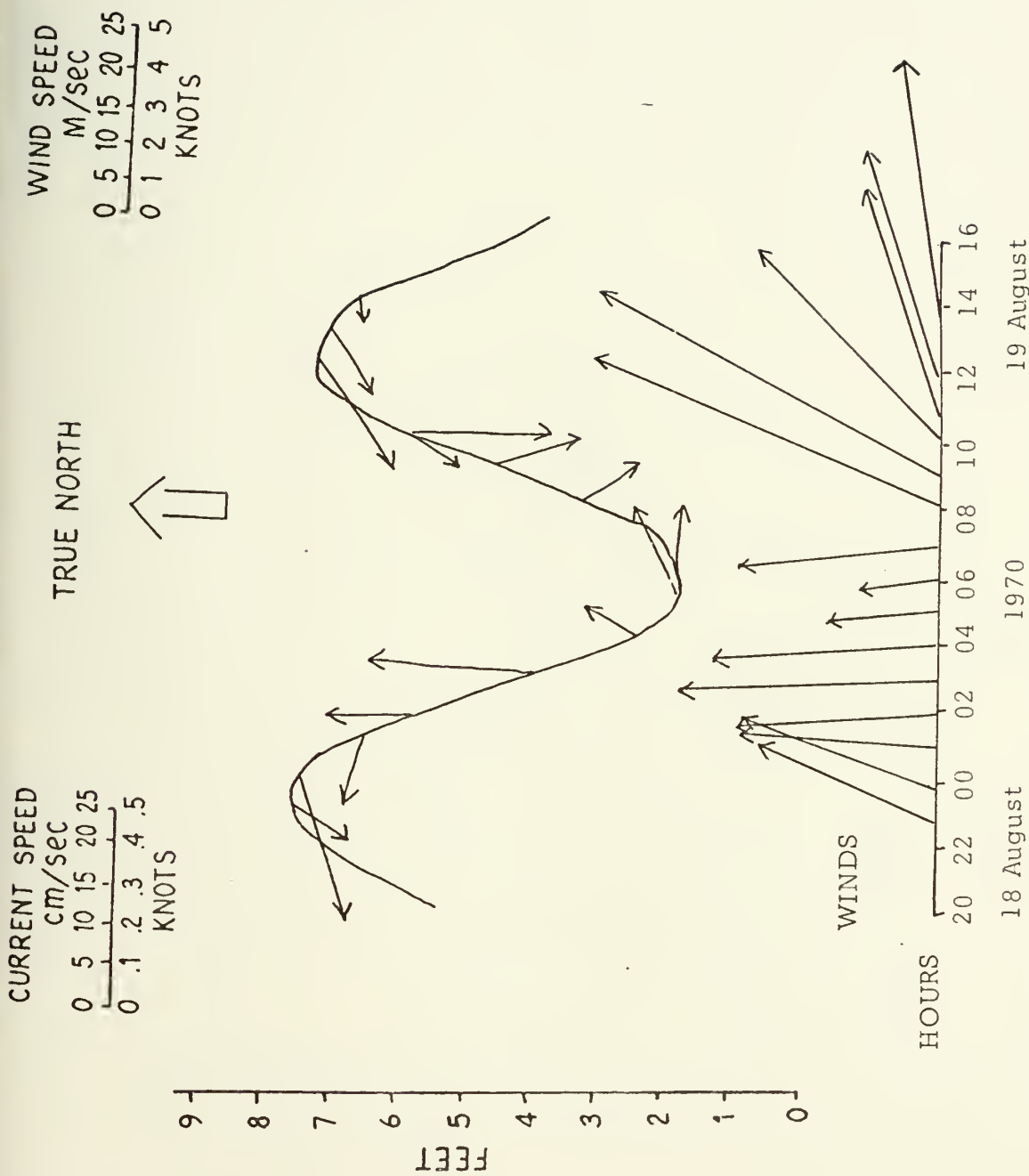
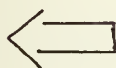


Figure A-24. Currents vs. Tides and Winds for Drogue 10.

WIND SPEED
M/sec
0 5 10 15 20 25
0 1 2 3 4 5
KNOTS

TRUE NORTH



CURRENT SPEED
cm/sec
0 5 10 15 20 25
0 .1 .2 .3 .4 .5
KNOTS

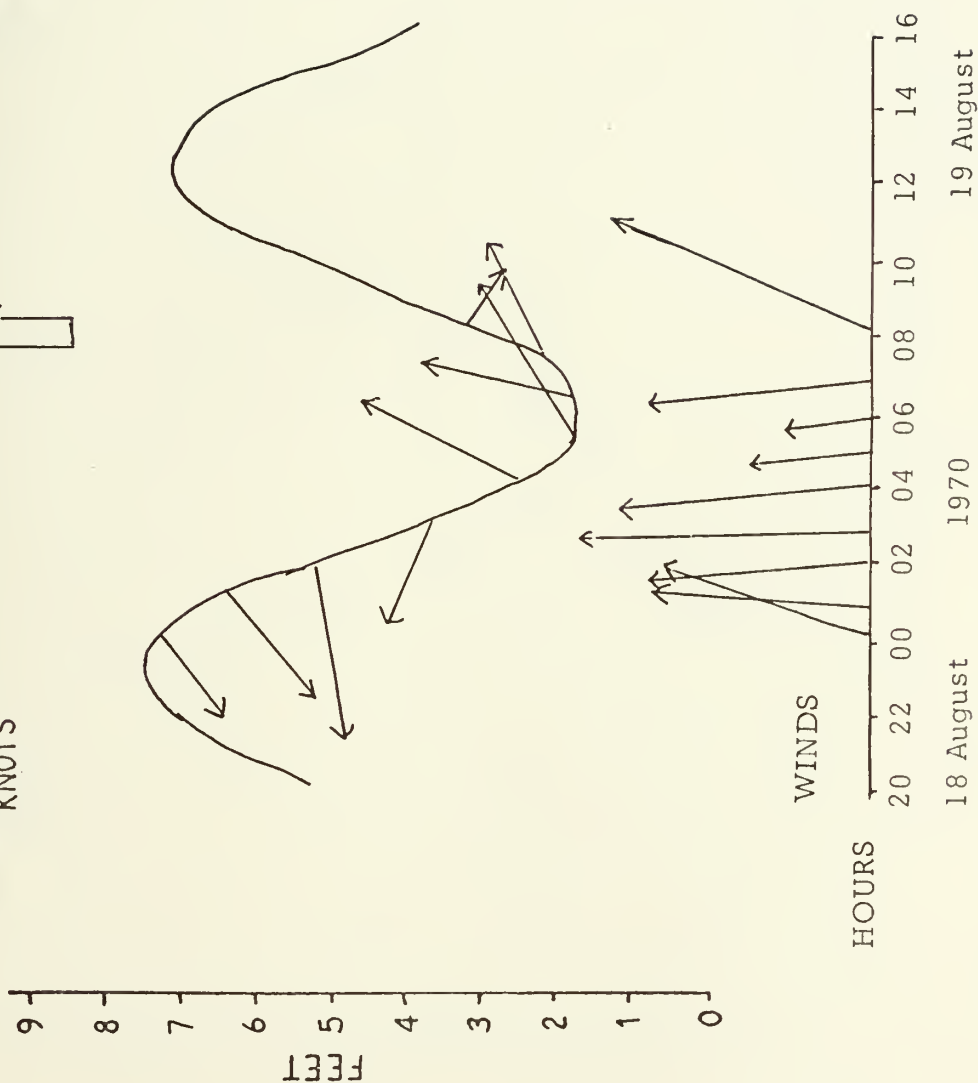


Figure A-25. Currents vs. Tides and Winds for Droque 12.

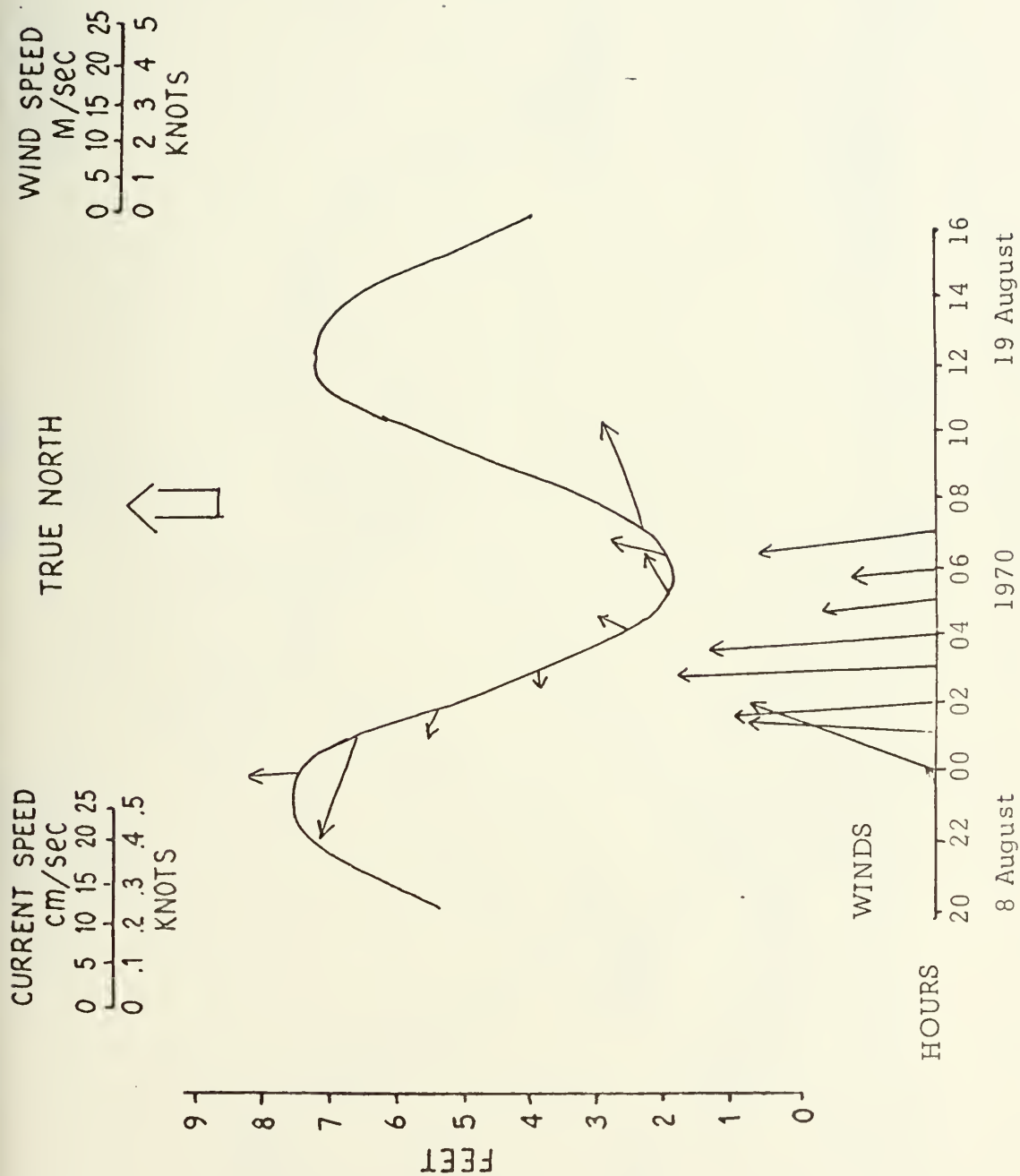


Figure A-26. Currents vs. Tides and Winds for Droque 13.

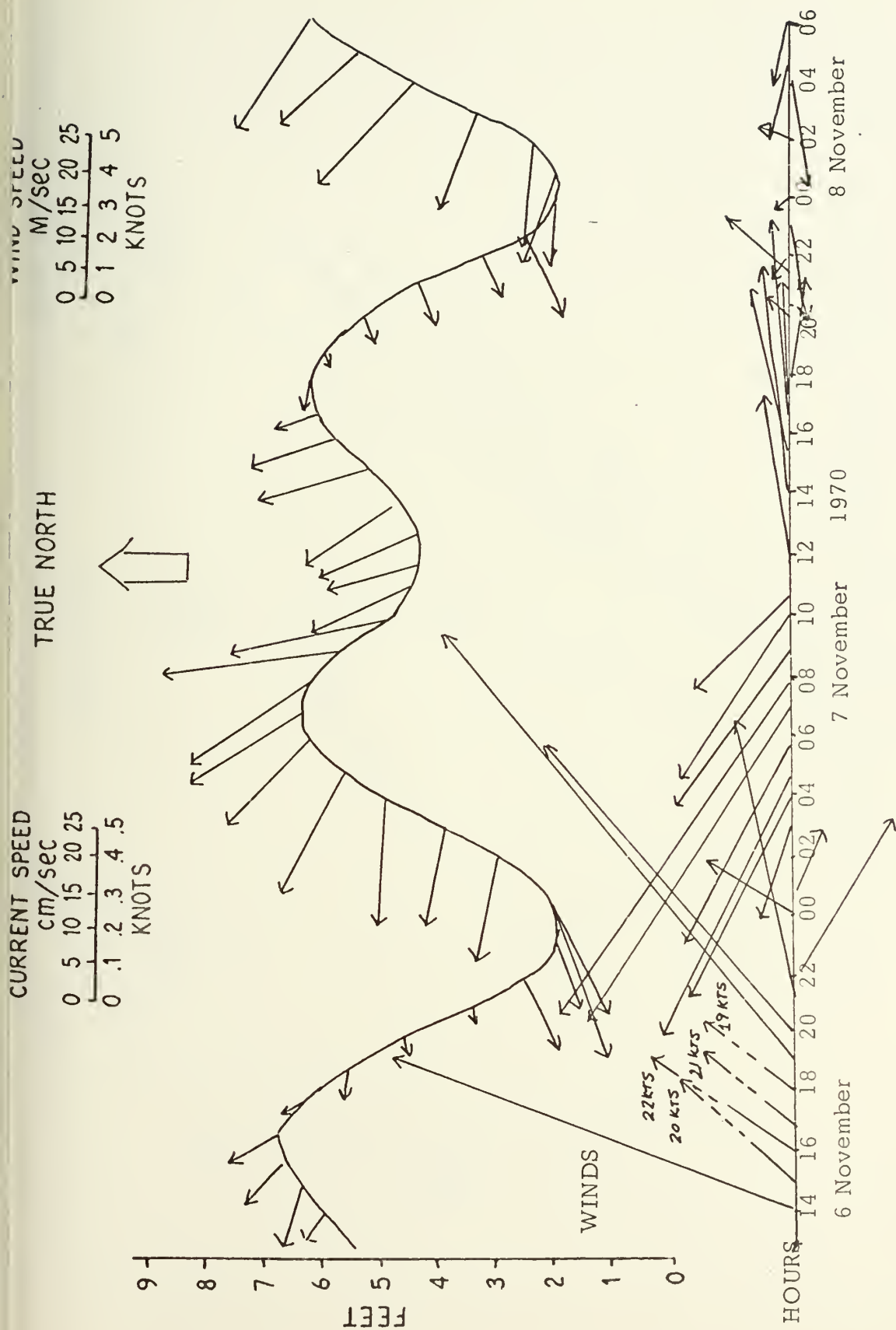


Figure A-27. Currents vs. Tides and Winds for Droque 28.

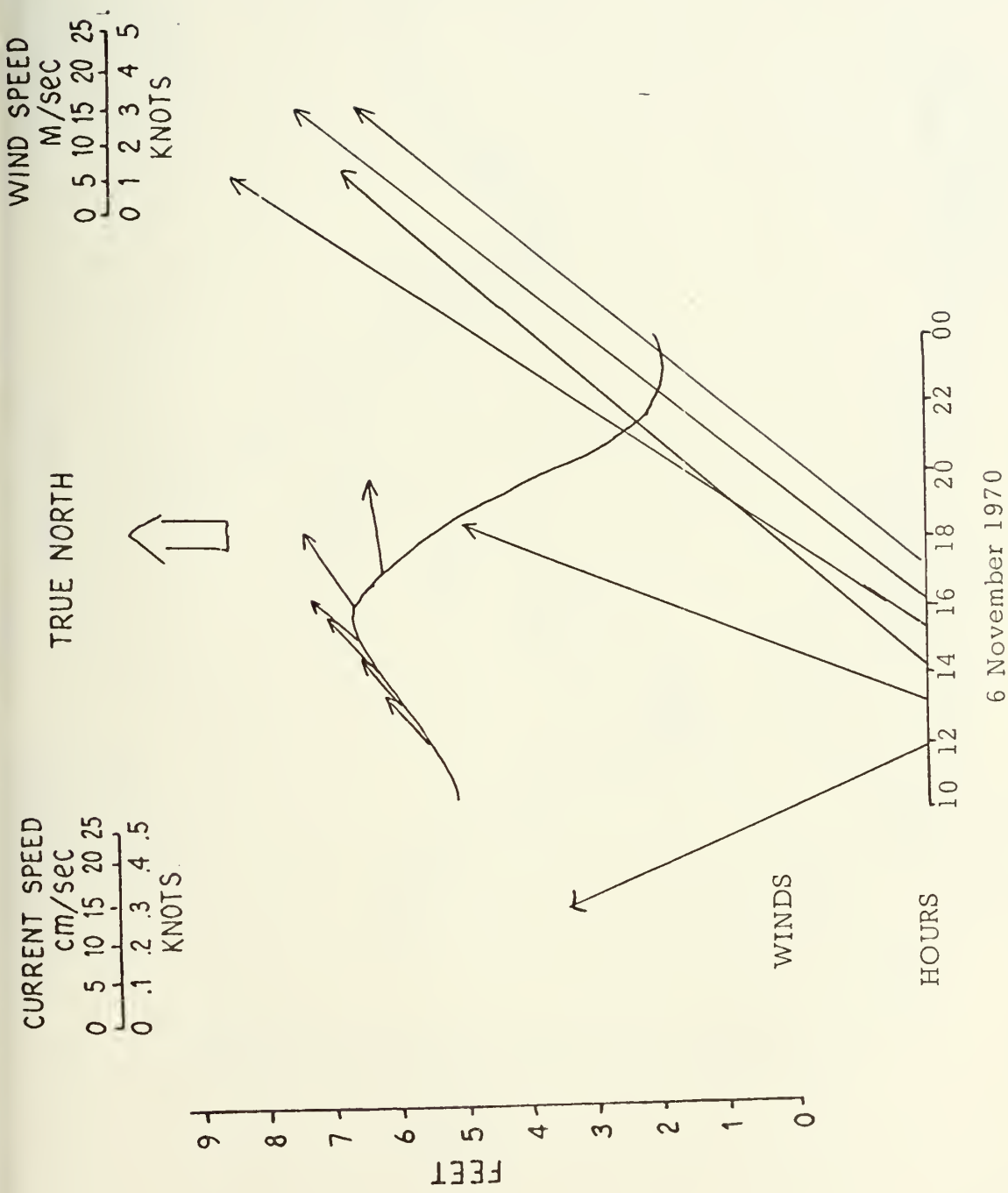
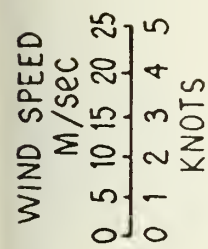


Figure A-28. Currents vs. Tides and Winds for Drogue 29.



TRUE NORTH

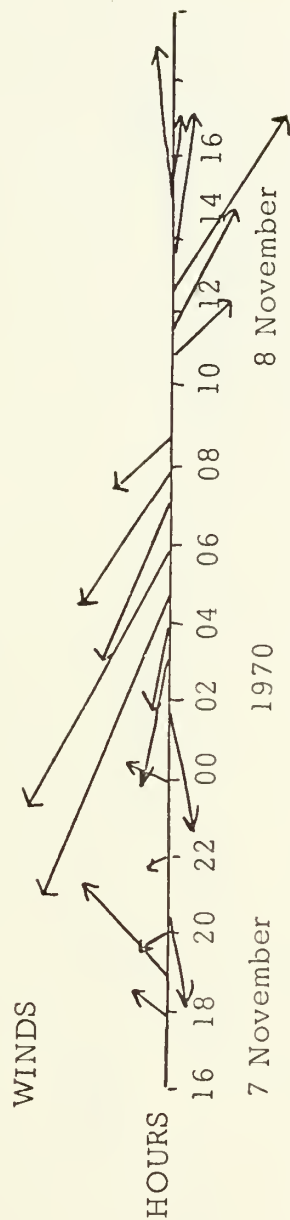
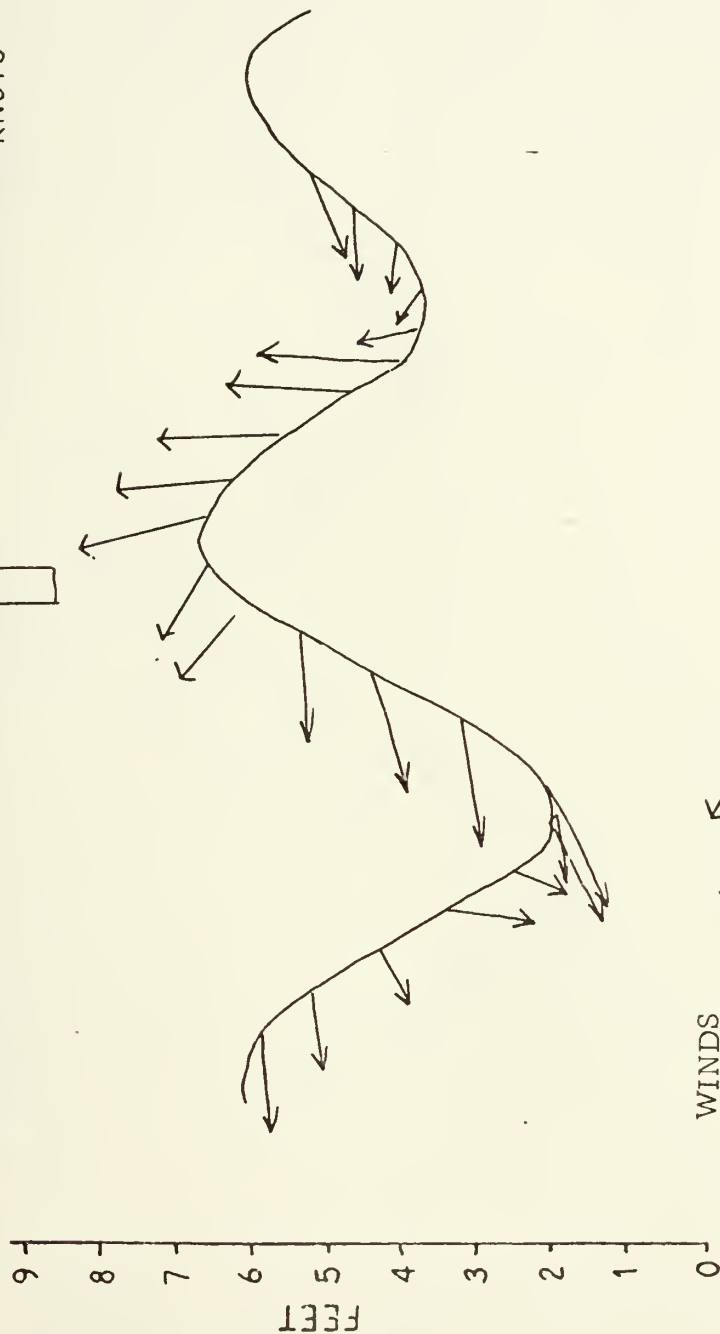
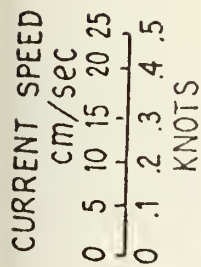
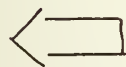


Figure A-29. Currents vs. Tides and Winds for Droque 30.

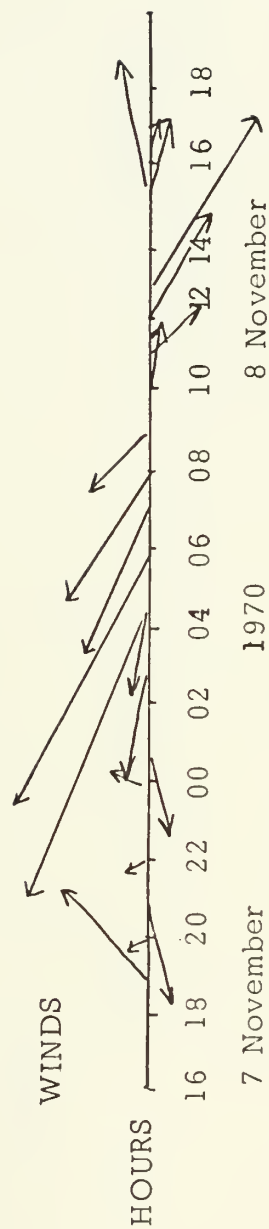
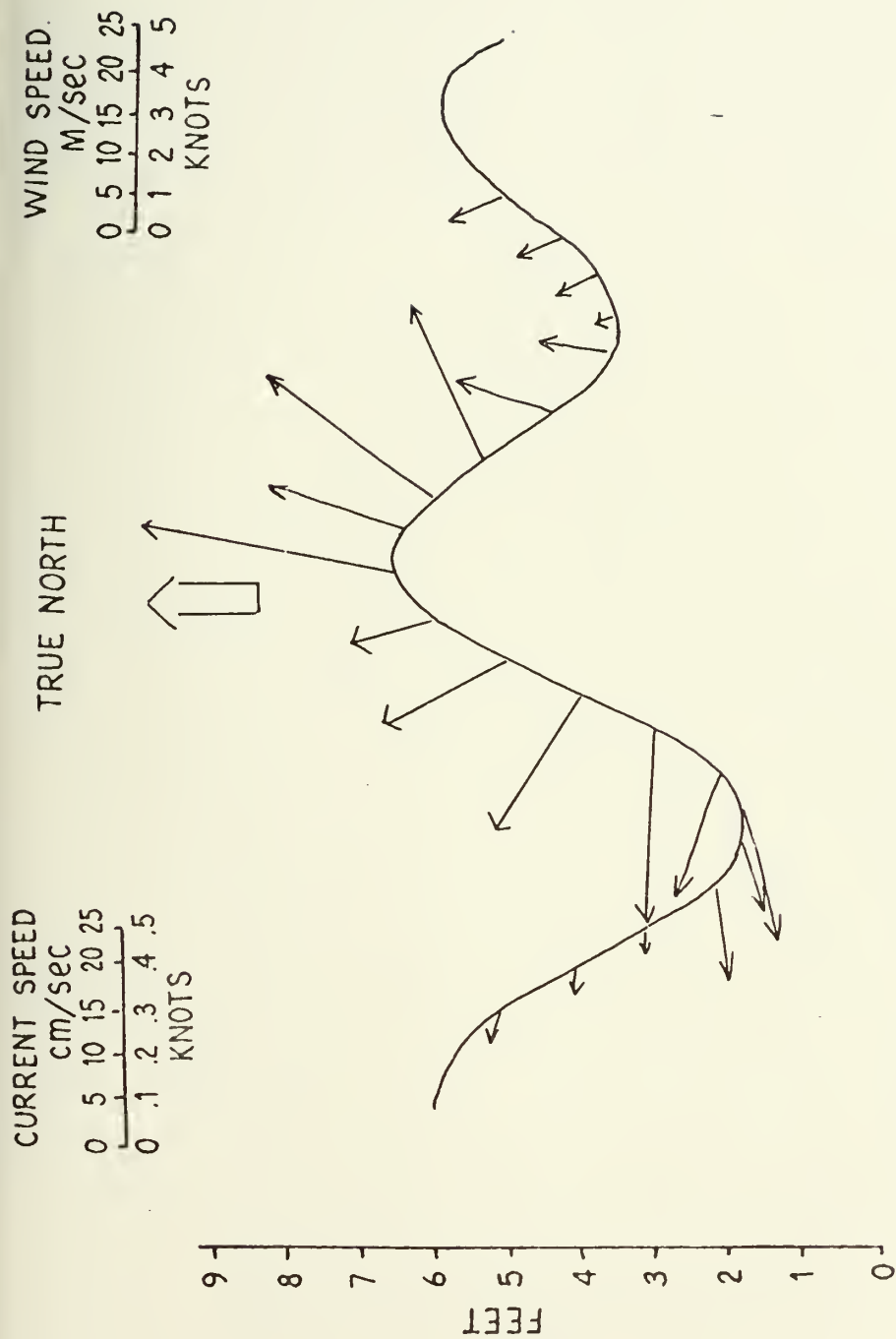


Figure A-30. Currents vs. Tides and Winds for Droque 31.

WIND SPEED
M/sec
0 5 10 15 20 25
0 1 2 3 4 5
KNOTS

TRUE NORTH

CURRENT SPEED
cm/sec
0 5 10 15 20 25
0 .1 .2 .3 .4 .5
KNOTS

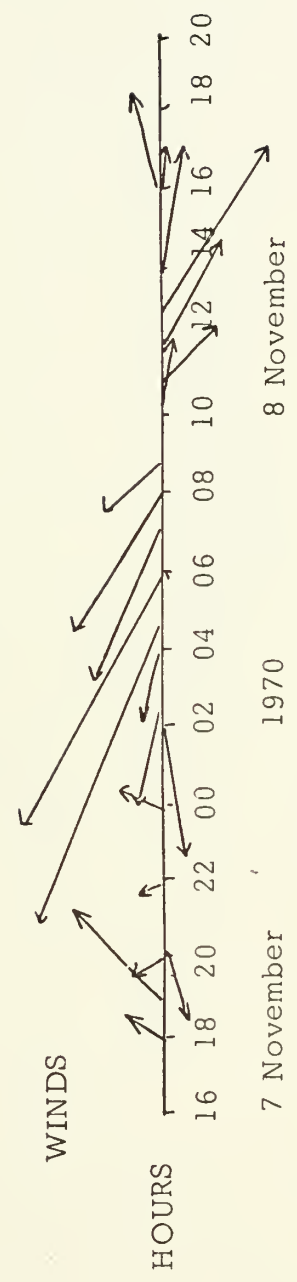
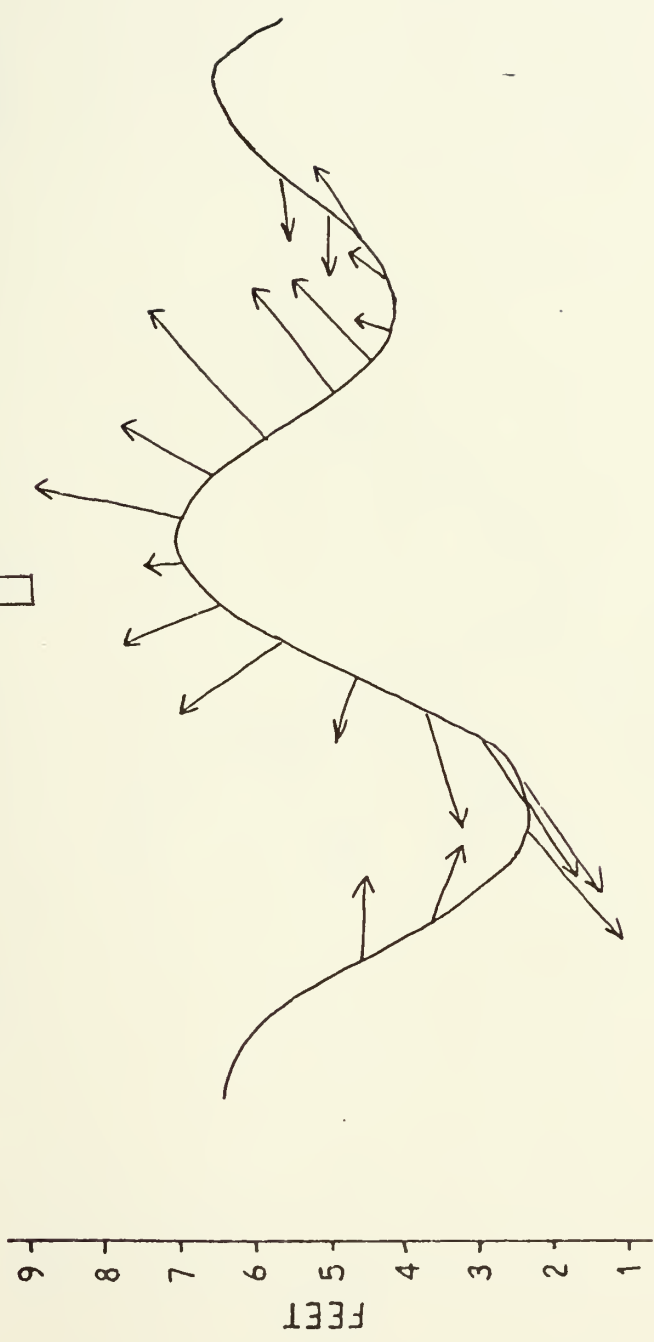


Figure A-31. Currents vs. Tides and Winds for Droque 33.

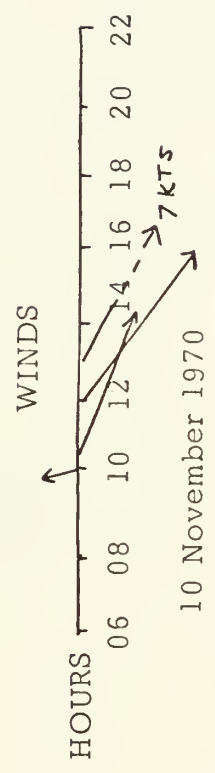
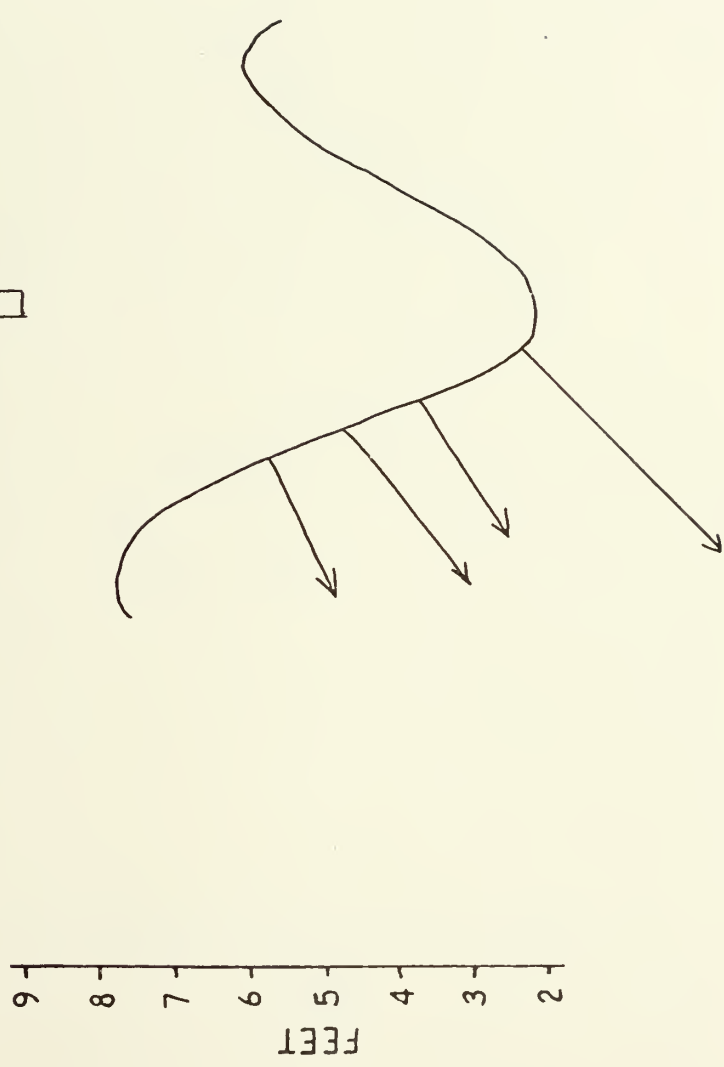
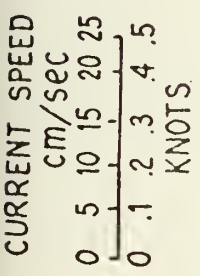
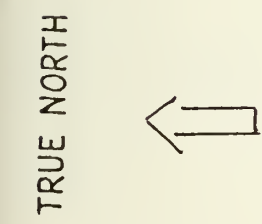
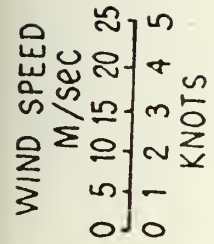
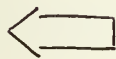


Figure A-32. Currents vs. Tides and Winds for Drogue 34.

CURRENT SPEED
cm/sec
0 5 10 15 20 25
0 .1 .2 .3 .4 .5
KNOTS

WIND SPEED
M/sec
0 5 10 15 20 25
0 1 2 3 4 5
KNOTS

TRUE NORTH



FEET
9
8
7
6
5
4
3
2

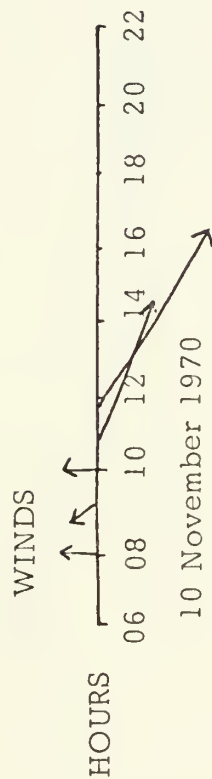
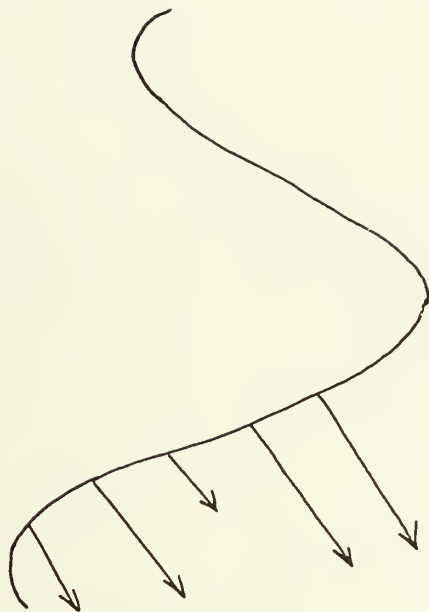
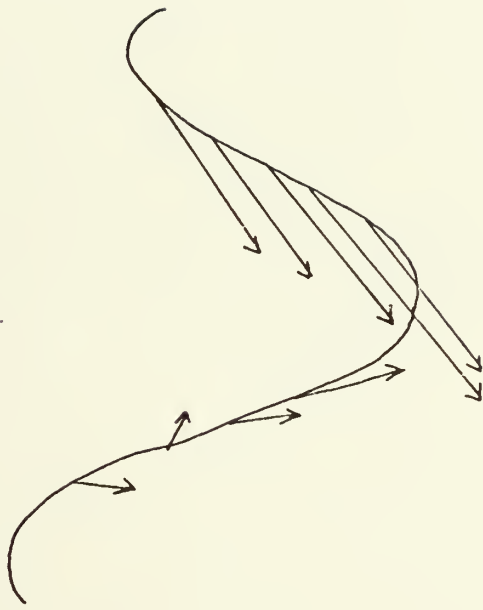
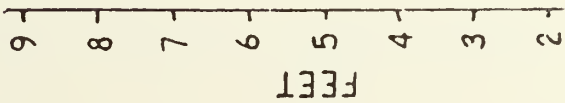
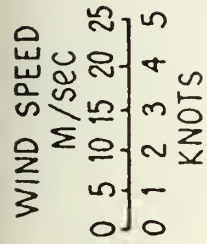
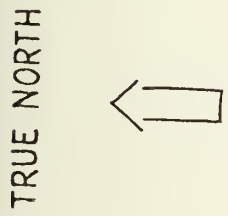
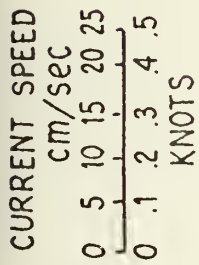


Figure A-33. Currents vs. Tides and Winds for Droque x.



WINDS

HOURS

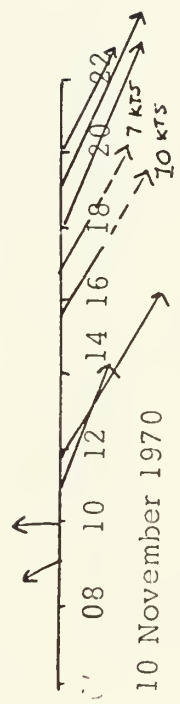
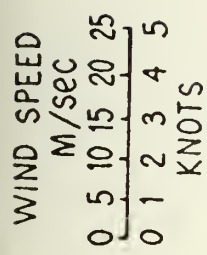
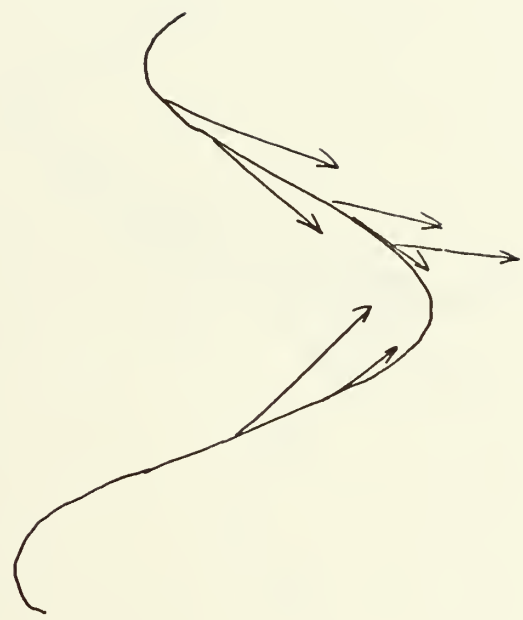
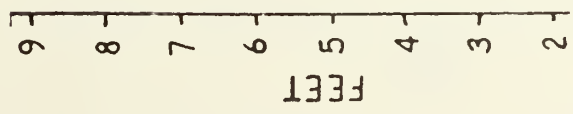
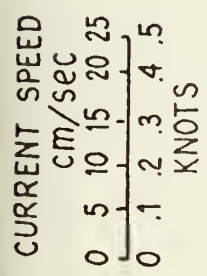
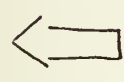


Figure A-34. Currents vs. Tides and Winds for Droque y.



TRUE NORTH



WINDS

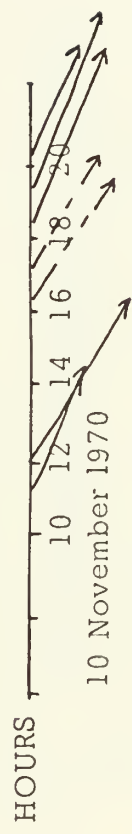
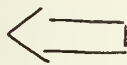


Figure A-35. Currents vs. Tides and Winds for Droque z.

CURRENT SPEED
cm/sec
0 5 10 15 20 25
0 .1 2 .3 4 .5
KNOTS

TRUE NORTH



WIND SPEED
M/sec
0 5 10 15 20 25
0 1 2 3 4 5
KNOTS

10
9
8
7
6
5
4
3
2
FEET

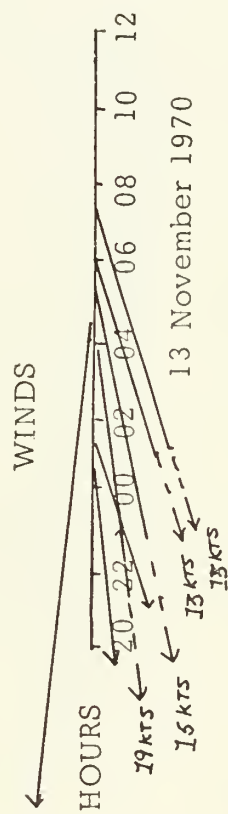
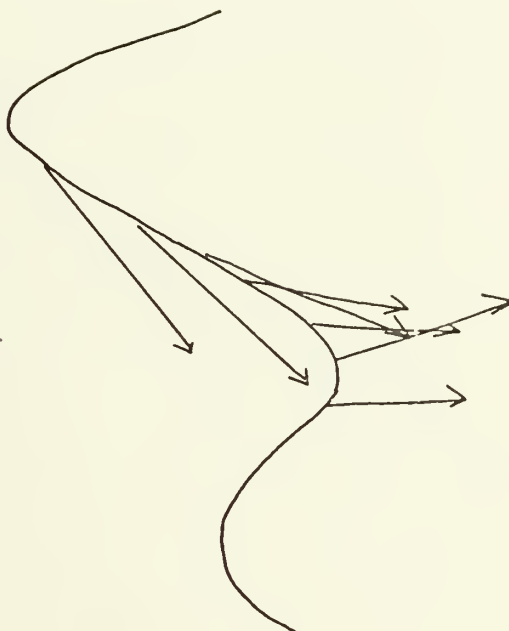
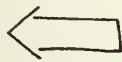


Figure A-36. Currents vs. Tides and Winds for Droque 35.

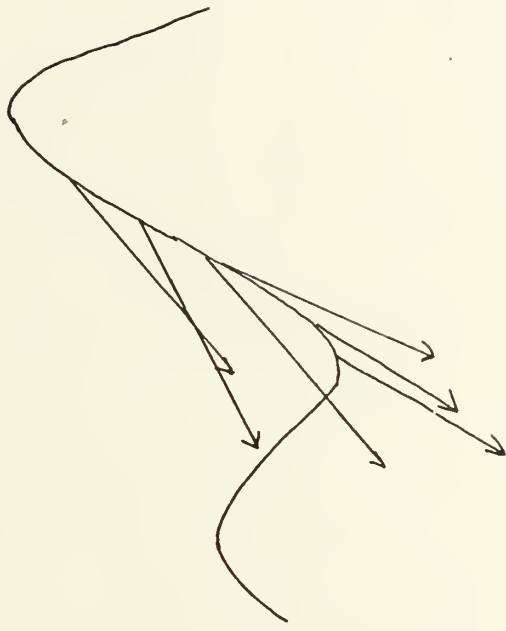
CURRENT SPEED
cm/sec
0 5 10 15 20 25
0 .1 2 .3 .4 .5
KNOTS

TRUE NORTH



WIND SPEED
M/sec
0 5 10 15 20 25
0 1 2 3 4 5
KNOTS

10
9
8
7
6
5
4
FEET



WINDS

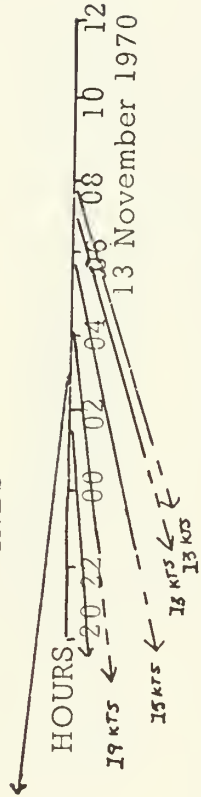
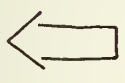


Figure A-37. Currents vs. Tides and Winds for Drogue 36.

CURRENT SPEED
cm/sec
0 5 10 15 20 25
0 .1 .2 .3 .4 .5
KNOTS

WIND SPEED
M/sec
0 5 10 15 20 25
0 1 2 3 4 5
KNOTS

TRUE NORTH



10
9
8
7
6
5
4
FEET

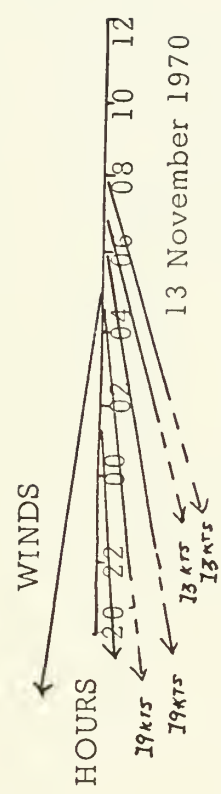
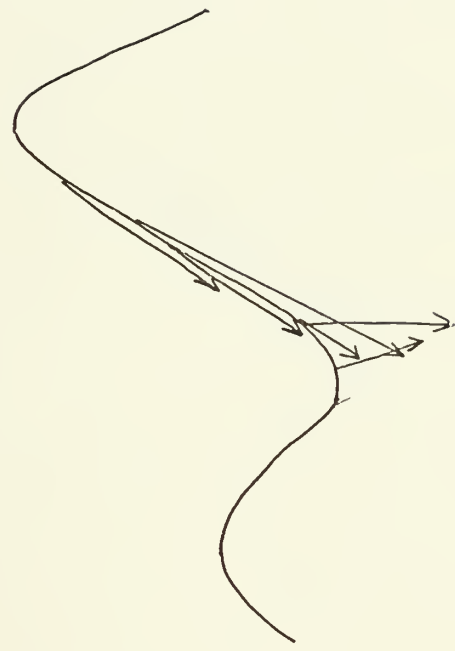
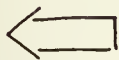


Figure A-38. Currents vs. Tides and Winds for Droque 37.

CURRENT SPEED
cm/sec
0 5 10 15 20 25
0 .1 .2 .3 .4 .5
KNOTS

WIND SPEED
M/sec
0 5 10 15 20 25
0 1 2 3 4 5
KNOTS

TRUE NORTH



10
9
8
7
6
5
4
FEET

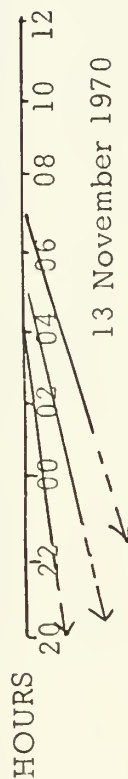


Figure A-39. Currents vs. Tides and Winds for Droque 38.

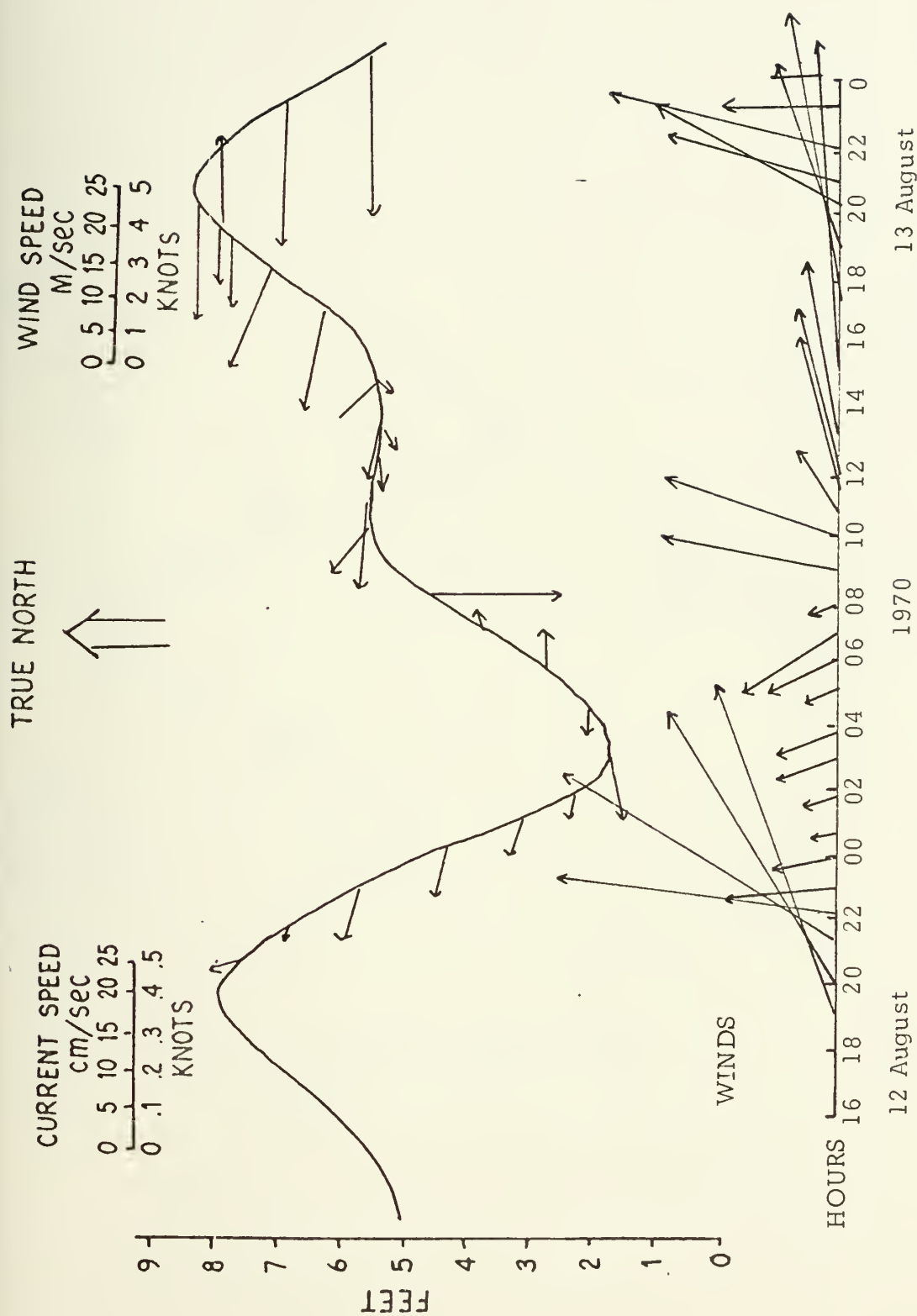


Figure A-40. Currents vs. Tides and Winds for Current Meter Station 1.

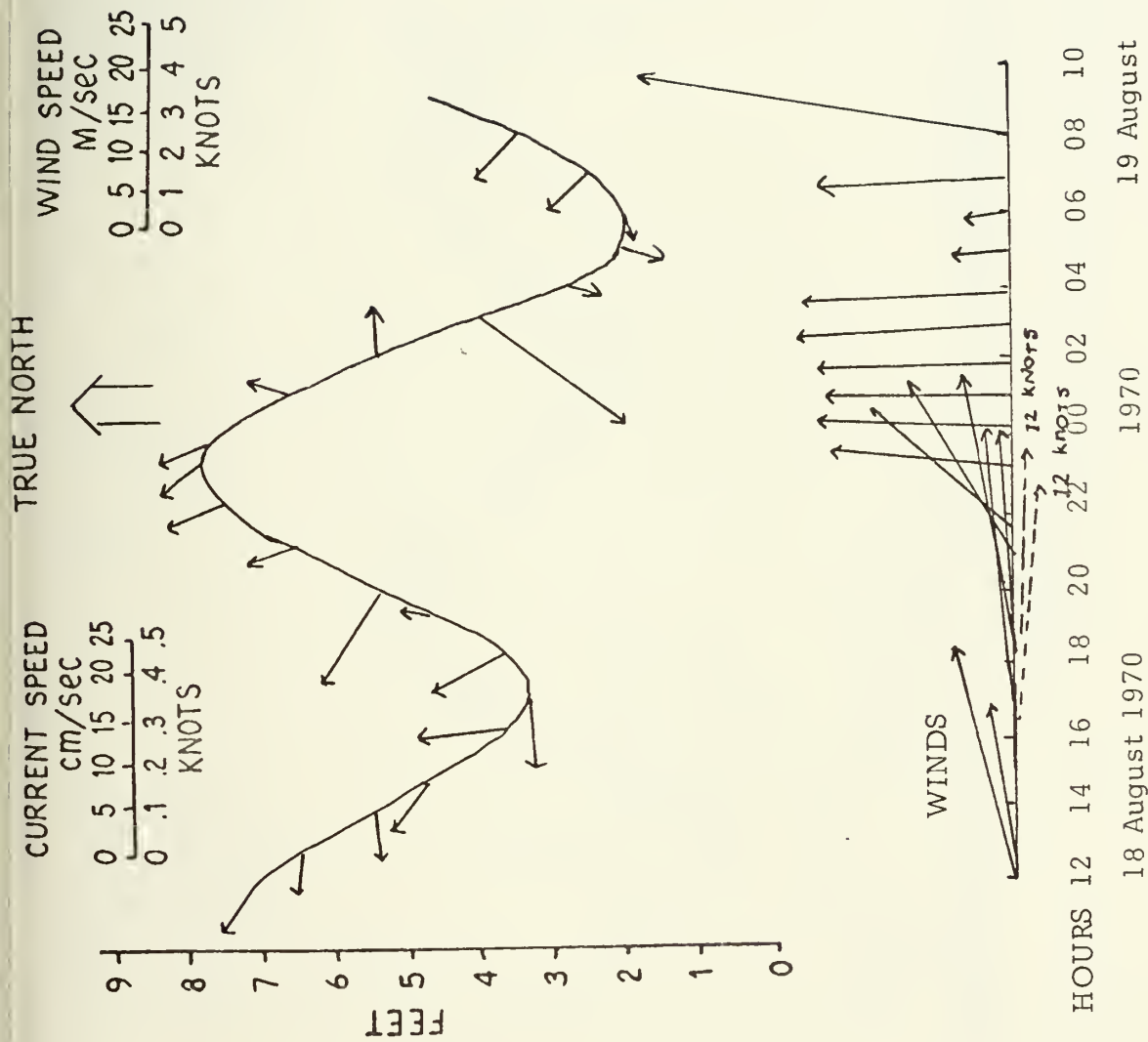
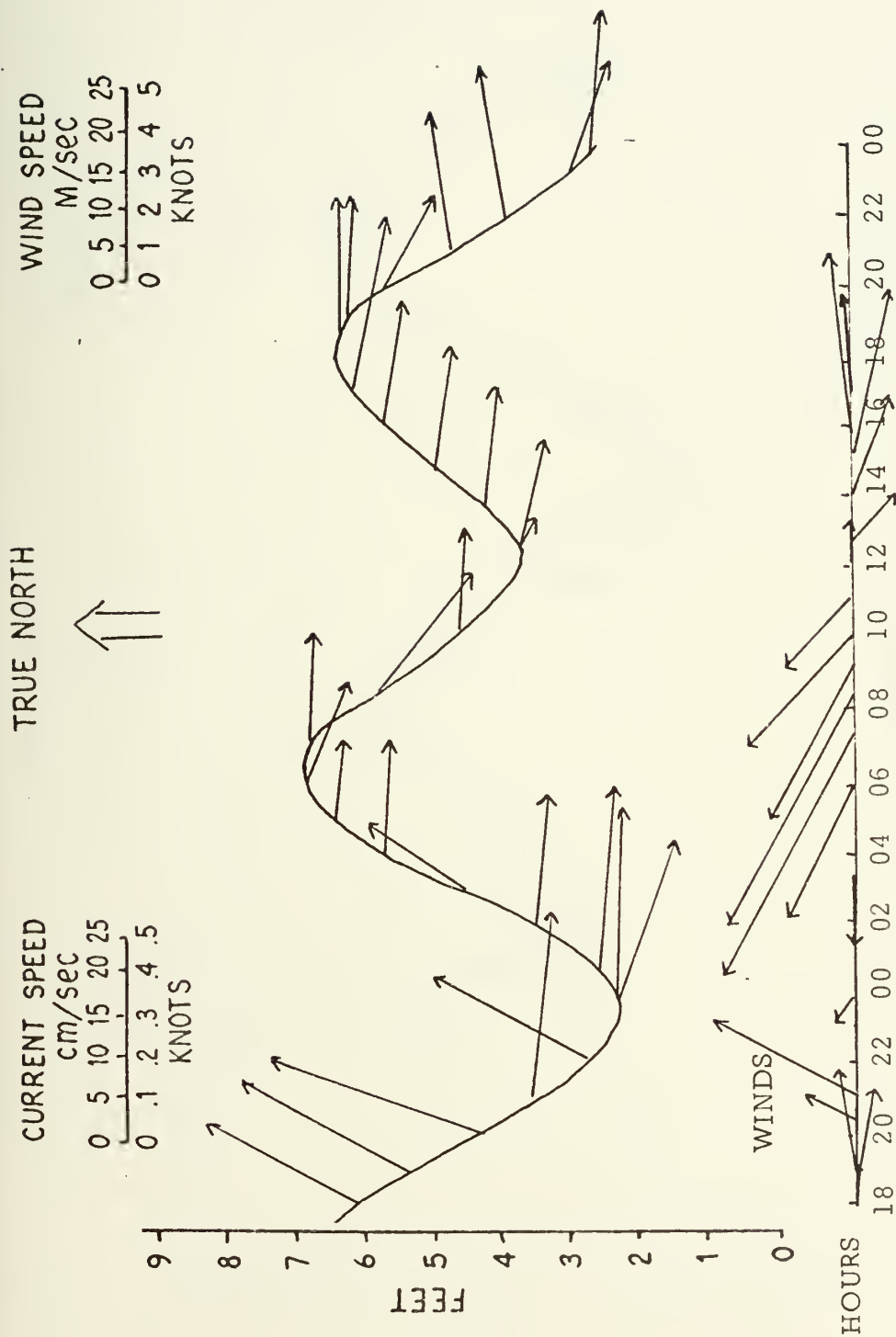


Figure A-41. Currents vs. Tides and Winds for Current Meter Station 1.



8 November 1970

Figure A-42. Currents vs. Tides and Winds for Current Meter Station 2.

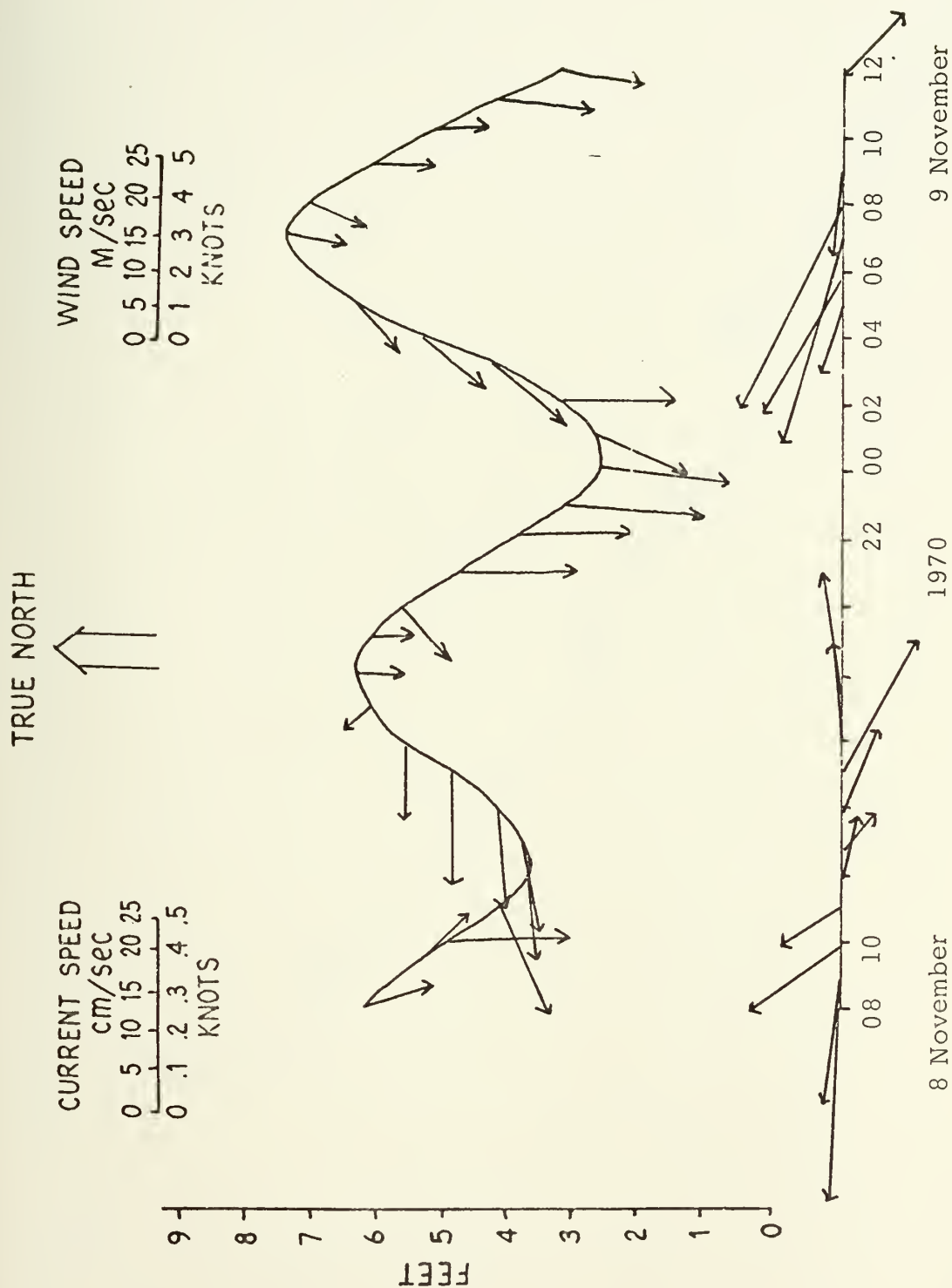


Figure A-43. Currents vs. Tides and Winds for Current Meter Station 3.

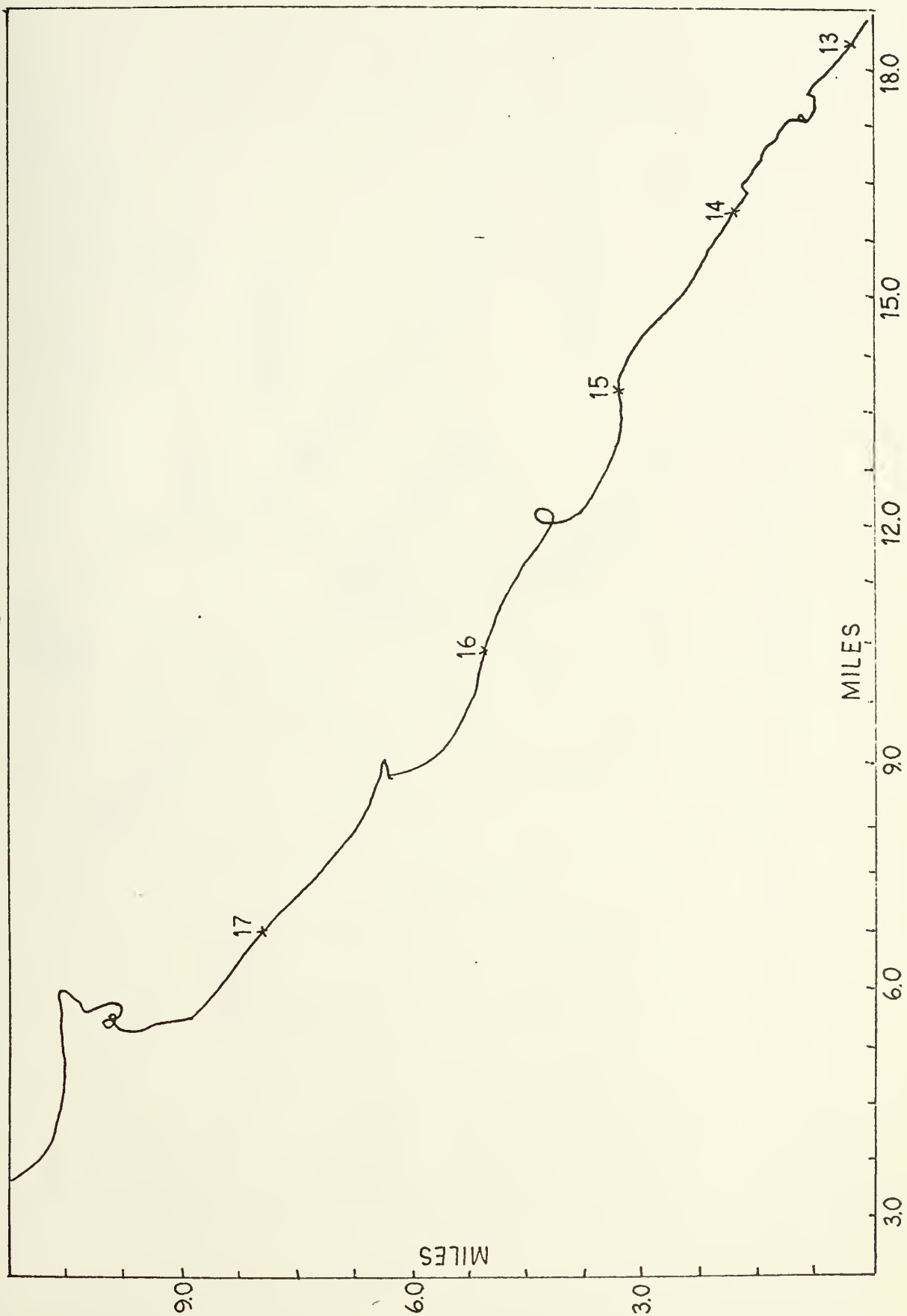


Figure A-44. Current in Lagrangian Format for Current Meter Station 1.

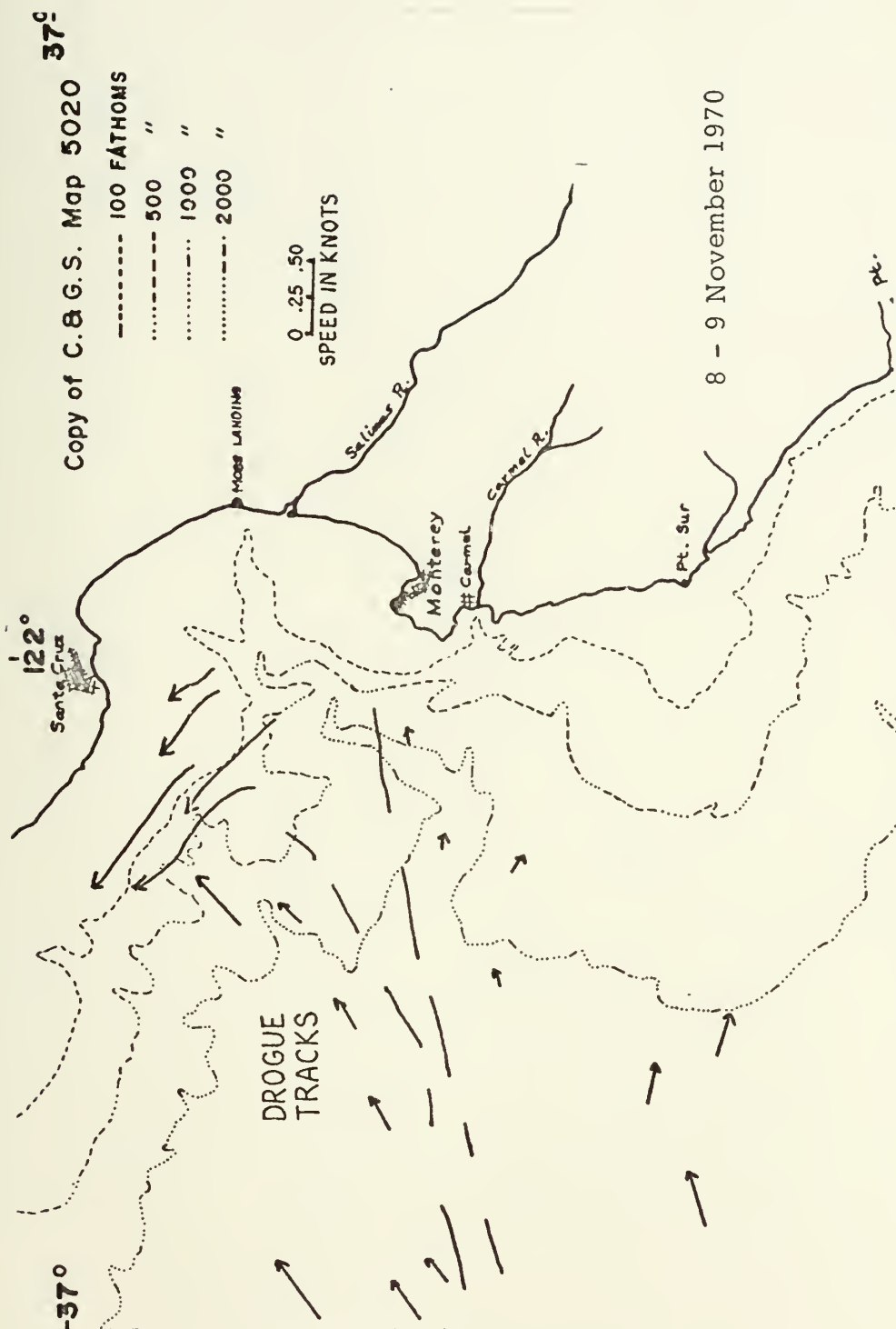


Figure A-45. Currents in Ocean adjacent to Monterey Bay.

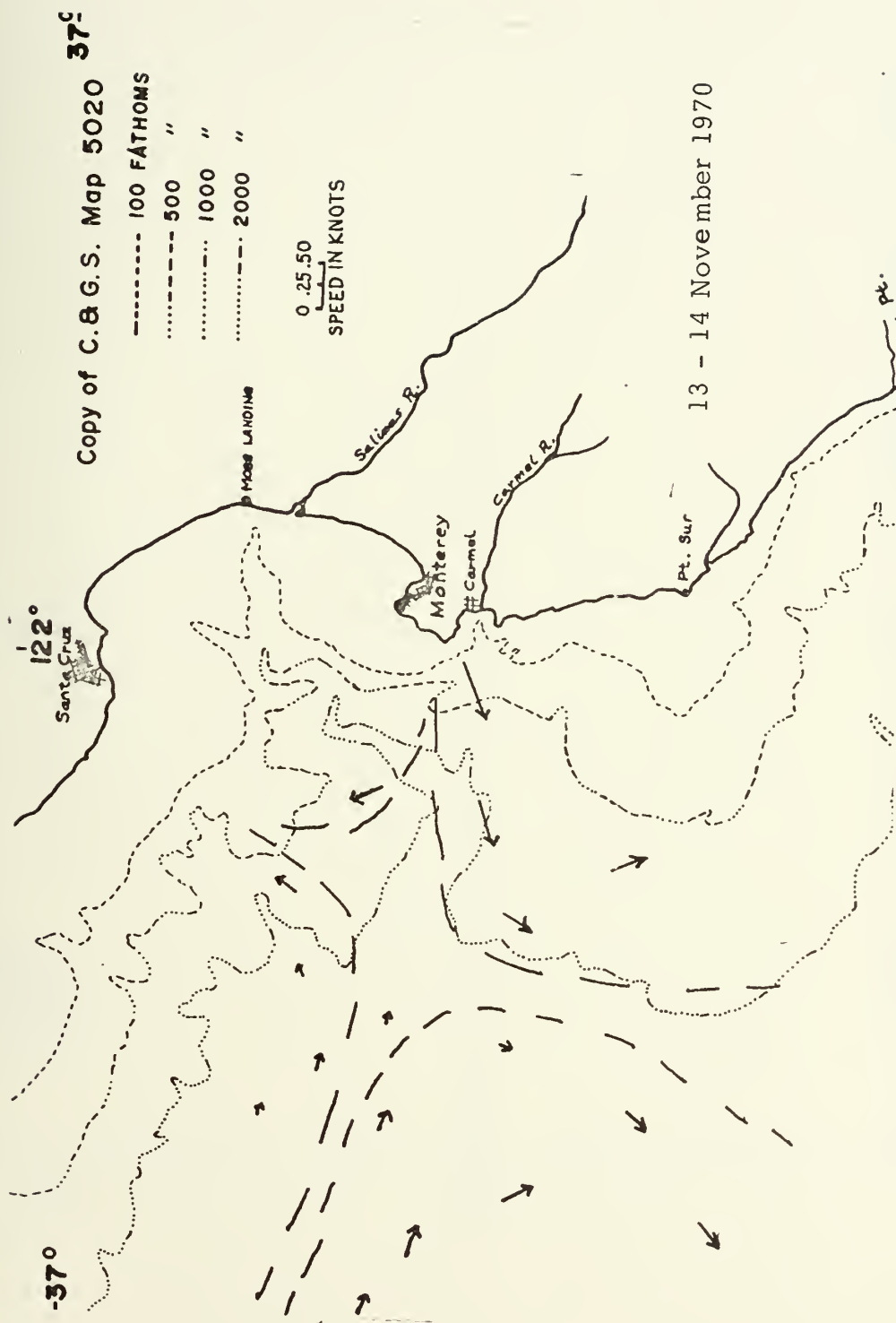


Figure A-46. Currents in Ocean adjacent to Monterey Bay.

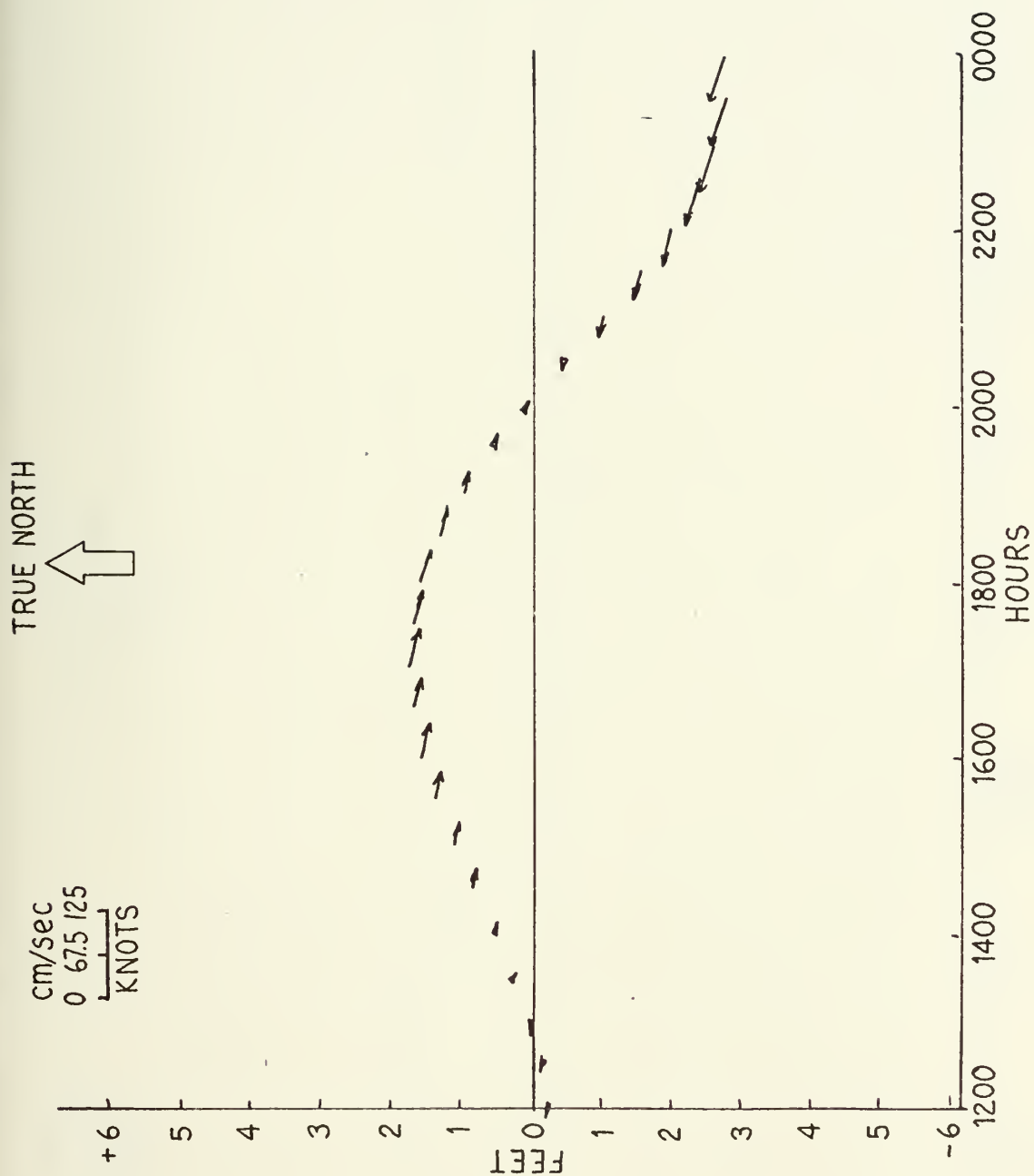


Figure A-47. Calculated Tides and Currents in Monterey Harbor for 7 November 1970.

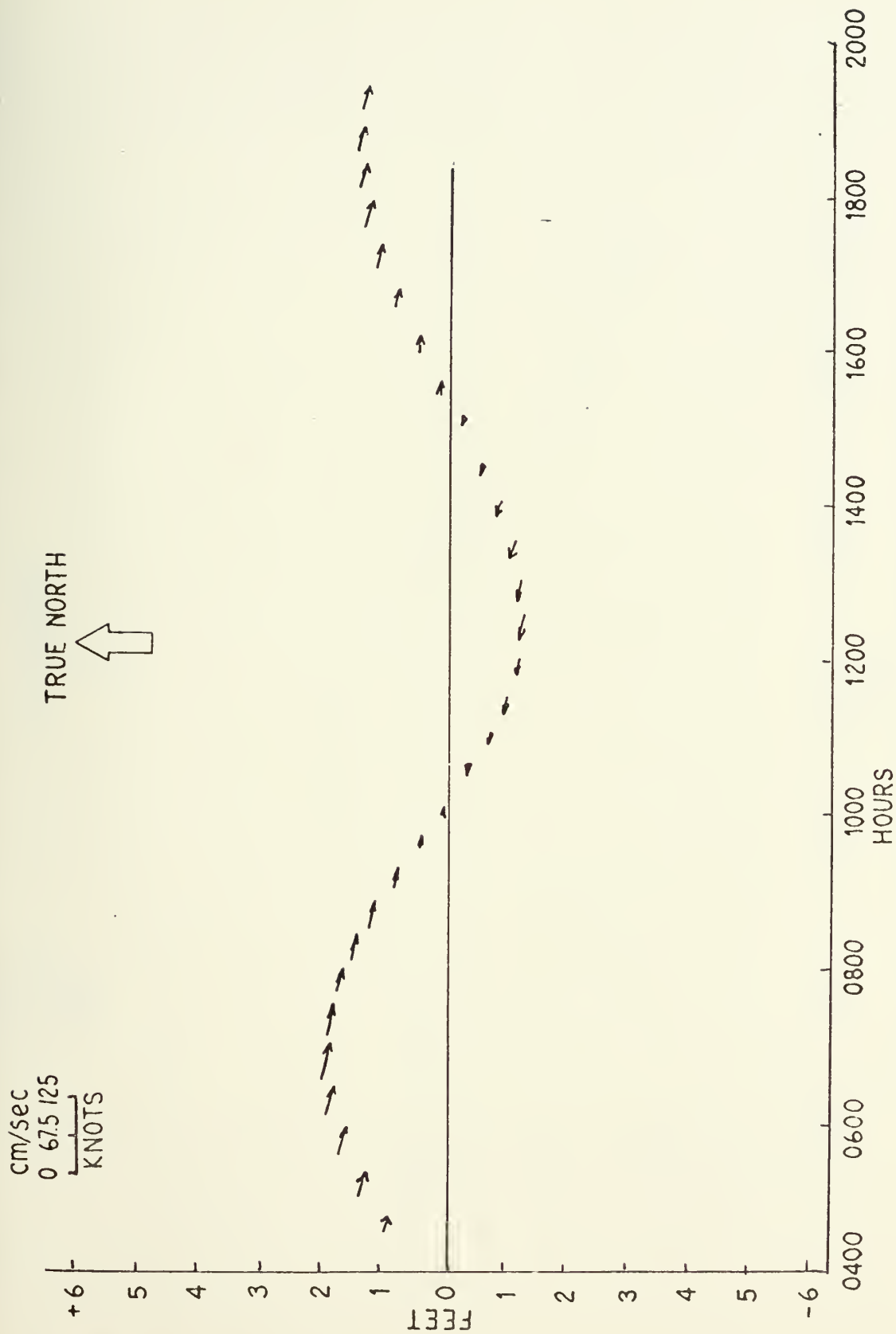


Figure A-48. Calculated Tides and Currents in Monterey Harbor for
8 November 1970.

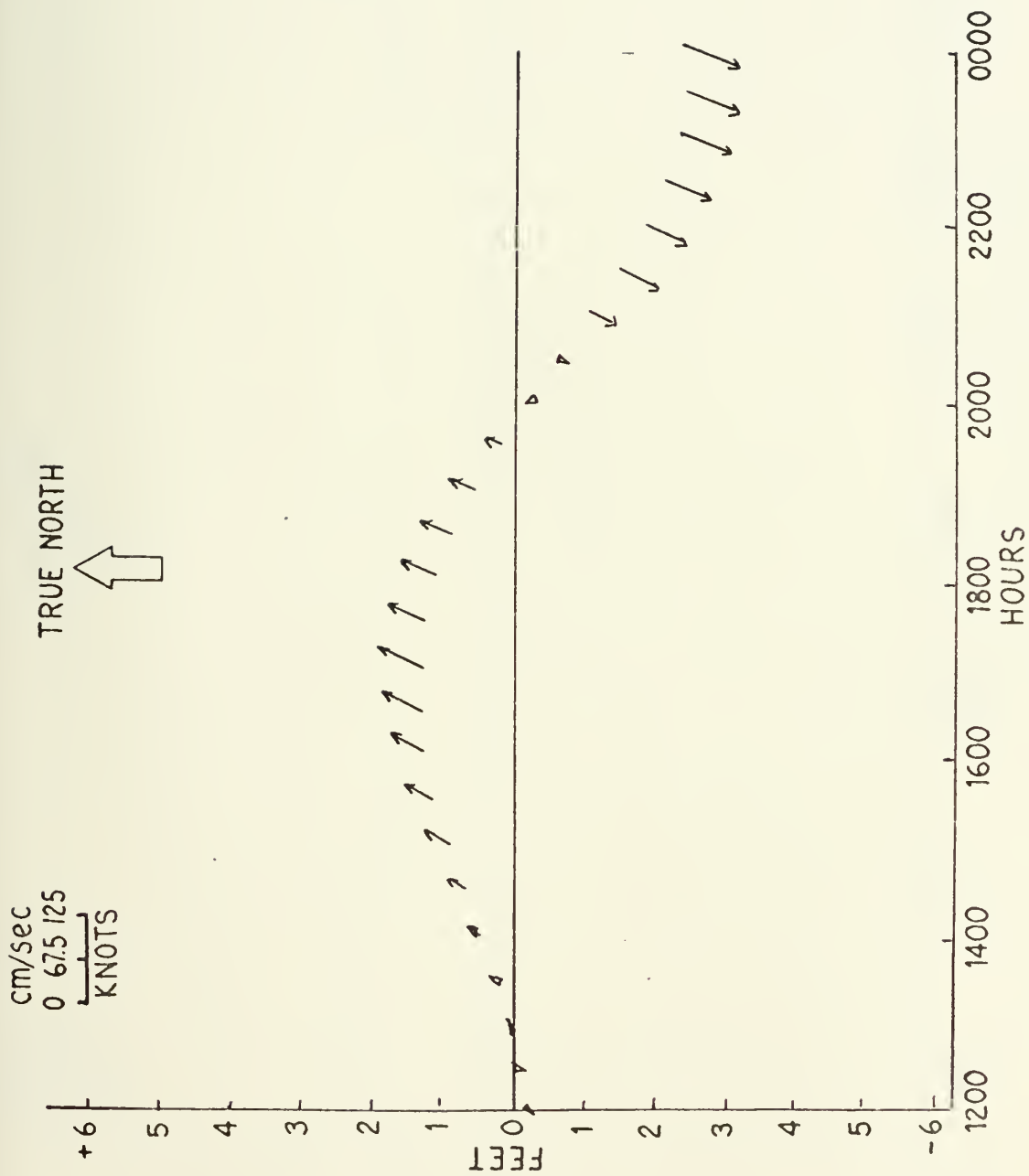


Figure A-49. Calculated Tides and Currents at Santa Cruz for
7 November 1970.



Figure A-50. Calculated Tides and Currents at Santa Cruz for
8 November 1970.

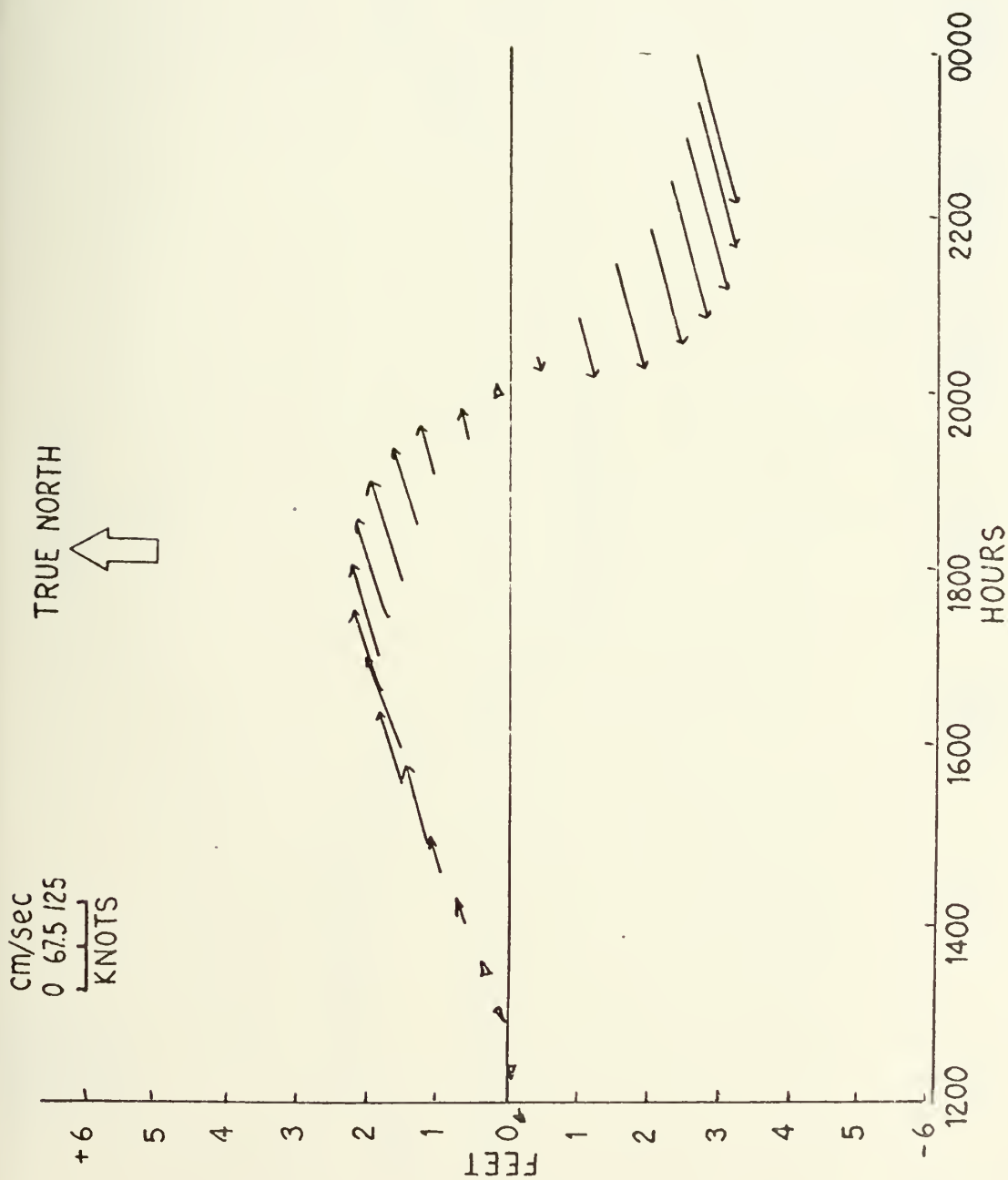


Figure A-51. Calculated Tides and Currents at Moss Landing for
7 November 1970.



Figure A-52. Calculated Tides and Currents at Moss Landing for
8 November 1970.

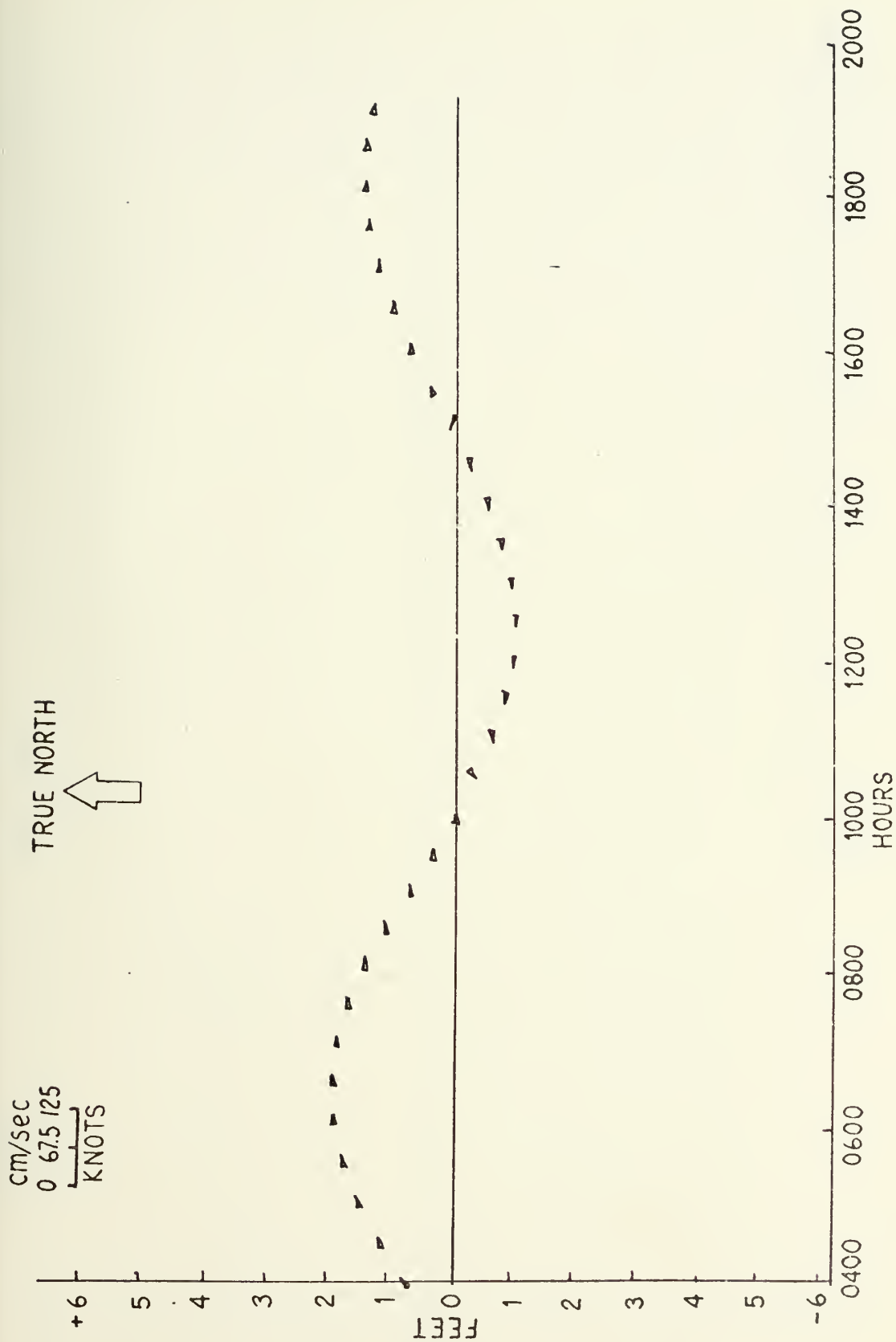


Figure A-53. Calculated Tides and Currents in Deep part of Monterey Canyon
8 November 1970.

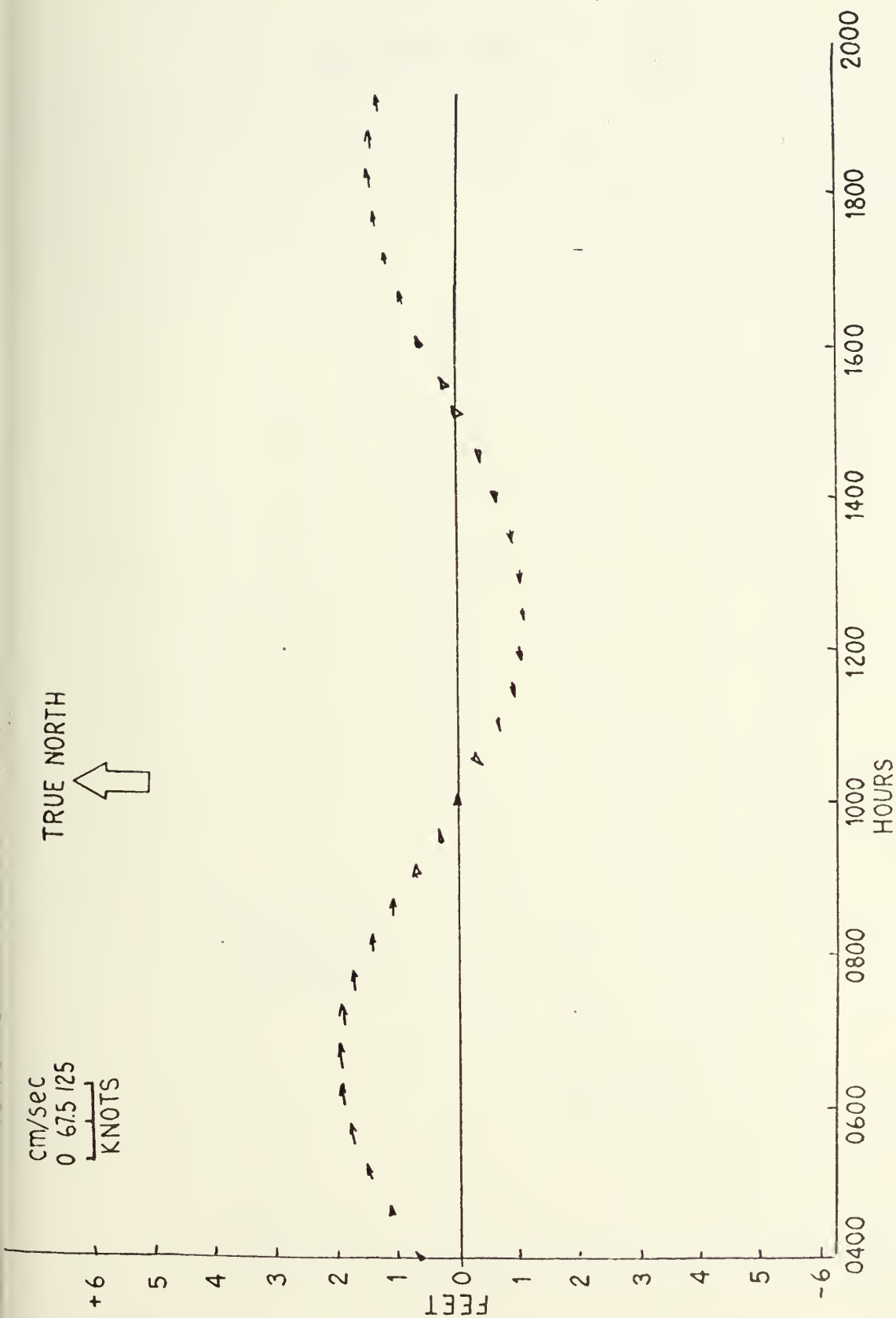


Figure A-54. Calculated Tides and Currents in Shallow part of Monterey Canyon for 8 November 1970.

MONTEREY BAY

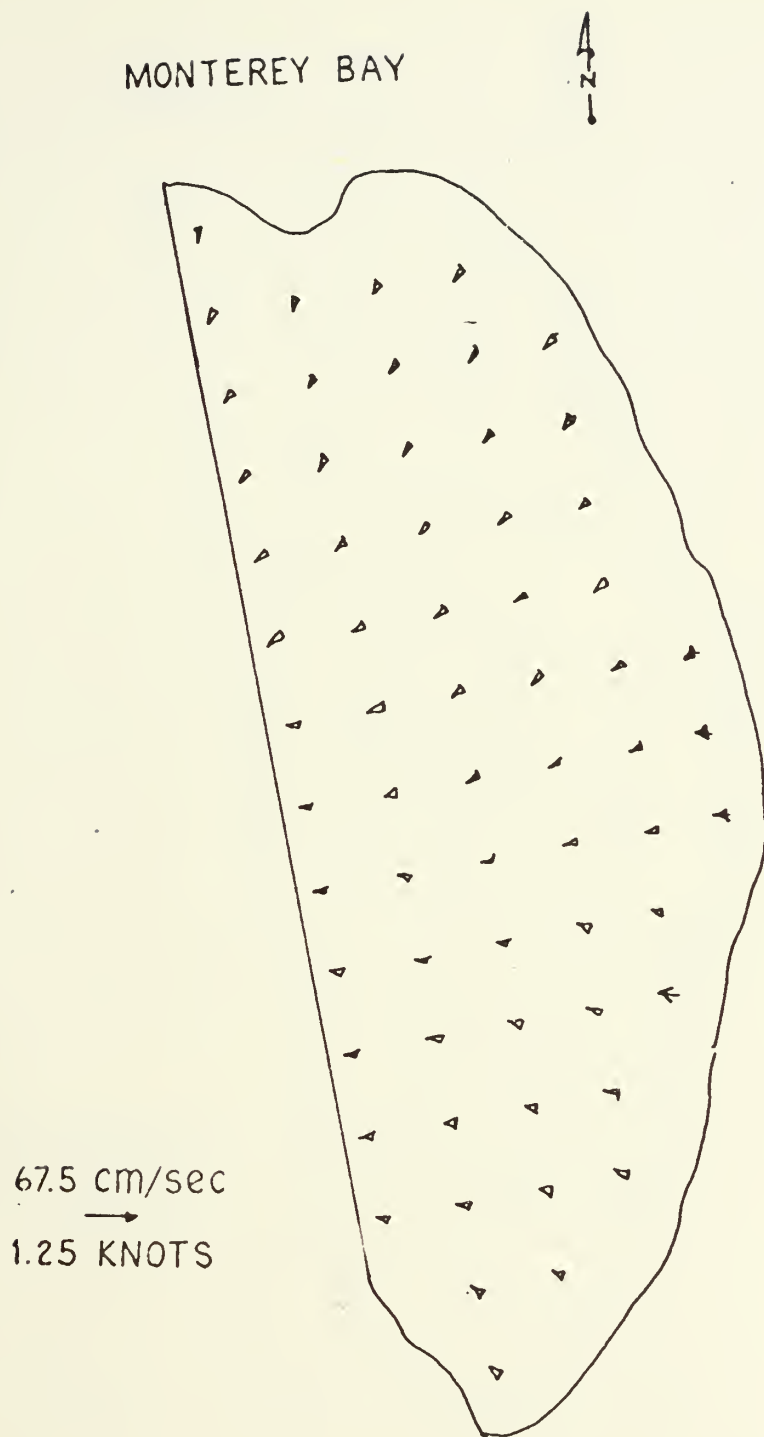


Figure A-55. Calculated Currents in Monterey Bay at Higher Low Water plus 0.5 hours.

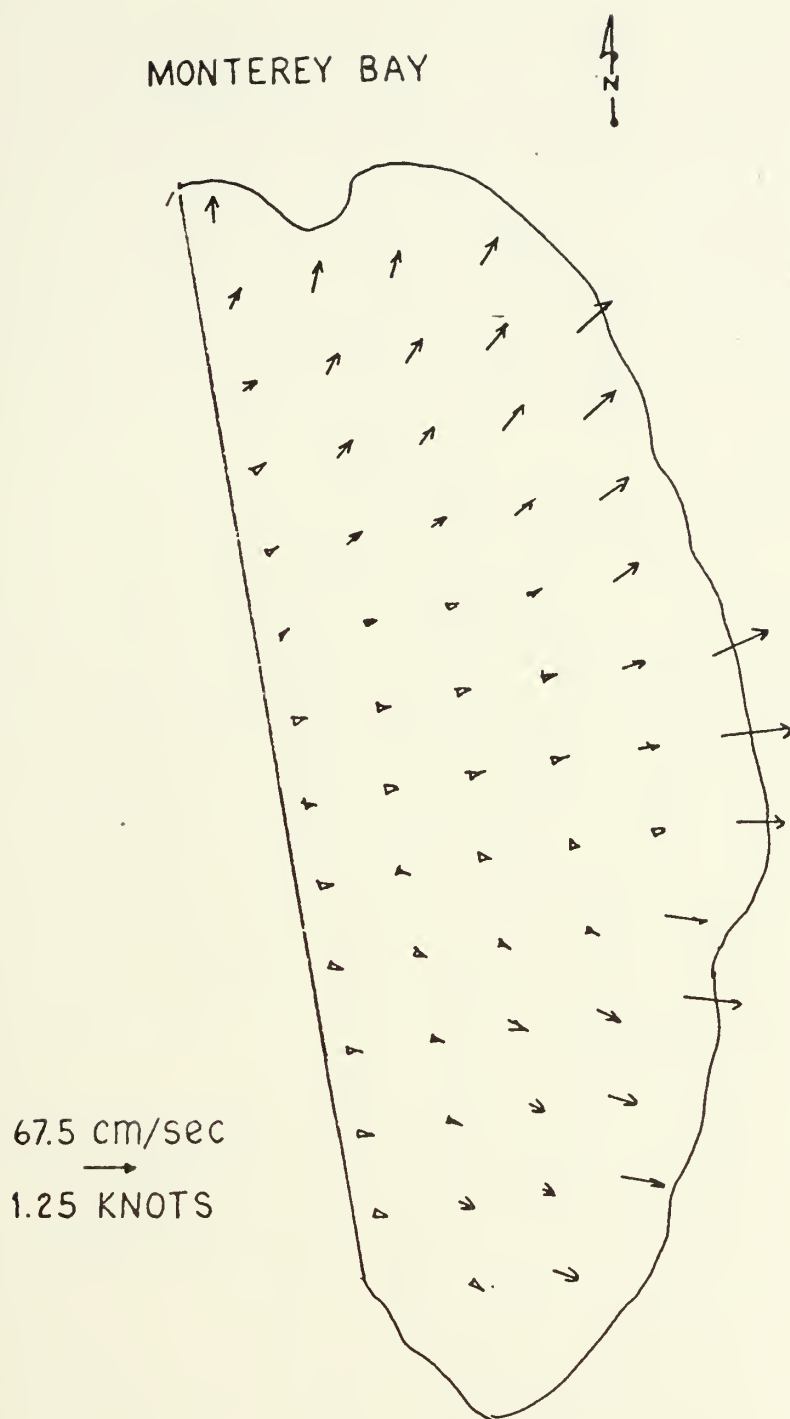


Figure A-56. Calculated Currents in Monterey Bay at Lower High Water minus 2 hours.

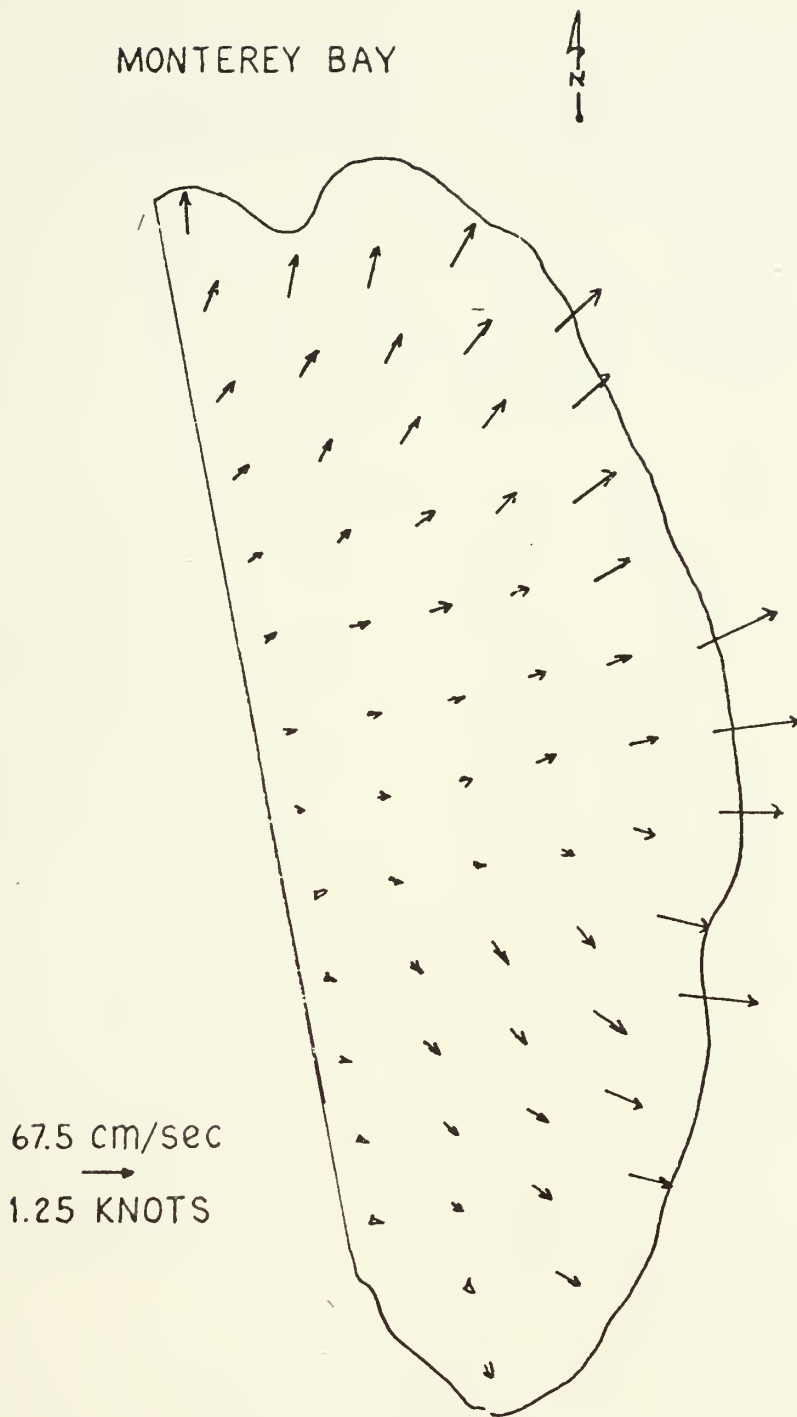


Figure A-57. Calculated Currents in Monterey Bay at Lower High Water plus 1 hour.

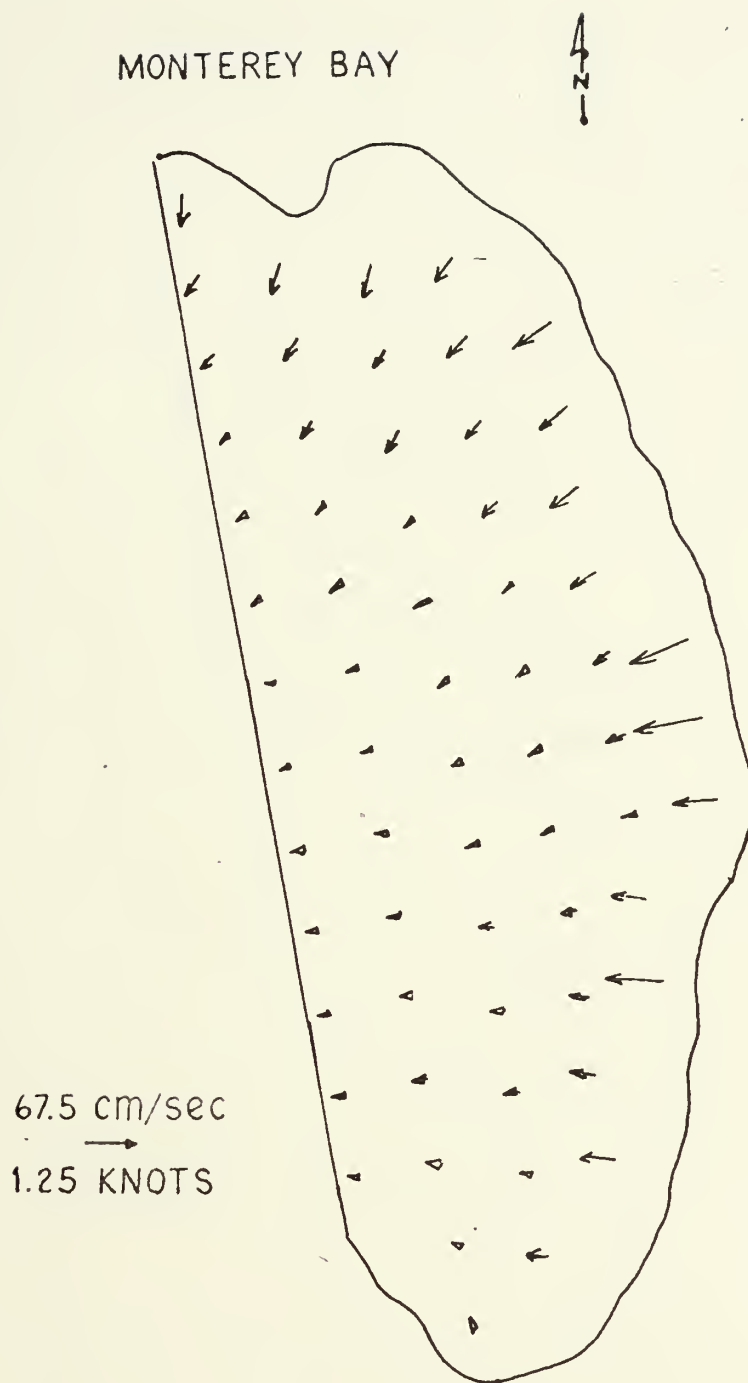


Figure A-58. Calculated Currents in Monterey Bay at Lower Low Water minus 2.5 hours.

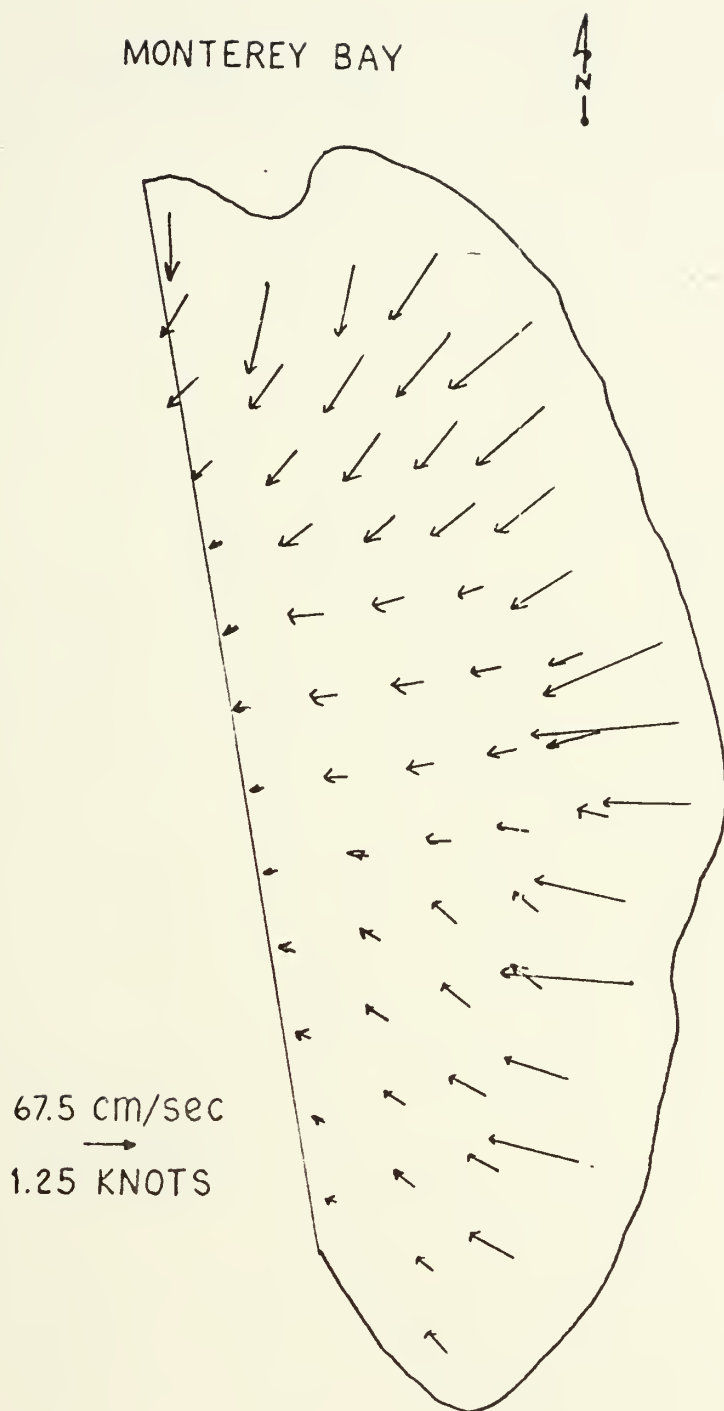


Figure A-59. Calculated Currents in Monterey Bay at Lower Low Water.

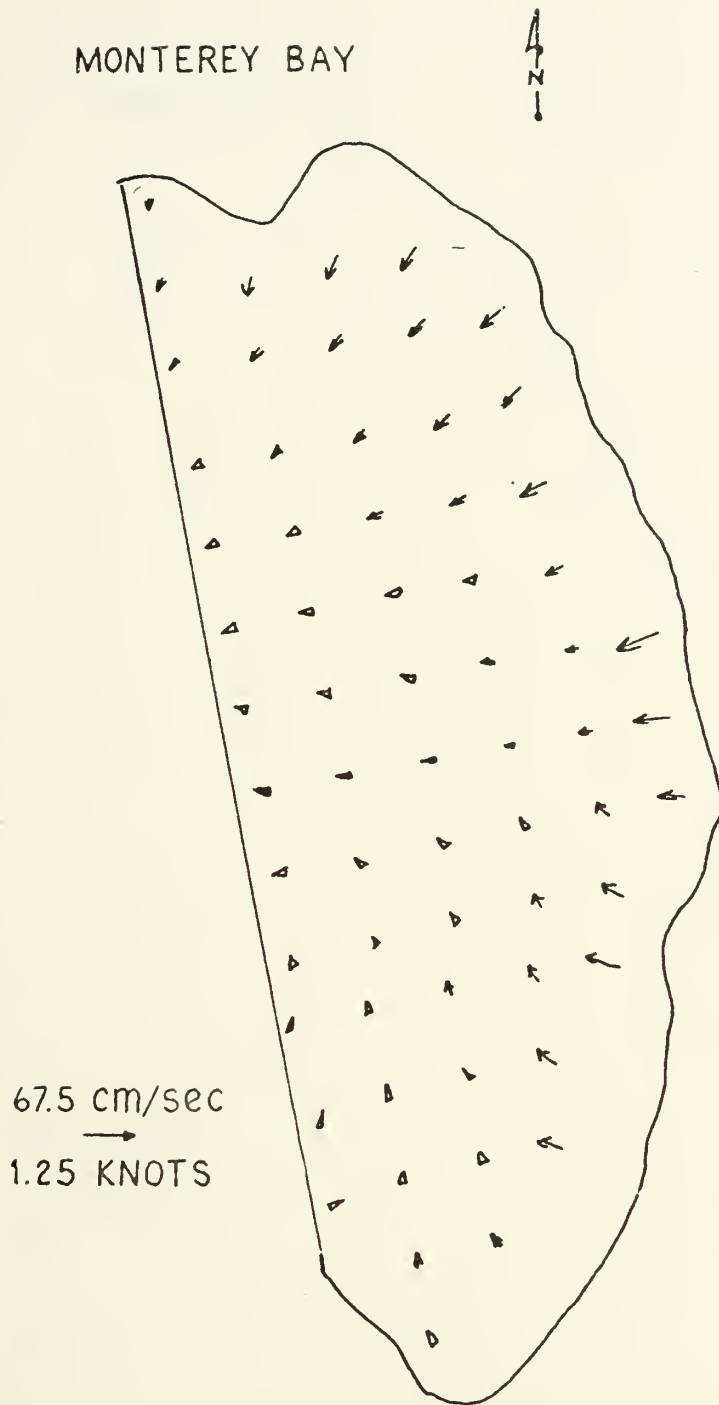


Figure A-60. Calculated Currents in Monterey Bay
at Lower Low Water plus 3.5 hours.

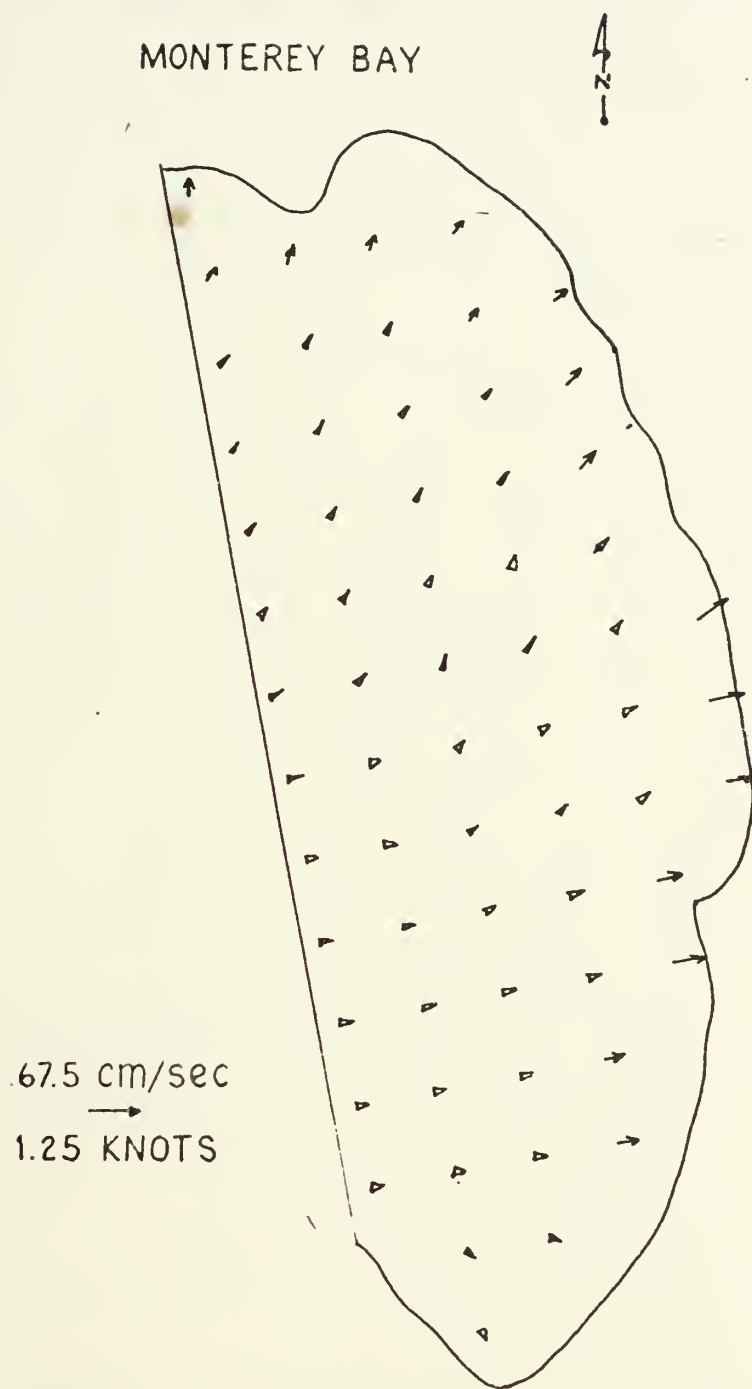


Figure A-61. Calculated Currents in Monterey Bay
at Higher High Water minus 2.5 hours.



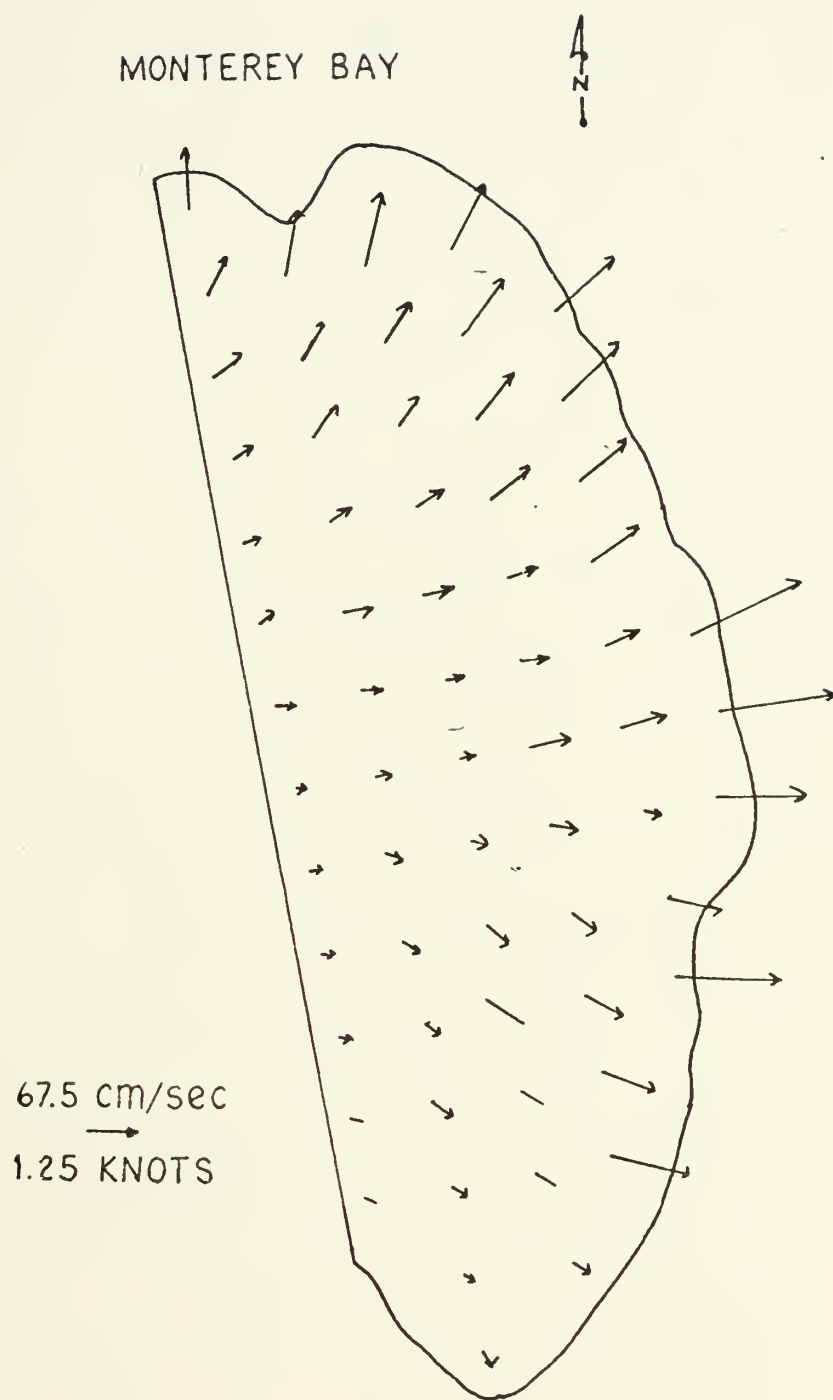


Figure A-62. Calculated Currents in Monterey Bay
at Higher High Water plus 0.5 hours.

MONTEREY BAY

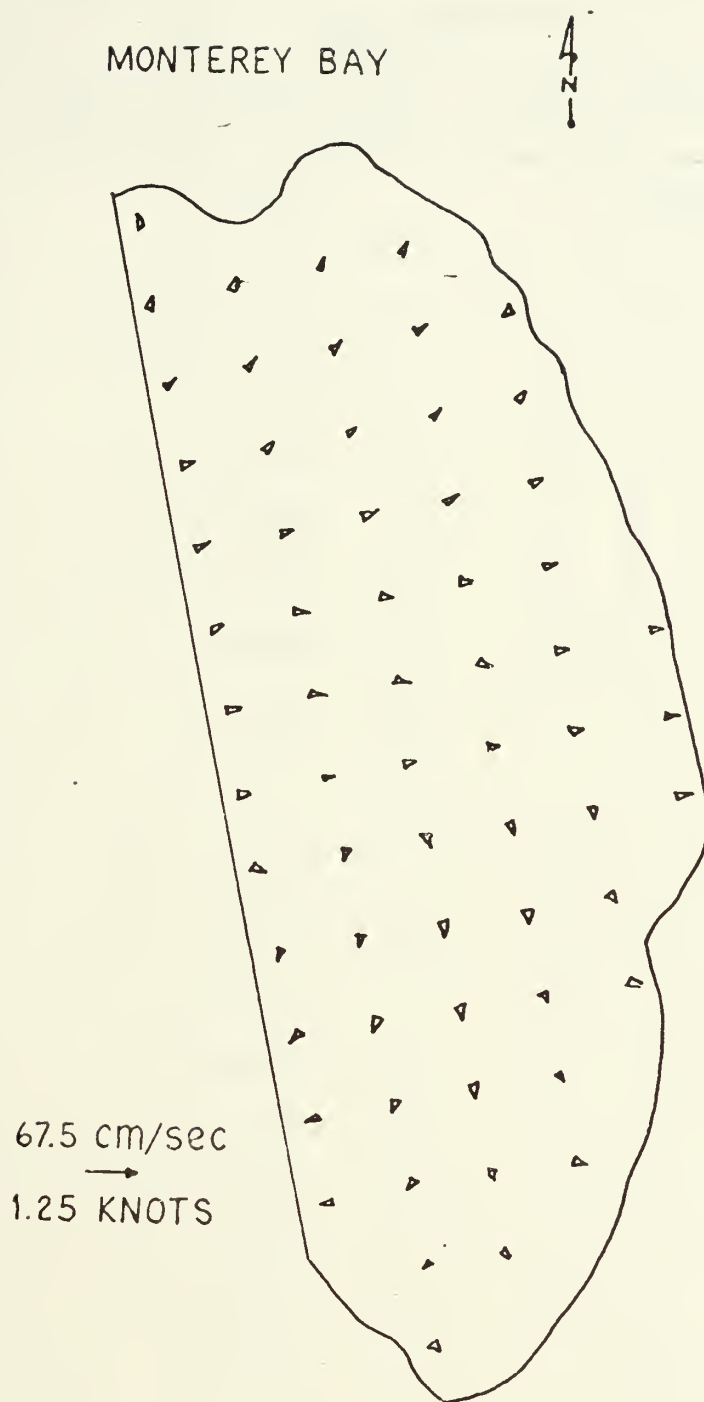


Figure A-63. Calculated Currents in Monterey Bay
at Lower-Low Water minus 2.5 hours.

Table A-I. Comparison of Tides at Monterey Bay Reference Stations

Monterey			Santa Cruz			Moss Landing		
Day/Time (PST)	High- Low	Diff- erence	Day/Time (PST)	High- Low	Diff- erence	Day/Time (PST)	High- Low	Diff- erence
<u>August</u>			<u>August</u>			<u>August</u>		
12/0200	3.35		12/0300	2.2				
		3.10			3.10			
12/0900	6.45		12/1000	5.3				
		0.15			0.2			
12/1200	6.3		12/1230	5.1		12	5.65	
		2.6			2.6			2.9
12/1900	8.9		12/1930	7.7		12	8.55	
		6.0			6.0			6.05
13/0300	2.9		13/0300	1.7		13	2.50	
		3.9			3.9			3.85
13/1000	6.8		13/1000	5.6		13	6.35	
		0.5			0.45			0.35
13/1300	6.3		13/1300	5.15		13	6.00	
		3.1			3.05			3.15
13/2000	9.4		13/2000	8.20		13	9.15	
17/2200	9.4		17/2230	8.4				
		6.9			7.15			
18/0500	2.5		18/0300	1.25		18	8.9	
		5.6			5.75			7.2
18/1130	8.1		18/1100	7/00		18	1.7	
					3.65			5.85
			18/1700	3.35		18	7.55	
					4.35			3.85
			18/2300	7.7		18	3.70	
					5.7			4.95
			19/0600	2.0		19	8.65	
					5.45			6.0
19/1200	8.5		19/1200	7.45		19	2.65	
		4.2			4.3			5.65
19/1800	4.3		19/1800	3.15		19	8.3	
		3.7			3.85			
20/0000	8.0		20/0000	7.00				

Comparison of Tides at Monterey Bay Reference Stations (Cont'd)

Monterey			Santa Cruz			Moss Landing		
Day/Time (PST)	High- Low	Diff- erence	Day/Time (PST)	High- Low	Diff- erence	Day/Time (PST)	High- Low	Diff- erence
<u>November</u>			<u>November</u>			<u>November</u>		
						06/0503	6.6	
								0.8
			06/1000	5.25		06/1000	5.8	
					1.6			1.35
			06/1600	6.85		06/1530	7.15	
					4.75			4.55
			06/2300	2.10		06/2300	2.6	
					4.3			4.4
			07/0600	6.40		07/0600	7.0	
					2.0			2.0
			07/1100	4.40		07/1100	5.0	
					1.9			1.9
			07/1630	6.30		07/1700	6.9	
					4.15			4.3
			08/0000	2.15		08/0000	2.6	
					4.6			4.6
			08/0630	6.75		08/0600	7.2	
					3.10			3.0
			08/1230	3.65		08/1300	4.2	
					2.65			2.5
08/1800	7.6		08/1800	6.3		08/1800	6.7	
		3.9			3.75			3.55
09/0000	3.7		09/0000	2.55		09/0000	3.15	
		5.0			4.75			4.75
09/0700	8.7		09/0700	7.3		09/0700	7.9	
		4.85			4.45			4.45
09/1300	3.85		09/1300	2.85		09/1330	3.45	
		3.85			3.4			3.3
09/1900	7.7		09/1900	6.25		09/1900	6.75	
		3.65			3.10			3.15
10/0700	4.5		10/0100	3.15		10/0100	3.6	
		5.15			4.6			4.7
10/1400	3.2		10/1400	2.15		10/1430	2.7	
		4.5			4.05			3.95
10/2030	7.5		10/2000	6.2		10/2000	6.65	
		2.9			2.75			2.7
11/0130	4.6		11/0200	3.45		11/0200	3.95	
		4.9			4.65			4.8

Comparison of Tides at Monterey Bay Reference Stations (Cont'd)

Monterey			Santa Cruz			Moss Landing		
Day/Time (PST)	High- Low	Diff- erence	Day/Time (PST)	High- Low	Diff- erence	Day/Time (PST)	High- Low	Diff- erence
<u>November</u>			<u>November</u>			<u>November</u>		
11/0800	9.5		11/0800	8.10		11/0800	8.75	
		7.1			6.75			6.8
11/1500	2.4		11/1500	1.35		11/1500	1.95	
		4.9			4.65			4.55
11/2200	7.3		11/2130	6.00		11/2100	6.5	
		2.4			2.25			2.2
12/0230	4.9		12/0200	3.75		12/0200	4.3	
		4.8			4.45			4.45
12/1000	9.7		12/0830	8.2		12/0800	8.75	
		7.9			7.4			7.25
12/1200	1.8		12/1600	0.8		12/1530	1.5	
		5.5			4.55			5.45
12/2300	7.3		12/2200	5.35		12/2230	6.25	
		2.3			1.55			1.65
13/0300	5.0		13/0300	3.0		13/0300	4.6	
		4.5			4.4			4.3
13/1000	9.5		13/0900	8.2		13/0900	8.9	
		8.0			7.5			7.65
13/1700	1.5		13/1630	0.7		13/1630	1.25	
		5.7			5.05			5.0
14/0100	7.2		13/2300	5.75		13/2300	6.25	
		1.1			1.15			1.15
14/0430	6.1		14/0300	4.60		14/0330	5.1	
		3.5			3.6			3.7
14/1100	9.6		14/1000	8.2		14/1000	8.8	
		7.8			2.45			7.45
14/1830	1.8		14/1700	0.75		14/1700	1.35	

Date	Time (PST)	Santa Cruz		Moss Landing		Marina		USNS Desteiguer	
		Speed Knots	Direc- tion Degrees	Speed Knots	Direc- tion Degrees	Speed Knots	Direc- tion Degrees	Speed Knots	Direc- tion Degrees
Aug. 12	1500	5	315	12	271	17	225	10	270
	1600			12	257				
	1700			10	260				
	1800			9	262			10	310
	1900			10	250				
	2000	4	270	9	239			15	310
	2100			9	214				
	2200			8	189			10	90
	2300			3	166				
	0000	4	135	2	167			calm	
Aug. 13	0100			1	165				
	0200			1	164			calm	
	0300			2	158				
	0400	2	90	2	161			calm	
	0500			1	167				
	0600			2	159				
	0700			3	148				

Table A-II. Wind Measurements in Monterey Bay.

Date	Time (PST)	Santa Cruz		Moss Landing		Marina		USNS Desteiguer	
		Speed Knots	Direction Degrees	Speed Knots	Direction Degrees	Speed Knots	Direction Degrees	Speed Knots	Direction Degrees
Aug. 13	0800			1	164				
	0900			5	187				
	1000			5	199				
	1100			3	240				
	1200			5	243				
	1300			5	250				
	1400			7	249				
	1500			8	260	13	225		
	1600	3	225	8	259				
	1700			8	250				
	1800			8	244				
	1900			6	241				
	2000	13	345	7	215				
	2100			7	206				
	2200			8	196				
	2300			4	173				
	0000			2	167				

Table A-II. (Continued)

Date	Time (PST)	Santa Cruz		Moss Landing		Marina		USNS Desteiguer	
		Speed Knots	Direc- tion Degrees	Speed Knots	Direc- tion Degrees	Speed Knots	Direc- tion Degrees	Speed Knots	Direc- tion Degrees
Aug. 18	1200	9	225	6	274			10	340
	1300			8	266				
	1400			9	272				calm
	1500			9	268	15	225		
	1600	11	225	11	276				calm
	1700			11	265				
	1800			9	269			12	280
	1900			8	269				
	2000	6	200	8	255			12	280
	2100			7	246				
	2200			6	233			13	280
	2300			5	210				
	0000	2	100	6	200			7	280
	0100			6	188				
	0200			5	176				
	0300			8	177				

Table A-II. (Continued)

Date	Time (PST)	Santa Cruz		Moss Landing		Marina		USNS Desteiguer	
		Speed Knots	Direc- tion Degrees	Speed Knots	Direc- tion Degrees	Speed Knots	Direc- tion Degrees	Speed Knots	Direc- tion Degrees
Aug. 19	0400	0	225	7	177				
	0500			3	176				
	0600			2	172				
	0700			5	172				
	0800			10	204				
	0900			10	208				
	1000			8	225				
	1100			7	252				
	1200	9	180	7	253				
	1300			8	233				
	1400			8	261				
	1500			10	265	17	225		
	1600	13	225	11	261				
	1700			12	254				
	1800			11	249				
	1900			12	238				
	2000	8	45	13	228				

Table A-II. (Continued)

Date	Time (PST)	Santa Cruz		Moss Landing		Marina		USNS Desteiguer	
		Speed Knots	Direc- tion Degrees	Speed Knots	Direc- tion Degrees	Speed Knots	Direc- tion Degrees	Speed Knots	Direc- tion Degrees
Aug. 19	2100			12	196				
	2200			5	165				
	2300			2	172				
	0000			4	144				
	1200			10	156				
Nov. 6	1300			13	207				
	1400			20	221				
	1500			23	214	14	170		
	1600			22	219				
	1700			19	220				
Nov. 7	1800			16	234				
	1900			17	231				
	2000			16	229				
	2100			9	259				
	2200			7	301				
	2300			6	251				
	0000	11	000	3	212				

Table A-II. (Continued)

Date	Time (PST)	Santa Cruz		Moss Landing		Marina		USNS Desteiguer	
		Speed. Knots	Direc- tion Degrees	Speed Knots	Direc- tion Degrees	Speed Knots	Direc- tion Degrees	Speed Knots	Direc- tion Degrees
Nov. 7	0100			2	295				
	0200			1	130				
	0300			4	109				
	0400	4	000	8	118				
	0500			9	115				
	0600			8	118				
	0700			11	124				
	0800	4	45	12	123				
	0900			7	126				
	1000			7	124				
	1100			4	132				
	1200			5	250				
	1300			8	263				
	1400			7	261				
	1500			7	263	7	225		
	1600			8	269				
	1700			8	270				

Table A-II. (Continued)

Date	Time (PST)	Santa Cruz		Moss Landing		Marina		USNS Desteiguer	
		Speed Knots	Direc- tion Degrees	Speed Knots	Direc- tion Degrees	Speed Knots	Direc- tion Degrees	Speed Knots	Direc- tion Degrees
Nov. 7	1800			3	274				
	1900			2	266				
	2000			1	224				
	2100			4	225				
	2200			1	134				
	2300			3	87				
	0000			1	138				
Nov. 8	0100	5	000	0	146				
	0200			1	203				
	0300			0	208				
	0400	02	000	3	89				
	0500			2	108				
	0600			4	122				
	0700			8	117				
	0800			8	118				
	0900			4	114				
	1000			4	132				

Table A-II. (Continued)

Date	Time (PST)	Santa Cruz		Moss Landing		Marina		USNS Desteiguer	
		Speed Knots	Direc- tion Degrees	Speed Knots	Direc- tion Degrees	Speed Knots	Direc- tion Degrees	Speed Knots	Direc- tion Degrees
Nov. 8	1100			2	133				
	1200			2	274				
	1300			2	314				
	1400			3	298				
	1500			6	302	5	180		
Nov. 10	0800	5	315	1	182				
	0900			1	148				
	1000			1	173	12	225		
	1100			3	295				
	1200	6	225	6	305				
	1300			8	302				
	1400			8	301				
	1500			12	296				
	1600	11	215	10	304				
	1700			8	304				
	1800			6	292				
	1900			5	293				

Table A-II. (Continued)

Date	Time (PST)	Santa Cruz		Moss Landing		Marina		USNS Desteiguer	
		Speed Knots	Direction Degrees	Speed Knots	Direction Degrees	Speed Knots	Direction Degrees	Speed Knots	Direction Degrees
Nov.10	2000			3	282				
Nov.13	0100			4	74				
	0200			6	89				
	0300			8	94				
	0400	2	90	11	82			11	090
	0500			19	83				
	0600			16	79				
	0700			16	74				
	0800			14	82				
								calm	

Table A-II. (Continued)

Table A-III
DROGUE COURSE/SPEED DATA

	<u>Time</u>	<u>Approx. Course</u>	<u>Approx. Speed(kts)</u>
Drogue #1:			
	121800 Aug.	088	0.70
	1900	046	0.70
	2000	099	0.50
	2100	112	0.40
	2200	124	0.30
	2300	114	0.25
	130000	152	0.15
	0100	144	0.25
	0200	134	0.40
	0300	166	0.34
	0400	179	0.20
	0500	187	0.10
	0600	198	0.15
	0700	218	0.10
	0800	162	0.05
Drogue #2:			
	122000 Aug.	328	0.20
	2100	285	0.30
	2200	275	0.20
	2300	267	0.10
	130000	255	0.30
	0100	255	0.20
	0200	255	0.10
	0300	298	0.25
	0400	274	0.25
	0500	272	0.20
	0600	258	0.34
	0700	237	0.05
	0800	201	0.10
	0900	167	0.20
Drogue #3: No track (never gained contact)			
Drogue #4:			
	130200 Aug.	143	0.15
	0300	130	0.15
	0400	156	0.10
	0500	160	0.10
	0600	182	0.15
	130700	191	0.10

0800	026	0.10
0900	028	0.10
1000	030	0.15

Drogue #5:

130200 Aug.	132	0.40
0300	169	0.40
0400	150	0.34
0500	168	0.20
0600	175	0.15
0700	135	0.15
0800	094	0.20
0900	097	0.20

Drogue #6:

182100 Aug.	112	0.25
2200	090	0.25
2300	124	0.20
190000	238	0.175
0100	221	0.20
0200	215	0.25
0300	120	0.075
0400	132	0.125
0500	043	0.10
0600	097	0.075
0700	065	0.025
0800	056	0.30
0900	069	0.225
1000	130	0.30
1100	134	0.25
1200	144	0.375
1300	143	0.20
1400	132	0.225
1500	133	0.275

Drogue #7:

182100 Aug.	017	0.225
2200	074	0.125
2300	334	0.20
190000	327	0.20
0100	342	0.30
0200	019	0.275
0300	031	0.40
0400	034	0.275
0500	034	0.20
190600	034	0.425
0700	069	0.50
0800	101	0.425
0900	107	0.50
1000	163	0.25

1100	200	0.225
1200	096	0.225
1300	081	0.15
1400	084	0.275
1500	143	0.20

Drogues #8:

182200 Aug.	034	0.20
2300	353	0.325
190000	328	0.225
0100	328	0.275
0200	003	0.45
0300	030	0.20
0400	071	0.20
0500	089	0.275
0600	080	0.15
0700	087	0.125
0800	090	0.25

Drogue #9: No track (lost contact after 15 min.)

Drogues #10:

182300 Aug.	214	0.175
190000	252	0.40
0100	285	0.175
0200	356	0.30
0300	003	0.45
0400	037	0.15
0500	065	0.275
0600	093	0.175
0700	087	0.175
0800	146	0.20
0900	165	0.25
1000	180	0.375
1100	207	0.40
1200	235	0.325
1300	237	0.225
1400	263	0.05

Drogues #11: Very short track. Moved due south 250 yds., 2300-2400. Shifted to approximate head 250 for 30 min. covering 200 yds. Reversed track to about 070 for 2 hrs. covering 400 yds. Lost contact at 190230 (shadow zone?)

Drogue #12:

190000 Aug.	230	0.275
0100	229	0.325
0200	261	0.425
0300	293	0.275
0400	026	0.40

0500	056	0.425
0600	012	0.375
0700	064	0.30
0800	117	0.175

Droque #13:

190000 Aug.	355	0.125
0100	292	0.30
0200	305	0.075
0300	272	0.05
0400	028	0.075
0500	055	0.125
0600	016	0.175
0700	068	0.325

Droque #28:

061300 Nov.	310	0.275
1400	310	0.125
1500	290	0.20
1600	311	0.20
1700	327	0.20
1800	327	0.10
1900	281	0.10
2000	257	0.05
2100	257	0.05
2200	244	0.25
2300	246	0.175
070000	248	0.325
0100	253	0.425
0200	283	0.333
0300	280	0.325
0400	273	0.375
0500	298	0.40
0600	315	0.375
0700	327	0.40
0800	330	0.475
0900	352	0.55
1000	348	0.45
1100	338	0.325
1200	342	0.30
1300	336	0.325
1400	327	0.325
1500	342	0.34
1600	342	0.275
1700	336	0.125
1800	277	0.10
1900	250	0.05
2000	248	0.10
2100	247	0.15
2200	247	0.15
2300	247	0.275
180000	276	0.225

0100	290	0.30
0200	275	0.325
0300	292	0.30
0400	314	0.425
0500	316	0.34
0600	304	0.40

Drogue #29:

061200 Nov.	048	0.175
061300	048	0.175
1400	051	0.20
1500	040	0.15
1600	056	0.25
1700	082	0.25

Drogue #30:

071800 Nov.	268	0.25
1900	263	0.175
2000	244	0.15
2100	183	0.20
2200	207	0.125
2300	241	0.225
080000	249	0.30
0100	248	0.275
0200	258	0.325
0300	253	0.30
0400	263	0.275
0500	311	0.25
0600	302	0.225
0700	345	0.325
0800	352	0.30
0900	358	0.325
1000	002	0.325
1100	002	0.325
1200	348	0.175
1300	310	0.10
1400	276	0.10
1500	264	0.15
1600	244	0.275

Drogue #31:

071900 Nov.	293	0.10
2000	278	0.05
2100	278	0.05
2200	259	0.225
2300	251	0.175
080000	260	0.40
0100	290	0.30
0200	272	0.45
0300	303	0.375
0400	294	0.325

0500	319	0.225
0600	339	0.65
0700	002	0.325
0800	010	0.34
0900	021	0.475
1000	046	0.40
1100	031	0.25
081200	009	0.175
1300	333	0.05
1400	333	0.10
1500	338	0.10
1600	338	0.125

Drogue #32: Very short track. Moved for 1-1/2 hours on approximate heading 170 covering 550 yds. Lost contact (shadow zone?)

Drogue #33:

072000 Nov.	095	0.175
2100	117	0.20
2200	152	0.15
2300	229	0.325
080000	234	0.275
0100	237	0.34
0200	253	0.30
0300	284	0.175
0400	325	0.275
0500	344	0.225
0600	359	0.10
0700	012	0.375
0800	030	0.225
0900	048	0.40
1000	051	0.325
1100	043	0.275
1200	021	0.10
1300	041	0.125
1400	054	0.275
1500	267	0.15

Drogue #34:

101000 Nov.	246	0.34
1100	233	0.45
1200	238	0.375
1300	226	0.40

Drogue "X":

100800 Nov.	240	0.25
0900	234	0.34
1000	231	0.20
1100	232	0.375
1200	236	0.45
1300	244	0.34

Drogue "Y":

100900 Nov.	190	0.15
1000	164	0.20
1100	118	0.125
1200	166	0.25
----	---	--- *
1600	236	0.40
1700	232	0.425
1800	229	0.475
1900	232	0.425
2000	236	0.475

Drogue "Z": 101100 Nov.

1200	137	0.40
----	---	--- *
1600	192	0.34
1700	195	0.325
1800	210	0.45
1900	219	0.375
2000	203	0.45

Drogue #35:

132000 Nov.	180	0.325
0300	164	0.425
0400	182	0.34
0500	191	0.375
0600	201	0.575
0700	223	0.575
0800	231	0.575

Drogue #36:

130300 Nov.	210	0.45
0400	213	0.45
0500	205	0.475
0600	229	0.70
0700	241	0.65
0800	230	0.675

Drogue #37:

130300 Nov.	162	0.225
0400	180	0.325
0500	205	0.375
0600	214	0.45
0700	212	0.50
0800	214	0.475

Drogue #38:

130500 Nov.	219	0.275
0600	225	0.45
0700	228	0.525

*Interrupted Track

BIBLIOGRAPHY

1. Broenkow, W. X., 1971, personal communication, Moss Landing Biological Station, Moss Landing, California.
2. Cardone, V. J., 1969, Specification of the Wind Distribution in Marine Boundary Layer for Wave Forecasting, New York University, Department of Meteorology and Oceanography, Geophysical Sciences Laboratory TR-69-1.
3. Carter, R. C. and E. J. Kazmierczak, 1968, Special Oceanographic Studies, Engineering-Science, Inc. Final Report, Task VII-1a, State of California State Water Quality Control Board, San Francisco Bay-Delta Quality Control Program.
4. Defant, A., 1961, Physical Oceanography, Volume 1, Pergamon Press, New York.
5. Dronkers, J. J., 1964, Tidal Computations in Rivers and Waters, North-Holland Publishing Company, Amsterdam.
6. Garcia, R. A., 1971, Numerical Simulation of Currents in Monterey Bay, M.S. Thesis, Naval Postgraduate School, Monterey, California.
7. Hansen, W., 1966, The Reproduction of the Motion in the Sea by means of Hydrodynamical-Numerical Methods, Mitteilungen des Instituts für Meereskunde der Universität Hamburg, Subcommittee on Oceanographic Research Technical Report 25, Hamburg, Germany.
8. Jensen, H. E., S. Weywadt and A. Jensen, 1966, Forecasting of Storm Surges in the North Sea, Part I, NATO Subcommittee Oceanographic Research Technical Report 28.
9. Laevastu, T. and P. Stevens, 1969, Application of Numerical Hydrodynamical Models in Ocean Analysis Forecasting, Part I - The Single-Layer Model of Walter Hansen, Fleet Numerical Weather Central, Technical Note 51.
10. Lazanoff, S. M., 1969, An Investigation of Seiches in DaNang Bay, Vietnam, U.S. Naval Oceanographic Office IR No. 69-81.
11. Lazanoff, S. M. and D. K. Clark, 1970, Preliminary Report on the Numerical Prediction of Tides and Tidal Currents for Various Wind Conditions in the South China Sea, U.S. Oceanographic Office IR No. 70-41.

12. Lynch, J. L., 1970, Long Wave Study of Monterey Bay, M. S. Thesis, Naval Postgraduate School, Monterey, California.
13. McKay, D. A., 1970, A Determination of Surface Currents in the Vicinity of the Monterey Submarine Canyon by the Electromagnetic Method, M.S. Thesis, Naval Postgraduate School, Monterey, California.
14. Mungall, J. C. J. and J. B. Matthews, 1970, A Variable-Boundary Numerical Tidal Model, University of Alaska, Institute of Marine Sciences, Report Number R70-4.
15. Ortiz, N. G., 1964, Numerisch-Hydrodynamische Untersuchungen in Golf von Mexico, Ph.D. Dissertation, Universitat Hamburg, Hamburg, Germany.
16. Pacific Gas and Electric Company Engineering Research Department, 1970, personal communication, Emoryville, California.
17. Pekeris, C. L. and Y. Accad, 1969, Solution of Laplace Equation for the M2 Tide in the World Oceans, Philosophical Transactions of The Royal Society of London, Mathematical and Physical Sciences Volume 265, No. 1165, pages 413-436.
18. Pore, N. A. and R. A. Cummings, 1967, A Fortran Program for the Calculation of Hourly Values of Astronomical Tide and Time and Height of High and Low Water, Weather Bureau, Techniques Development Laboratory, WRTM TDL-6.
19. Schureman, P., 1958, Manual of Harmonic Analysis and Prediction of Tides, United States Coast and Geodetic Survey Special Publication No. 98.
20. Simmons, H. B., 1966, Tidal and Salinity Model Practice, Estuary and Coastline Hydrodynamics, A. T. Ippen, ed. McGraw-Hill Book Company, New York.
21. Stoddard, H. S., 1971, Feasibility Study on the Utilization of Parachute Droques and Shore Base Radar to investigate Surface Circulation in Monterey Bay, M.S. Thesis, Naval Postgraduate School, Monterey, California.

INITIAL DISTRIBUTION LIST

	No. Copies
1. Defense Documentation Center Cameron Station Alexandria, Virginia 22314	2
2. Library, Code 0212 Naval Postgraduate School Monterey, California 93940	2
3. Oceanographer of the Navy The Madison Building 732 N. Washington Street Alexandria, Virginia 22314	1
4. Department of Oceanography, Code 58 Naval Postgraduate School Monterey, California 93940	3
5. Dr. E. B. Thornton, Code 58Tm Department of Oceanography Naval Postgraduate School Monterey, California 93940	3
6. Dr. W. C. Thompson, Code 58Th Department of Oceanography Naval Postgraduate School Monterey, California 93940	1
7. U.S. Army Corps of Engineers Waterways Experiment Station Vicksburg, Mississippi 39180	1
8. Mr. Sheldon M. Lazanoff U.S. Naval Oceanographic Office Representative Fleet Numerical Weather Central Monterey, California 93940	5
9. Commander U.S. Naval Oceanographic Office Washington, D. C. 20390	1
10. Mr. Leo J. Fisher U.S. Naval Oceanographic Office Code 7300 Washington, D. C. 20390	5

	No. Copies
11. Commanding Officer Fleet Numerical Weather Central Monterey, California 93940	1
12. Mr. Walter Howard U.S. Ship Research and Development Laboratory Code 746 Panama City, Florida 32401	1
13. Mr. Orville T. Magoon U.S. Army Engineer District Corp of Engineers 100 McAllister Street San Francisco, California 94102	1
14. Mr. M. J. Doyle, Jr. Pacific Gas and Electric Company Department of Engineering Research 4245 Hollis St. Emeryville, California 94608	1
15. Mr. W. T. Burns Kaiser Refractories Moss Landing, California 95039	1
16. Mr. R. H. Bethel Park/Recreation Department Civic Auditorium Santa Cruz, California 95060	1
17. Dr. D. J. Baumgartner Federal Water Quality Administration Northwest Region Pacific Northwest Water Laboratory 200 Southwest 35th Street Corvallis, Oregon 97330	1
18. Mr. Robert Ford State of California Department of Water Resources P.O. Box 9137 Sacramento, California 95816	1
19. Dr. Phillips Hopkins Marine Station Cabrillo Point Pacific Grove, California 93940	1
20. Dr. John Harville Moss Landing Marine Laboratory Moss Landing, California 95039	1

	No. Copies
21. Dr. R. G. Dean Coastal and Oceanographic Engineering Department University of Florida Gainesville, Florida 32601	1
22. Environmental & Fishery Forecasting Center National Marine Fisheries Service National Oceanic & Atmospheric Administration U.S. Department of Commerce c/o Fleet Numerical Weather Central, NPS Monterey, California 93940	2

DOCUMENT CONTROL DATA - R & D*

(Security classification of title, body of abstract and indexing annotation must be entered when the overall report is classified)

1 ORIGINATING ACTIVITY (Corporate author)

Naval Postgraduate School
Monterey, California 93940

2a. REPORT SECURITY CLASSIFICATION

Unclassified

2b. GROUP

3 REPORT TITLE

An Evaluation of a Numerical Water Elevation and Tidal Current
Prediction Model Applied to Monterey Bay

4 DESCRIPTIVE NOTES (Type of report and, inclusive dates)

Master's Thesis; March 1971

5 AUTHOR(S) (First name, middle initial, last name)

Sheldon Mark Lazanoff

6 REPORT DATE

March 1971

7a. TOTAL NO. OF PAGES

148

7b. NO. OF REFS

21

8a. CONTRACT OR GRANT NO.

b. PROJECT NO.

c.

d.

9a. ORIGINATOR'S REPORT NUMBER(S)

9b. OTHER REPORT NO(S) (Any other numbers that may be assigned
this report)

10. DISTRIBUTION STATEMENT

Approved for public release; distribution unlimited.

11. SUPPLEMENTARY NOTES

12. SPONSORING MILITARY ACTIVITY

Naval Postgraduate School
Monterey, California 93940

13. ABSTRACT

The Hansen Hydrodynamical - Numerical model was evaluated for Monterey Bay with actual field data. Tides and winds are the principal driving forces of the Hansen model. Analysis of the field data indicated that the principal driving force of the circulation in the bay was the oceanic currents and not the tides and winds. The tidal heights and phases and current directions were calculated correctly by the model, but the calculated current speeds were an order of magnitude too large. The inaccuracy of the current speeds was attributed to the inaccurate calculations of the currents along the open boundary and the large bathymetric gradients of the Monterey Submarine Canyon.

KEY WORDS

LINK A

LINK B

LINK C

ROLE

WT

ROLE

WT

ROLE

WT

Tides

Currents

Numerical Model

Shallow Water Embayments

Thesis

L345

c.1

Lazanoff

An evaluation of a
numerical water eleva-
tion and tidal current
prediction model ap-
plied to Monterey Bay.

126453

DUDLEY KNOX LIBRARY



3 2768 00036716 3